Structuring of Liquid Crystals for Optical Technologies

Kedar Sathaye

N° d'ordre : 2012telb0214

Sous le sceau de l'Université européenne de Bretagne

Télécom Bretagne

En habilitation conjointe avec l'Université de Bretagne-Sud

Ecole Doctorale – sicma

Structuring of Liquid Crystals for Optical Technologies

Thèse de Doctorat

Mention : "***Sciences pour l'ingénieur***"

Présentée par ***Kedar SATHAYE***

Département : **Optique**

Soutenue le 29 Mars 2012

Jury:

Directeur de these: Jean-Louis de Bougrenet de la Tocnaye, Professeur, Département d'optique, Télécom Bretagne

Rapporteurs: Dominique Bosc, HDR, ENSSAT – Rennes I, Plateforme CCLO
Christian Legrand, Professeur, Université du Littoral

Examinateurs: Jean-François Blach, Maître de conferences, Unité de Catalyse et de la Chimie du Solide, Faculté Jean Perrin
Jean-François Feller, Professeur, Université de Bretagne de Sud
Laurent Dupont, Professeur, Département d'optique, Télécom Bretagne

Contents

Glossary

LC: Liquid crystal
LCP: Liquid Crystal Polymer
FLC: Ferroelectric Liquid Crystal
NLC: Nematic Liquid Crystal
CLC: Cholesteric Liquid Crystal
PSCLC: Polymer Stabilised Cholesteric Liquid Crystal
PSFLC: Polymer Stabilised Ferroelectric Liquid Crystal
PDLC: Polymer Dispersed Liquid Crystal
LCD: Liquid Crystal Display
FP: Fabry-Perot
TFT: Thin Film Transistor
LPP: Linearly Photo-polymerisable Polymer
UV: Ultra-violet
QWP: Quarter Waveplate
SmC: Smectic C
SmA: Smectic A
RM: Reactive Mesogen
ITO: Indium Tin Oxide
TE: Transverse Electric
TM: Transverse Magnetic
MUX: Multiplexer
DEMUX: Demultiplexer

List of Figures for Chapter 1

List of Figures for Chapter 2

List of Figures for Chapter 3

List of Figures for Chapter 4

List of Figures for Chapter 5

List of Figures for Chapter 6

List of Tables

List of Graphs

Acknowledgments

I would like to dedicate this work to my parents, Mr. Shriram R. Sathaye and Mrs. Manjiri S. Sathaye, without their support it would have been impossible to reach this day. My other family members especially my brother, Mr. Shantanu S. Sathaye and his wife Mrs. Ketaki Pandit, both of them have been instrumental to make this day happen. The words will fall short to explain the help and the support of my family.

I would like to express my sincere gratitude towards Prof. Jean-Louis de Bougrenet de la Tocnaye for giving me this opportunity to work in his team. He has been very supportive throughout this work and I would like to thank him for all his timely support during this period of 3 and half years. Also, he has been pivotal in finding the required finance for this work. He himself has vast knowledge and experience in the field of optics, photonics and especially liquid crystals, which he has shared with me throughout this work to help me attain the objectives decided for the work. He has always taken time from his busy schedule to answer my questions in a welcoming manner.

Prof. Laurent Dupont has been influential during this work. His knowledge is an excellent blend of technological aspects as well as the theoretical facets of the subject. This has played immense role in not only coming up with an idea but also the ways to execute that idea. He has always answered my queries and has welcomed me any time to have discussion on the scientific issues in his office. Needless to say, those discussions have always paid rich dividends.

Special thanks one of my best friends Mervin Obeegadoo, who happen to be not only my professional colleagues but also my flatmate, for his support. He has been very helpful and really has been of brotherly influence.

Vinicius Nunes Henriques Silva deserves a separate paragraph to express my appreciation because not only he is my colleague in liquid crystal group but also my one of my best friends. His sense of humour and witty presence has given some moments to cherish in life to come. He has been of great help in performing the experiments in the clean room as well as in the optics laboratories.

I would like to thank Dr. Nicolas Fraval for his help in understanding the basics of liquid crystals and also giving me the required knowledge of French language. Not to forget that this teaching went in a very jovial manner. Also, I would like to express a word of appreciation for Dr. Alexey Denisov, Dr. Antoine Tan and Dr. Bob Bellini for their help in

clean room as well as in the laboratory affairs. I want to thank one of my fellow citizens, Dr. Abhishek Srivastava, who was part of this department for 6 months as a post doctorate fellow and during this time he has given me some important insight in the field of liquid crystals. I would like to thank ever green Bernard Della to make my work easier by offering his experience help. I am grateful to Prof. Michel Gadonna and Dr. Azar Maalouf for allowing and welcoming me in their laboratory in CCLO, Lannion, to perform few experiments.

Departmental colleagues especially the fellow PhD students have made the life, in a foreign country with foreign language, easy and have brightened it up. It was easier because for me to blend in this multicultural, multiethnic department. I would like to thank my fellow colleagues and friends Dr. Damien Malarde, Dr. Bogdan Uscumulic, ever helping Charbel Nassour, ever smiling Lida Sadeghioon, Aurelie Chang Yong, Hani Al Hajjar, Hou Bo, Yuliya, Rabiaa and a very good friend Ghayath El Haj Shhade for their support and also for their encouraging words.

I would like to express a special word of appreciation for entire staff members of Department of Optics especially Frederick Lucarz and Dr. Daniel Stonescou for their help and support. Finally, Anne Catherine Cariou and Jennifer Romer who have been the secretaries of the Department have made things easier on the administrative front with their constant help and support.

Motivation and Introduction

Liquid crystals have variety of applications and these applications cover diverse domains in the world of science and technology. Optically, electrically and magnetically anisotropic nature, reorientation of molecules in desired direction, sensitive to electric and magnetic fields, ability to change the already possessing large birefringence with respect to applied electric field and temperature puts liquid crystal on the cutting edge of the technology. We take an overview of the existing alignment technologies and also the ones which we exploited for devised applications. The work presented here covers diverse applications with liquid crystals as one of the integral parts of all them. The essence of the work lies in the alignment technologies for many applications. Hence alignment technology is the theme which connects all the applications covered in this work. It would be very difficult to point out one single objective in this work; however, a generalised objective can be said as the use of alignment technology to build various applications in telecom industry. As it can be seen that most of the targeted applications belong to telecom or will be useful in telecom industry. In this section we will take a brief overview what each chapter of this work will evolve.

To begin with we have introduced fundamentals of liquid crystals, their types and their basic physical properties. We have been working mainly with thermotropic liquid crystals; hence we have restricted our attention on this type and its sub-types only. Again each of the sub-type mentioned has peculiar physical properties of its own; however, we have mentioned the ones we exploited further in this work.

The successive chapter takes into account of the existing alignment technologies. We have detailed the alignment technologies, which are later on exploited by the author in this work. Brief overview of the origin of the alignment and necessity of molecular alignment has been taken. The chapter especially focuses on the alignment using light. We have further discussed the alignment of different liquid crystals using photo-alignment. We propose basic applications purely based on photo-alignment technique. There is a brief account of the role of polymers in liquid crystal technology.

The third chapter focuses on various different applications based on mainly cholesteric liquid crystals but with other liquid crystals. Fabrication of Fabry-Perot using different techniques and also different alignment method has been realised. Tunability, switchability and also other reflective properties of cholesteric liquid crystals have been exploited to achieve the fabrication of cold cavities.

The fourth chapter deals with the alignment of ferroelectric liquid crystals and the problems arising in their alignment. There are certain kinds of defect which appear in these liquid crystals and these defects deteriorate the quality. We have proposed a novel technique to overcome such defects in these liquid crystals. We have introduced the role of liquid crystal in 3D cinema by detailing the fabrication of shutters required for active 3D glasses.

From then the research follows an interesting path of fabrication of waveguides in liquid crystal. This particular research describes yet another facet and adaptability of liquid crystals in a completely different domain. In order to build a waveguide in liquid crystal it was necessary to make a brief theoretical study on the waveguides. The reason for using liquid crystal for fabricating the waveguides rather than any other polymer and the presence of different phases of liquid crystal on the same substrate has been mentioned. We have utilized the presence of different phases of liquid crystal on the same substrate for making the separation of polarisations travelling in a waveguide. Another important use of polymer-liquid crystal pair has been mentioned.

The sixth chapter deals with the fabrication of waveguides in liquid crystals. The entire fabrication process was realised on silicon substrates. Part of the fabrication especially the etching experiments were carried out in CCLO, Lannion, France as the project was collaborative and they possess certain facilities that our laboratory does not have. Once the waveguides were fabricated it was necessary to inject light into the waveguide and analyse them for losses, more importantly for separation of polarisations. As one will find out that the later part of the experiments especially coupling of light in the waveguide and analysis for polarisation separation was not completed within the time limits of this document. However, those experiments are still going on and we are very optimistic that the objectives will be attained.

It can be seen that a liquid crystal technology is the soul of this work and all the applications mentioned revolve around it. In the final chapter we have drawn few conclusions of the work. We have also proposed few improvements, the scope and the potential for these amazing materials possess.

Chapter 1: Introduction to Liquid Crystals

1.1. Introduction to Liquid crystals

Liquid crystals, as the name suggests, are the materials which have a phase of matter which finds itself *in limbo!* The reason is simple as they possess properties that are in between the properties of liquid and that of crystalline solid i.e. they can flow like ordinary liquid but at the same time posses certain crystalline properties as orientational, positional order, optical, electrical and magnetic anisotropy etc [1].

There are two main types of liquid crystal phase: Thermotropic and lyotropic liquid crystals. In the former type of liquid crystals the phase sequence is dependent on applied temperature; while the latter type of liquid crystals the phase change is not only dependent on temperature but also the concentration of the solvent in which they are [2]. In this work we will be dealing with the former type of liquid crystals.

These thermotropic liquid crystals can be made using several organic materials whose molecules are normally highly anisotropic in shape like a rod or a disc [2]. All Liquid crystals phases posses long range orientational order [3]. These phases occur over defined range of temperature, pressure and concentration. The smectic phases posses both orientational and positional order.

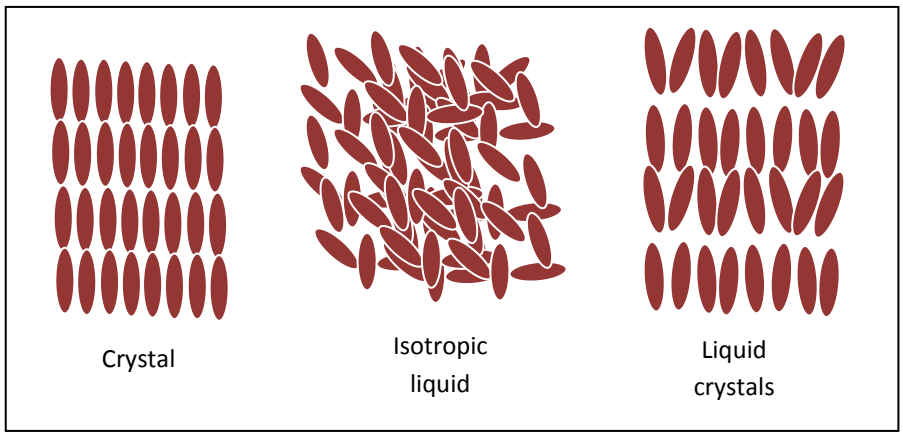

FIGURE 1- 1: PHASES OF MATTER

In this work we have realised applications based on each of these liquid crystals. We will now take overview of physical properties, their structure etc.

1.1.1 Nematic liquid crystals

These are the most widely used liquid crystals and the most common type of liquid crystals. The word “nema” comes from Greek which is known as “thread” because of the topological

defects which look like the threads. The structure of the nematic liquid crystal is very similar to the one shown in Figure 1- 2. These are made up of rod-like molecules which possess no positional order but they do tend to point in certain direction [4]. This direction is generally called as the director **n**. These are known as the uniaxial liquid crystal. In figure below n denotes the direction of the molecules.

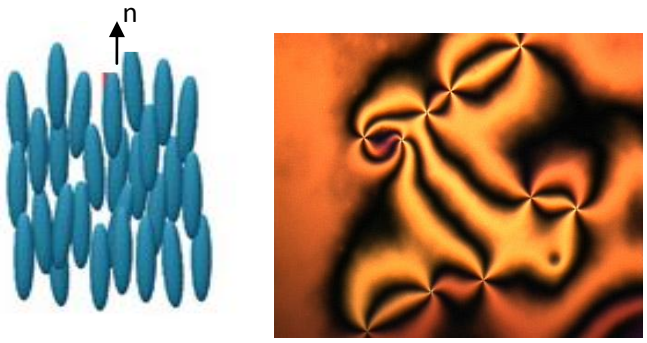

FIGURE 1- 2: NEMATIC LIQUID CRYSTAL

There is another type of nematic liquid crystals which are called chiral nematics. We will discuss in the section under the cholesteric liquid crystals.

Spatial deformation of the director is associated to an amount of elastic free energy. The free energy density can be resumed by the formula developed by Frank:

$$F = \frac{1}{2}K_1(\nabla.\vec{n}) + \frac{1}{2}K_2(\vec{n}.\nabla \times \vec{n}) + \frac{1}{2}K_3(\vec{n} \times \nabla \times \vec{n}) \quad \textbf{(1- 1)}$$

The first term correspond to the splay deformation, the second to the twist deformation and the third the bend deformation.

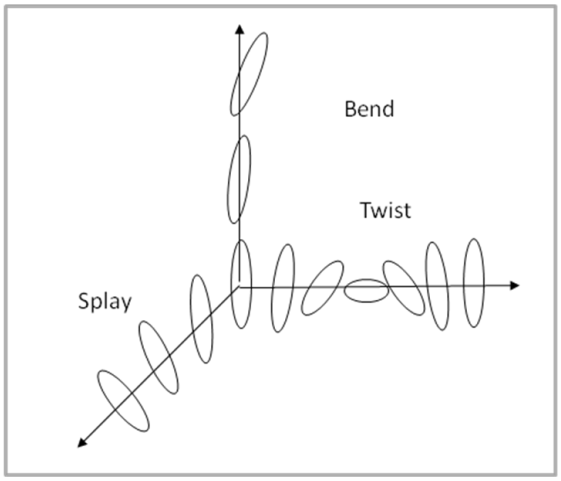

FIGURE 1- 3: SPLAY, TWIST AND BEND DEFORMATION

1.1.2 Cholesteric liquid crystals

These are the oldest forms of liquid crystalline phases. The name cholesteric comes from the "cholesterol" because when Austrian botanist Freidrich Reinitzer was looking at the cholesterol extracts from carrot he found that the compound exhibits *two* melting points and it showed some dramatic colour changes at different temperature. They were at that time called as the *flowing crystals* [5]. That is why these liquid crystals are known as cholesterics.

In case of cholesteric liquid crystal the director has a helical structure. The length of the helical period is called as pitch and this pitch can be from several nanometres to several microns covering wide range spectrum. These types of liquid crystals can be also known as the chiral nematics as the chiral dopant can vary the pitch for desired wavelength. These liquid crystals possess some remarkable structural properties which lead to some optical functions and we have tried to exploit these properties in our work.

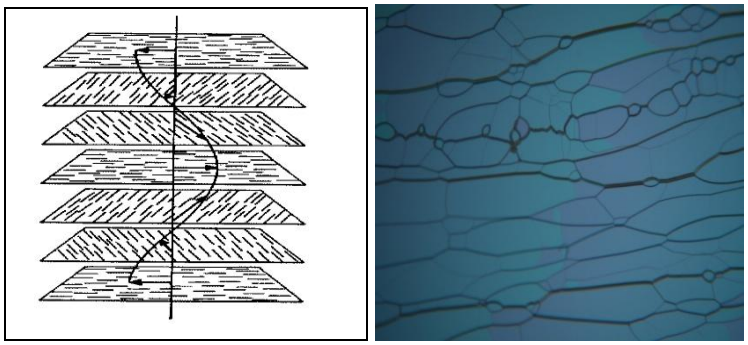

FIGURE 1- 4: CHOLESTERIC LIQUID CRYSTALS. THE LINES IN THE PICTURE ARE TYPICAL CHOLESTERIC DEFECTS (OILY STREAKS). THE PHOTO WAS TAKEN USING 10X MAGNIFICATION OBJECTIVE

In the above diagram we can see the cholesteric structure. It can be observed that the director is in a plan perpendicular to the helix axis and it winds to make a complete 360° rotation.

1.1.3 Smectic Liquid Crystals

The name smectic is derived from the Greek word for soap. Because they appear like the thick and often slippery found after washing using soap. These liquid crystals can be considered as the solid like nematics. Molecules of these liquid crystal not only point themselves along the director but also possess a positional order i.e. molecules of these liquid crystals align themselves in planes or layers as shown in figure below.

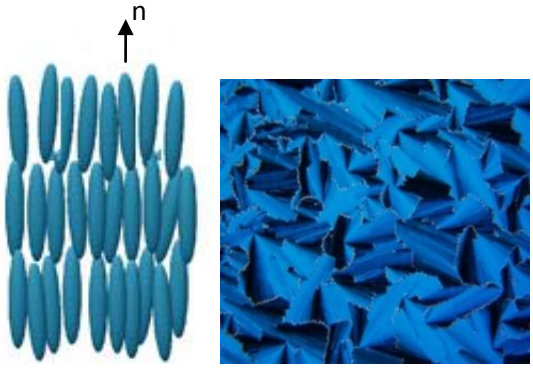

FIGURE 1- 5: SMECTIC LIQUID CRYSTALS. THE IMAGE WAS TAKEN WITH 10X MAGNIFICATION OBJECTIVE

There are several different types of smectic phases; there are as many as 12 different ones that are identified. Smectic A and Smectic C are the most used. In case of smectic C phase, the director is making an angle with respect to the layers normal while smectic A phase the director is along the normal of the layers. In the smectic C phase the director can rotate on a cone. Figure 1- 5 shows the appearance of Smectic C phase under the polarising microscope.

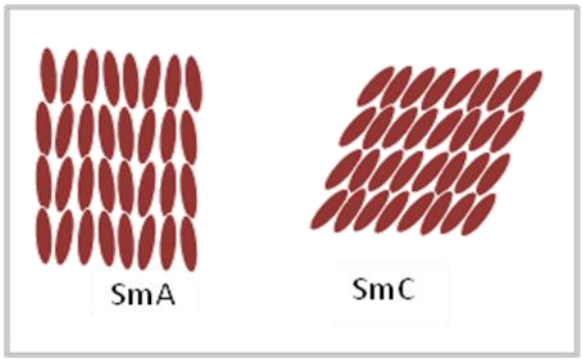

FIGURE 1- 6: SMECTIC PHASES

There is another type of smectic C phase which is known as Smectic C* or chiral smectics. The C_2 point group symmetry of this mesophase is compatible with the existence of a spontaneous polarization P_s perpendicular to the tilt plan. In case of chiral smectic phase as shown in Figure 1- 7, the orientation of the director has a helical distribution with respect to Z-axis. The pitch is defined as the distance when the similar molecular orientation is retraced. This tilt angle induces a spontaneous polarisation perpendicular to the plan defined by the director and the normal to the layers. The SmC* is locally a ferroelectric mesophase. Azimuthal angle ϕ can be defined using the projection of the molecule in X-Y plane.

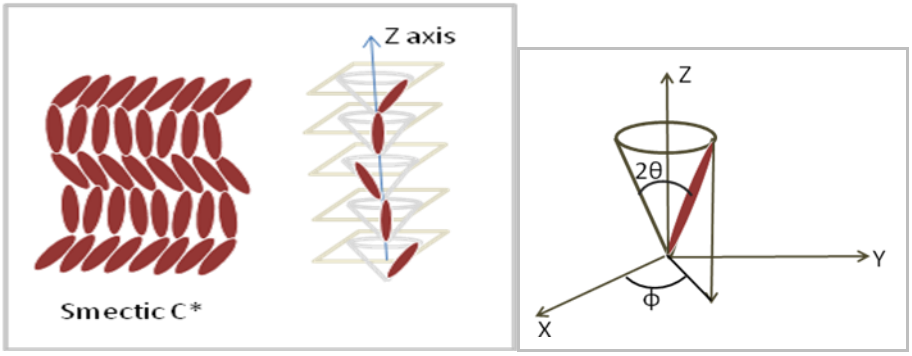

FIGURE 1- 7: SMECTIC C* AND TILT ANGLE OF THE SMECTIC LIQUID CRYSTALS

Application of electric field changes the direction of the director as shown in Figure 1- 8. The SmC* helix can be unwound by confining the liquid crystal in cell with small thickness, typically few micron (Clark-Lagerwall structure) [6]. This structure, known as bookshelf geometry, allows the switching of the director through the ferroelectric coupling torque: $P_s.E\sin\phi$. When the electric field is applied and upon reversing the direction of the field the director orientation reverses. The half of the angle between these two stable states is two times the tilt angle.

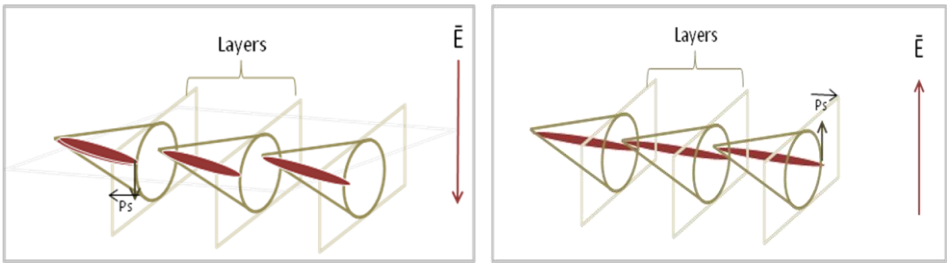

FIGURE 1- 8: THE SWITCHING OF THE MOLECULES

The smectic layers in confined geometry have a chevron structure. This structure results from the layer shrinkage observed in SmC due to the tilt of the director. With a strong surface anchoring a uniform layers displacement along the z direction is impossible. The only way is a tilt of the smectic layer in chevron-like structure. Two orientations of the chevron tilt are possible those who induce defects lines between domains with opposite chevrons [7] [8]

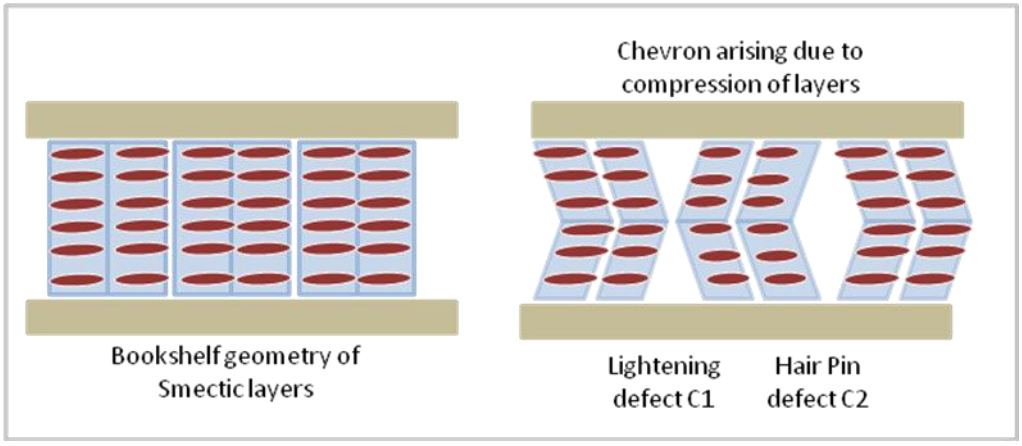

FIGURE 1- 9: COMPRESSION OF LAYERS IN A SURFACE STABILISED CELL

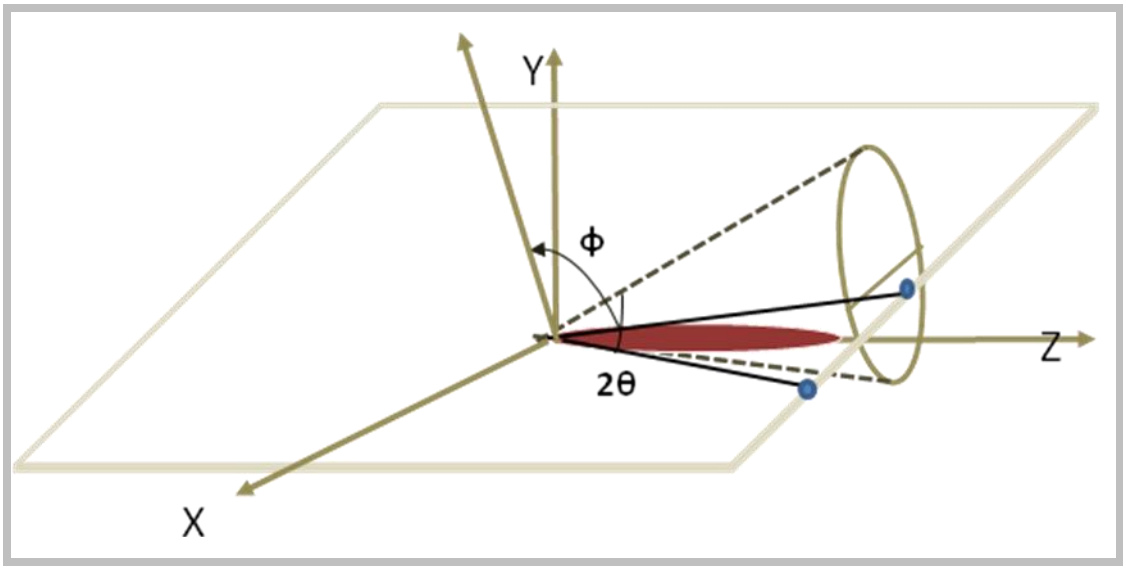

FIGURE 1- 10: EFFECTIVE TILT ANGLE IN A SSFLC CELL

Above figure represents Φ as the effective tilt angle surface stabilised ferroelectric liquid crystal cell. This tilt angle appears because compression of the smectic layers in cell geometry.

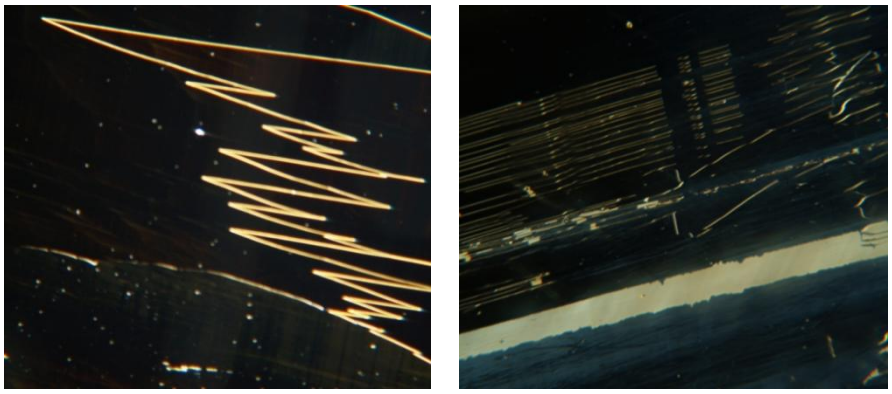

FIGURE 1- 11: LIGHTENING AND HAIR PIN DEFECTS 10X OBJECTIVE WITH FELIX 015/100 (CLARIANT)

The above photos were taken in the laboratory. In above figures one can see how the zigzag defects in smectic liquid crystal look like. The formation of C1 or C2 defect depends upon the surface treatment given to the surfaces and also the *pretilt angle* of the liquid crystal [7].

1.2 Optical Anisotropy

Another important intrinsic property of liquid crystal is optical anisotropy. These materials have two different refractive indices n_o and n_e; n_o is the ordinary refractive index i.e. the electric field vibrates perpendicular optical axis (director) while n_e is the extra-ordinary refractive index where the electric field vibrates parallel to optical axis [9]. The difference between these two indices of refraction is called as birefringence. Birefringence in liquid crystals is temperature (and wavelength) dependent: Increasing temperature causes a reduction of the birefringence until the liquid crystal passes liquid crystal-isotropic transition.

The birefringence property is intensively used to transform light polarisation: A polarised light wave when it enters the liquid crystals it splits into ordinary and extra-ordinary waves and they emerge from the material with a phase shift. The output polarisation is different from the input polarisation. Modifying the birefringence properties can be done by applying electric field on the material. This polarisation transformation combined with an output polariser allows light amplitude modulation. The optical phase retardation in the liquid crystal with thickness *d,* and birefringence Δn is given by,

$$\delta = \frac{2\pi \Delta n d}{\lambda_0} \qquad \textbf{(1- 2)}$$

Where, λ_0 is the wavelength of light in vacuum. Since birefringence is temperature and wavelength dependent the optical retardation also depends upon these two parameters.

1.3 Dielectric Anisotropy

Dielectric properties of the liquid crystals are related to the response of the liquid crystal molecules upon application of electric field. We have seen that the nematic and smectic have orientational order; hence these liquid crystals possess uniaxial symmetry. SmC has a symmetry which allows biaxial properties, but generally this mesophase is approximated to uniaxial material.

In a dielectric material an electric field E induces electric polarisation P and is given as,

$$P = \varepsilon_0 \vec{\chi} E \tag{1-3}$$

$\vec{\chi}$ is the electric susceptibility tensor.
The electric displacement is given by,

$$D = \vec{\varepsilon} E = \varepsilon_0 E + P \tag{1-4}$$

Where, E is the electric field, ε_0 permittivity of free space, P is polarisation and $\vec{\varepsilon}$ is the dielectric tensor since we are dealing with anisotropic media. The dielectric tensor is given as,

$$\vec{\varepsilon} = \varepsilon_0 (1 + \vec{\chi}) \tag{1-5}$$

$\vec{\varepsilon}$ for uniaxial (nematic and smectic A) and biaxial (Smectic C) are given as,

$$\vec{\varepsilon} = \underbrace{\begin{pmatrix} \varepsilon_\perp & 0 & 0 \\ 0 & \varepsilon_\perp & 0 \\ 0 & 0 & \varepsilon_\parallel \end{pmatrix}}_{\text{Uniaxial liquid crystal}}, \quad \vec{\varepsilon} = \underbrace{\begin{pmatrix} \varepsilon_1 & 0 & 0 \\ 0 & \varepsilon_2 & 0 \\ 0 & 0 & \varepsilon_3 \end{pmatrix}}_{\text{Biaxial liquid crystal}} \tag{1-6}$$

Where, $\varepsilon_\perp$ and $\varepsilon_\parallel$ are perpendicular and parallel components of dielectric constants, ε_i is the components of dielectric constants associated with all three axes.
The difference between these two dielectric constants is known as dielectric anisotropy and can be given as,

$$\Delta\varepsilon = \varepsilon_\parallel - \varepsilon_\perp \tag{1-7}$$

The dielectric anisotropy can be either positive or negative.

1.4 Liquid Crystal Switching

In this section we will detail the behaviour of liquid crystal director with different structures with respect to applied electric field.

1.4.1 Dielectric Coupling

When electric field is applied on the liquid crystal molecule with positive anisotropy ($\Delta\varepsilon>0$) it tends to align itself along the direction or parallel to the electric field. While in case of liquid crystal molecule with negative dielectric anisotropy ($\Delta\varepsilon<0$) it tends to align itself perpendicular to the direction of the electric field. The index of refraction is larger along the long axis of the molecules. The optical and dielectric anisotropies of liquid crystals enable the index of refraction to be controlled electrically, which is the underlying basis for many liquid crystal display applications.

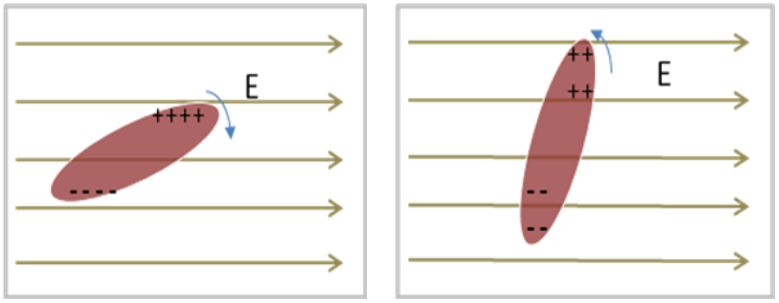

Figure 1- 12: RESPONSE TO ELECTRIC FIELD BY POSITIVE AND NEGATIVE ANISOTROPIC LIQUID CRYSTAL

1.4.2 Nematic and Cholesteric switching

The dielectric torque govern the reorientation mechanism of both nematic and cholesteric liquid crystal. The dielectric torque is balanced by the elastic energy torque within the liquid crystal and a progressive reorientation is observed increasing the electric field magnitude.

The refractive index of the liquid crystal starts to decrease with the electric field is applied to their molecules i.e. the birefringence value starts to reduce with application of electric field.

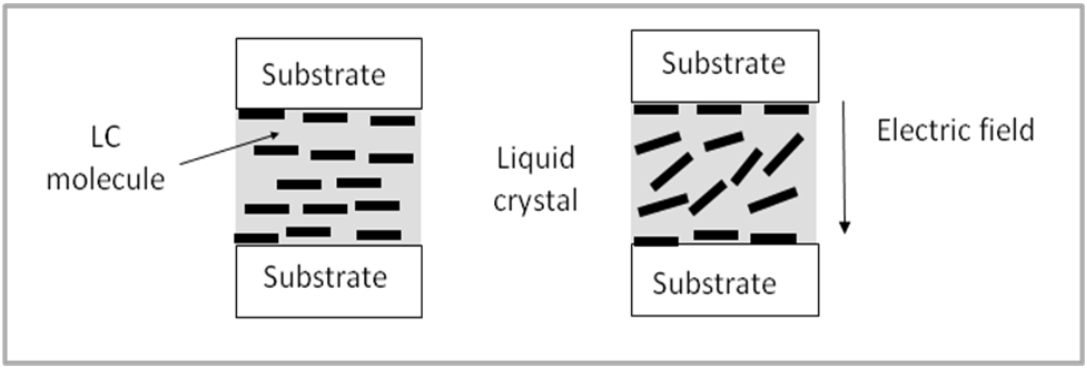

Figure 1- 13: REORIENTATION OF NEMATIC LIQUID CRYSTAL WITH ELECTRIC FIELD (FREDERICSZ TRANSITION)

There is critical field before which the director is not sensitive, but this critical electric field value is crossed the director continue to orient themselves with respect to electric field. In a planar aligned nematic cell the molecules in bulk start to orient to homeotropic direction until the field is reached where the entire cell is homeotropically aligned. Homeotropic state if seen under the cross polarisers appears dark and hence the cell is switching from ON state to OFF state [10]. The critical electric field value is given by,

$$E_c = 2\pi/d\,(\pi K_1/\Delta\varepsilon)^{1/2} \qquad \textbf{(1- 8)}$$

Where, K_1 is the splay elastic constant, d is thickness of the liquid crystal and $\Delta\varepsilon$ is the dielectric anisotropy.

Response times for Nematic liquid crystal can be given as

$$\tau_{ON} = \frac{\eta_1 d^2}{\pi^2 k_{11}}\left(\frac{\Delta\varepsilon}{\pi^2 k_{11}}V^2 - 1\right)^{-1} \qquad \textbf{(1- 9)}$$

$$\tau_{OFF} = \frac{\eta_1 d^2}{\pi^2 k_{11}} \qquad \textbf{(1- 10)}$$

Where, d is the thickness of the liquid crystal, $\Delta\varepsilon$ is the dielectric anisotropy, k_{11} is the elastic constant associated with the splay, η_1 is the viscosity of the liquid crystal and V is the applied voltage.

Without applied electric field the structure is planar twisted. The electric field break the helix structure into scattering multi domains texture. Finally increasing the electric field magnitude a homeotropic nematic liquid crystal is obtained.

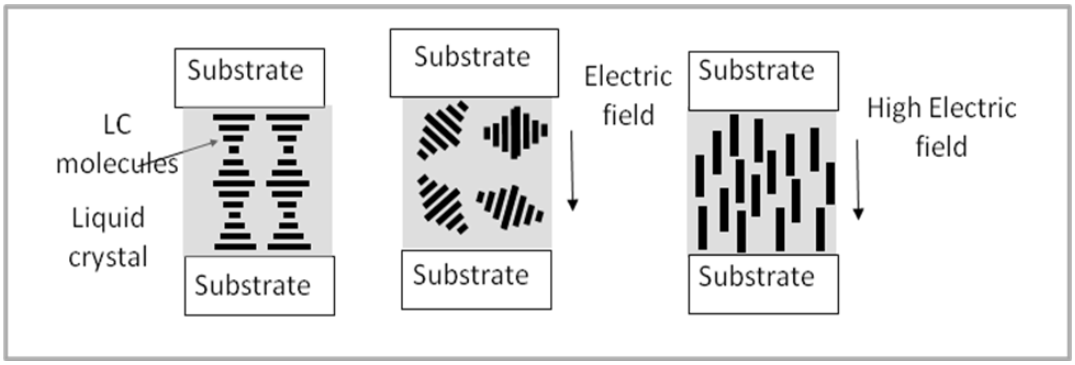

FIGURE 1- 14: REORIENTATION OF CHOLESTERIC LIQUID CRYSTAL WITH ELECTRIC FIELD: PLANAR TWISTED (WO ELECTRIC FIELD) TO FINGERPRINT STRUCTURE (W ELECTRIC FIELD) AND HOMEOTROPIC TEXTURE (W HIGH MAGNITUDE ELECTRIC FIELD)

1.4.3 Ferroelectric coupling

In case of smectic the switching of molecules is slightly different than nematics as these molecules switch between two stable states.

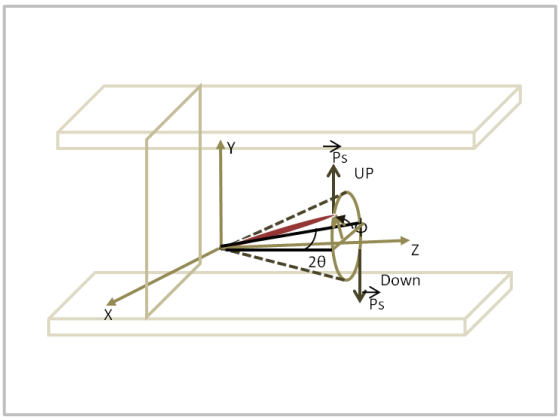

FIGURE 1- 15: SWITCHING IN SURFACE STABILISED (BOOKSHELF GEOMETRY) FERROELECTRIC LIQUID CRYSTALS

Taking the balance equation between ferroelectric torques and viscous torque, we obtain the response times for FLC, given by following equation.

$$\tau = \gamma_{\varphi}/PsE \qquad (1\text{-}11)$$

Where,

τ = the response time (s), γ_{φ}= Smectic rotational viscosity (mPa.s), Ps = Spontaneous Polarisation (C.m^{-2}, E = Applied electric field (V.m^{-1}).

1.5 Liquid crystal composite material: Polymer Stabilised Liquid Crystals and Polymer Dispersed Liquid Crystal

The role of polymer stabilisation is double: modify the electro-optic response of liquid crystal and increase the mechanical resilience of the material. For example using a nematic liquid crystal stabilised with a polymer network formed with mesogenic pre-polymer increase the relaxation speed. In the case of ferroelectric liquid crystal stabilisation induces monostable behaviour. These structures are obtained by mixing liquid crystal material with photo-curable mesogenic pre-polymer. The UV radiation induces a polymerisation and a phase separation and finally formation of a continuous liquid crystal structure stabilised by a polymer network [11] [12] [13]. There are several other composite liquid crystal structures. For example using a mixture of non-mesogenic pre-polymer and liquid crystal, polymer dispersed liquid crystals (PDLC) is obtained. These structures are sponge-like with liquid crystal droplets dispersion. Due to the isotropic property of the mixture, the liquid crystal is randomly oriented. These materials have light scattering modulation effect or pure phase shift modulation according the size of liquid crystal droplets that depends on both polymer concentration and kinetic of the polymerisation.

1.6 Potential Technologies of Liquid Crystals

The dielectric nature, the ability of the molecules to orient in any direction, selective reflection, response to electric and magnetic fields, optically anisotropic nature, large birefringence compared to any other crystal, ability to alter the birefringence with respect to applied electric and also with respect to temperature makes liquid crystals an attractive material in wide spectrum of applications. One of the biggest applications in the world is the fabrication of displays based on liquid crystals [14]. Market share of liquid crystals in the display industry has already overtaken the traditional cathode ray tube based displays and soon the latter will become redundant in display industry. As mentioned earlier change in the birefringence with respect to electric field and magnetic field has attracted lot of attention from the world of optical communications. Different types of liquid crystal present with different characteristics and by exploiting these characteristics one can think many applications. In case of chiral nematics or cholesterics, they reflect light depending upon the pitch which allows us many applications like tunable mirrors, colour sensors; also this pitch is temperature dependent this allows us to fabricate thermometers. Smectic liquid crystals are known for their ability switch fast and one can imagine several applications where one requires high speed switching (few tens of microseconds). Apart from these applications other applications like tunable filters, optical imaging, tunable lasers based on birefringence modulation of liquid crystals, failure analysis in

semiconductor industry, waveguides based on liquid crystals etc are few of the promising and upcoming frontiers of liquid crystal research [15-17].

Chapter 2: Textures and Alignment Techniques of Liquid Crystal

2.1 Introduction to Alignment of Liquid Crystals

One of the most critical aspects of the liquid crystal study is the orientation of these liquid crystalline molecules in a desired direction. Therefore, the study of alignment technologies is by far the most important and subtle feature of the liquid crystal research. The aim of this chapter is to analyse different alignment methods and also to study in particular the photo-alignment in detail. However, before discussing about the photo-alignment technique for aligning liquid crystals, it would be necessary to assess the need of alignment for liquid crystals.

Liquid crystals have not only become the backbone of the display applications but also they are capable of expanding their horizons to a wide spectrum of applications like telecommunications, diffractive optics, holograms, geometrical optics, etc [18] [19] [20]. The orientation of liquid crystal molecules in a desired direction is a prerequisite for many liquid crystal related applications. The groundwork for these numerous applications is an alignment layer deposited on a substrate, which induces an interaction between the substrate and the liquid crystal molecules eventually deciding the orientation of these molecules. This alignment layer is normally a polymer film deposited on a substrate using spin coating or some other means as dip-coating, spraying etc. It usually anchors these liquid crystal molecules either parallel (planar) or perpendicular (homeotropic) to the substrate. A specific treatment is then operated to induce the anisotropy (rubbing, anisotropic polymerization etc.). When the liquid crystal molecules come in contact with the anisotropic surface, the excess free energy of the molecules near the interface will be directionally dependent; the anisotropic part of this free surface energy induces an anchoring that tends to align the molecules in the same direction [21]. The parameters governing the anchoring energy are generally surface topology, the intermolecular forces like Van der Waal, polar and steric between the liquid-crystal-substrate interface [22]. Another important characteristic of the alignment layer is a generation of slight angle to the molecules of a liquid crystal near to the surface known as the pretilt angle. This means that the alignment layer not only exerts alignment in the azimuthal plane but also in the perpendicular direction. The energy supplied to the polymer chains near to the surface of the alignment layer is responsible for deciding the pretilt angle. It is possible to generate pretilts ranging from 0^0 to 90^0 making the alignment planar to homeotropic respectively.

2.1.1 Alignment by rubbing

The most widely used alignment technique is alignment by rubbing, which dates back to almost hundred years ago [23]. The mere idea and the execution of this technique make it such a remarkable alignment technique that till date it is still used in practice. By simply buffing the polymer film deposited on the substrate using a velvet cloth gives rise to alignment of liquid crystal molecules in the direction of buffing. Although the technique is so simple to align liquid crystal molecules, the parameters governing the orientation of the liquid crystal director are not yet lucid enough. There are mainly two explanations with two governing mechanisms. D.W. Berreman in his famous paper suggests that the rubbing of the polymer surface creates microscopic grooves on the polymer surface along the rubbing direction causing the molecules of liquid crystal aligning themselves along these periodic surface topologies [24]. In the molecular model of alignment first suggested by Castellano [25] and then by Geary *et al* [26], where they suggest that the rubbing causes a partial melting of few molecular layers of polymer films near the surface because of heat created due to friction and hence the alignment is *solely* due to the orientation of polymeric chains near the surface of alignment layer parallel to the applied shear field. This gives rise to the local anisotropy of the polymer film and liquid crystal molecules orient themselves accordingly. There are studies where they experimentally prove that the molecular model for alignment is responsible for the alignment [27]. There are studies from different groups suggesting that both these mechanisms play a pivotal part in the orientation of director of liquid crystals [28] [29] [30]. Irrespective of which governing mechanism, the alignment will originate from breaking of the symmetry at the surface of the polymer either macroscopically in case of Berreman model or microscopically in case of molecular model [31]. Like the parameters governing the rubbing mechanism, another important aspect about alignment by rubbing is generation of pretilt angles ranging from 0^0 to 90^0, is also ill understood [32]. Several groups have tried to elucidate the mechanism for generation of pretilt angle, which causes by interaction of polymers with liquid crystal [33], [34], [35]. Authors from [36] reported that the pretilt angle of the liquid crystal molecules on rubbed polymer film was determined by several factors associated with anchoring energy, mainly van der Waals forces, steric effect and electronic interaction.

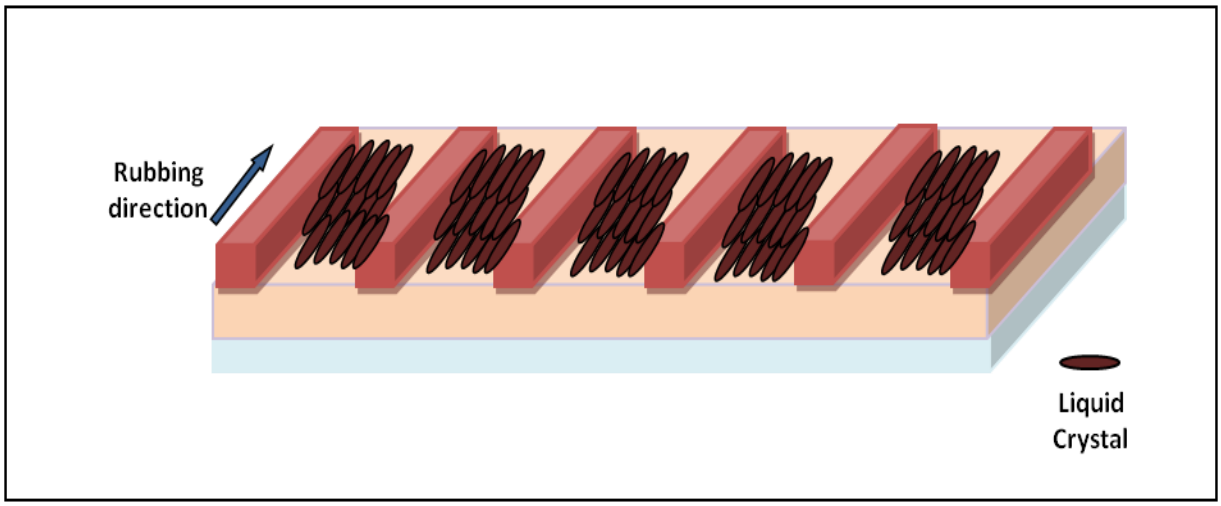

FIGURE 2- 1: BERREMAN MODEL OF ALIGNMENT BY RUBBING

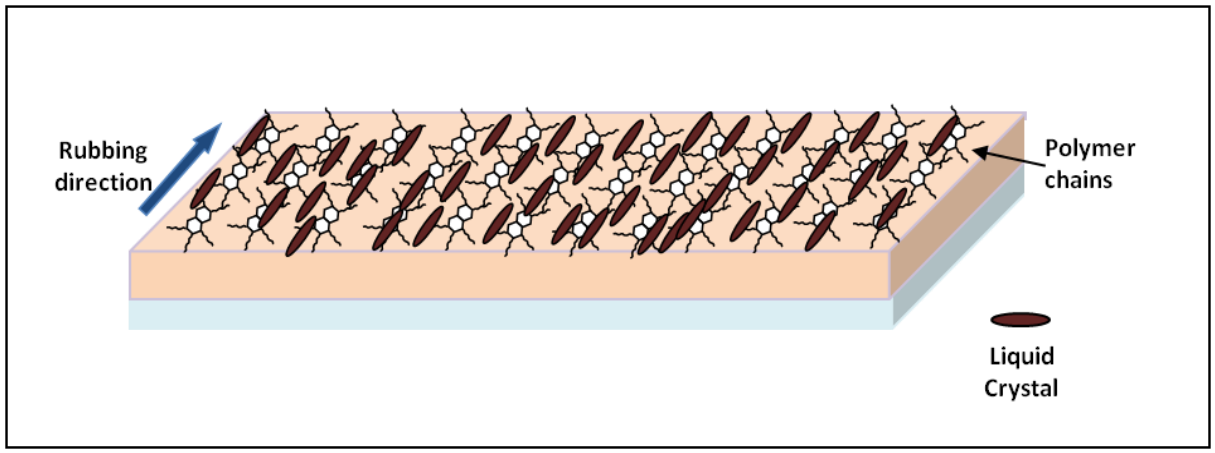

FIGURE 2- 2: MOLECULAR MODEL OF ALIGNMENT USING RUBBING

So far in this section we have been studying about the alignment by rubbing, now we will focus our attention on the execution of this technique for different liquid crystals. In liquid crystal studies, authors usually talk about the "cell", which comprises of two glass plates separated by few microns using glass rod spacers with a liquid crystal sandwiched between the glass substrates. Studies relating to these cells are normally orientation of liquid crystal inside them and the electro-optical response of the same. The former is the alignment technique and the latter we try to exploit for different applications. When nematic and cholesteric liquid crystals are filled at temperatures above isotropic temperature using a capillary effect in such a cell, which has been fabricated by using two rubbed polyimide substrates; then the molecules of these liquid crystals align themselves in the direction of rubbing. The only matter of detail while fabrication of the cell is that the direction of rubbing for each substrate should be in opposite direction as that of the other i.e. the cell is

fabricated in anti parallel fashion in order to have parallel alignment. Alignment of smectics on the other hand presents with some alignment difficulties and the molecular alignment for smectic liquid crystals and also novel method involved in the same has been addressed in coming sections. First, we will focus on the problems involved in alignment of smectic liquid crystals.

2.1.2 Other alignment techniques

Over the last few decades there are several alignment techniques have been extensively developed. This section will briefly address the mode of operation for these techniques. All techniques for the alignment result into an anisotropy of the alignment layer either physically and/or chemically. Here we will be mentioning few of the most relevant techniques. Apart from the techniques mentioned below there are various other techniques used for liquid crystal alignment; [12] takes brief overview of the existing technologies, their characteristics, the quality of alignment and their industrial feasibility.

2.1.2.1. Alignment by oblique evaporation of SiOx films

Liquid crystal alignment on the substrates can be controlled by the vacuum deposition of Silicon oxide films. The direction of the alignment is decided by the incident angle of the deposition [12]. Topology of the surface formed by the oblique evaporation is normally grooved like [37]. The magnitude of the anisotropy depends upon the angle of incidence between the surface of the substrate and the direction of evaporation, which shows that the direction of the liquid crystal director is a function of the same angle. From liquid crystal display the point of view the deposition of insulators like silicon oxides induces uniform alignment over patterned electrodes; they provide strong and stable alignment. Also, these inorganic films can sustain the temperatures up to 500°C [38]. Generation of pre-tilt angle starting from 0° to 85° can be precisely controlled using this technique. However, the cost of vacuum deposition technology and also because of lack of in plane uniformity of this technique makes industrial feasibility of it poor [32].

2.1.2.2. Micro-patterned polymers

This particular alignment method is made by photolithographically patterning the microgrooves on the polymer surface [32]. This mechanical process furnishes periodic topologies to the polymer surfaces giving rise to the physical anisotropy in the direction of the microgrooves. The principle of this alignment method follows closely the principle of Berreman's model for alignment by rubbing [24] of having periodic structures on the substrate. The periodic pattern is made by the master mould and it is further transferred

on the surface by stamping method. It is obvious that no re-orientation of polymer chains occurs and the alignment is solely due to grooved structure [39]. The liquid crystal molecules show fair long range order when confined to these microgrooves. Increase in the anchoring is observed with increase in the groove depth; however, it decreases with increasing the spatial period and the groove width [39].

2.1.2.3. Ion beam etching surfaces

There are two different approaches for achieving topological anisotropy using this technique; the first one being the bombardment of ion beam on to the substrate to form a film that can be used as an alignment layer and in the second method, bombardment of ion beam on to the already deposited film in order to achieve the alignment. Ion energy, the dose of ion bombardment and the angle of incidence are various parameters who govern the anchoring strength of the alignment layer. Pretilt angle is found to be function of ion beam incidence angle and the dose of the ion beam [40].

2.2 Introduction to Photo-alignment of Liquid Crystals

Anisotropic distribution of the alignment layer molecules by using the directional dependence of the polarisation of the incident light absorbed by these molecules is commonly known as photo-alignment. When an electric vector of the incident light wave is in concurrence with the transition moment of the molecule, the molecule strongly absorbs the light causing a photochemical reaction [12]. This particular process of aligning liquid crystal molecules is widely reckoned as a potential substitute to conventional alignment by rubbing as it possesses some obvious advantages as compared to its traditional counterpart. From the point of view of liquid crystal displays and also for other liquid crystal based devices, alignment due to traditional rubbing technique causes several problems; the quality of rubbing cloth degrades over the period of time due to repeated use causing the degradation in quality in alignment and also requires precise adjustment of the rubbing apparatus, rubbing traces reduce the contrast ratio, electro-static charges created due to friction damage the TFT based LCDs, alignment patterning within the individual pixel is not possible, since the pressure while rubbing varies on the elevated LCD substrate causing non uniform alignment and tilt angle discrepancies resulting in degradation of the grey scale; rubbing leaves debris on the substrate while the photo-alignment technique clean and dust free [32]. Moreover, rubbing technique is well suited to large substrate sizes and it is not at all suited for small components. To circumvent these problems photo-alignment has attracted strong interest because it is a contact free method, allows multi patterning with possible use of photo-masks, fine control over the pretilt and precise optical liquid crystal alignment. In 1988 Ichimura *et al* had reported for the first time isomerisation of azobenzene which

showed reversible photo-alignment [41]. In early 1990s two independent methods for photo-alignment were invented; first in 1991 Gibbons *et al* used azobenzene doped polyimide when exposed to linear polarised light aligns the liquid crystal molecules [42] and second in 1992 Schadt *et al* reported the photo-alignment using dimerisation of poly (vinyl cinnamate) exposed to linearly polarised UV light [22]. Photochemical reaction occurring during photo-alignment can be roughly categorised in two reactions *viz.* photoisomerisation and photodimerisation Gibbons *et al* used the former method whilst Schadt *et al* used the latter.

2.2.1 Photo-alignment using photoisomerisation

Photoisomerisation brings about a phase transition enabling the switching between two states with different molecular orientations. When a polarised ultraviolet light of appropriate wavelength is incident on the azobenzene dissolved in liquid crystal medium, azobenzene molecules experience *trans-cis* isomerisation, the dipole of the double bond aligns perpendicular to incident polarisation resulting in uniform alignment [43]. However, if the irradiation is continued the concentration of *cis* form will increase with time. The shape of *trans* form converts rapidly into the *cis* form and latter possessing more surface affinity rests near the cell walls. The combination of these two effects was used by Gibbons *et al* to demonstrate the first photo-alignment based LCD. Control over the pretilt angle can be achieved by making the exposure in two stages; first exposure aligns the liquid crystal molecule and in the second exposure by rotating the axis polarisation of polarised UV liquid crystal molecules will re-orient equal to the angle of rotation. Ichimura *et al* showed that the reversible change in the alignment i.e. the switching between homeotropic and homogeneous alignment can be achieved by perpendicularly aligning the azobenzene molecules in liquid crystal medium [41]. Successively, these molecules can be switched between different alignment states by using appropriate UV wavelengths. These azobenzene materials have the ability to switch the orientation of liquid crystal within the plane and therefore, they were called as the “command surfaces”. However, all the azobenzene based photo-alignment systems have one major shortcoming and that of the stability. Due to random *cis-trans* isomerisation and in-plane thermal motions lead to stability lasting from seconds to months [43] restraining the use of photo-alignment systems in liquid crystal applications.

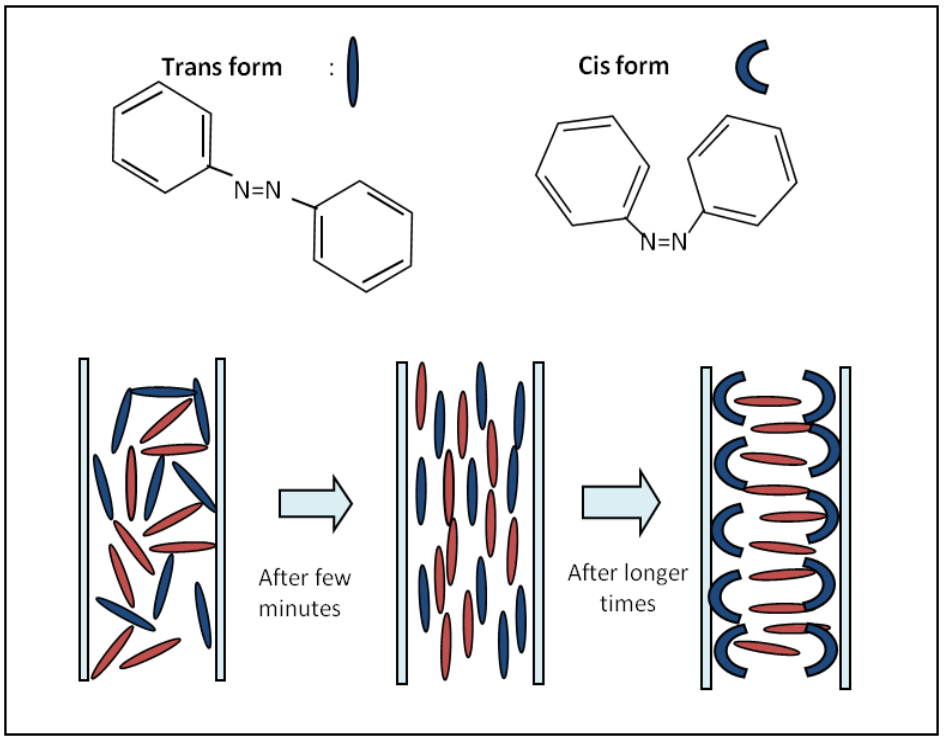

FIGURE 2- 3: PHOTOALIGNMENT OF LIQUID CRYSTAL USING GIBBONS METHOD

2.2.2 Photo-alignment using Photochemical Process

Since the process of aligning molecules using the azobenzene was not stable enough, one of the first substitutes for this method was use of molecules based on cinnamic acid. As these molecules are capable of not only undergoing the *cis-trans* and *trans-cis* isomerisation but also capable of undergoing (2+2) photocycloaddition reactions upon irradiation of UV light. Schadt *et al* proposed for the first time photo-alignment using poly (vinyl-*p*-methoxy-cinnamate) (PVCi); irradiation of polarised UV on spin coated PVCi provided the anchoring for liquid crystal molecules [22]. This paper turned out to be one of the milestones of the liquid crystal alignment research triggering the massive interest in the process and also in industrialisation of the same. Prior to the UV exposure PVCi molecules are isotropically distributed. When PVCi films are illuminated by linearly polarised UV light, different cross linking rates occur between the cinnamoyl side chains parallel to direction of polarisation and cinnamoyl side chains perpendicular to polarisation direction causing local anisotropy, which results in a linear dichroism and birefringence [44]. The choice of the UV wavelength is made on the basis of the absorption spectra of the PVCi; if the used wavelength lies in the absorption spectra then linear photopolymerisation of this wavelength will lead to optical anisotropies and homogeneous alignment. Unlike the photo-alignment using the azobenzene here the (2+2) cycloaddition method is more dominant than the *cis-trans* transitions [22], although the latter do take place during the

photochemical process. During the photopolymerisation double bonds parallel to the polarisation direction are broken, eventually getting reconnected and dimerised. There is no optical anisotropy before the UV irradiation; however, immediately after the polarised UV light is incident on PVCi, a weak anisotropy is observed, it increases rapidly with time saturating after certain UV dosage. Non dimerised side chains of PVCi have anisotropic shape giving rise to large refractive index along these chains (slow axis); thus, the slow axis of the photo exposed film lies perpendicular to polarisation indicating large population of these side chains. From the point of view of chemical structure of the PVCi there are three molecular entities, which play the important role in LC alignment. Cinnamoyl side chains, the cyclobutane photoderivatives and the hydrocarbon main chains [22]. The anisotropic interaction forces of these molecular entities lie in the same direction and hence it is considered to be responsible for the planar alignment of LC molecules [22]. This LPP alignment has advantage over the alignment using *cis-trans* isomerisation of being able to generate the linear alignment and also the pretilt in one exposure or simultaneously. Following figure shows the (2+2) cycloaddition reaction and also the direction of the molecular alignment. This process was later on industrialised by an enterprise called ROLIC, which produced photo-alignment materials for different optical devices. Two different products for aligning the liquid crystals were proposed. The first product was **L**inearly **P**hoto-polymerisable **P**olymer (LPP), which is an alignment layer which undergoes the exposure to linearly polarised light in order to boast optical anisotropy on the substrate. The second photo-alignment product was **L**iquid **C**rystal **P**re-polymer (LCP), is a liquid crystal-polymer solution used in combination with LPP to fabricate compensation films for various liquid crystal based applications. LCP is normally deposited on already photo-aligned LPP so that the molecules of liquid crystal align themselves with respect to anisotropy of the LPP layer. LPP layer possesses some useful properties from the point of view of liquid crystal applications; it has high photosensitivity, can generate high contrast ratio due to excellent orientation quality, high thermal and humidity stability, high pre-tilt angles in combination with LCP and can be patterned with high resolution (LPP datasheet from ROLIC). LCP also possesses properties like high thermal and humidity stability; it can withstand intense light intensities (LCP datasheet from ROLIC). The experiments mentioned in this chapter are performed using the combination LPP and LCP for few liquid crystal based applications.

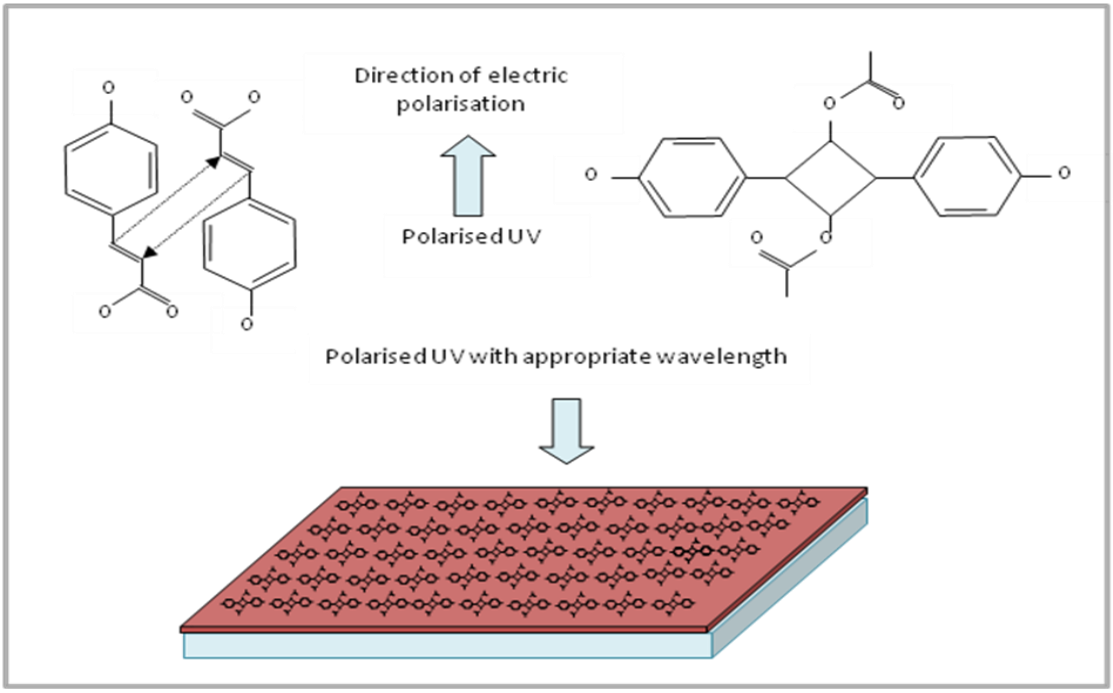

FIGURE 2- 4: (2+2) CYCLOADDITION OF AZOBENZENE MOLECULES

2.3 Photo-alignment of different liquid crystals

So far in this chapter we have been studying about the different alignment methods, now we will focus our attention on the execution of these techniques for different liquid crystals. As mentioned before in order to align the liquid crystals in desired direction we make use of the liquid crystal cells. In this section, first we will see alignment of nematic and cholesteric liquid crystal in such a cell. Applications based on photo-alignment are discussed in a separate chapter. Photo-alignment of smectic liquid crystal is also discussed in following sections.

2.3.1 Photo-alignment of Nematic Liquid Crystals

As mentioned above for the experiments involved in this section we have used the commercially available products LPP (ROP 103 – commercial name) and LCP (ROF -5102) from ROLIC for photo-alignment purposes. In order to prepare a well aligned nematic cell, we took two clean glass substrates. These two glass substrates were first coated by LPP at 3000 RPM for 60 seconds. The thickness of the LPP substrates was approximately 50 nm. They were later dried at 180^0 C for 5 minutes. Then they were separately exposed to linearly polarised light at energy of 1 J/cm^2 with a source of wavelength 300nm, the direction of electric polarisation was kept parallel to one of the sides of the substrate. LCP is manufactured for compensator films; hence at higher spin speeds also the thickness of

LCP film is few hundreds of nanometres. In order to provide sufficient anchoring energy to nematic liquid crystal molecules; LCP was diluted using the solvent cyclopentanon (same used by manufacturer for LCP) to as much as 3% of solid content (original solution is 25% of solid content). Technique of aligning the liquid crystals by fine liquid crystal film is similar to the technique proposed by Yaroshchuk *et al,* as it improves stability of the liquid crystal alignment [45]. This diluted solution was coated on the photo-aligned LPP substrates at 3000 RPM for 60 seconds. The newly coated substrates then underwent heat treatment *strictly* between 50-52 ^{0}C for 3 minutes to align the liquid crystal molecules in the direction of exposure. Then, they were polymerised using unpolarised UV light under nitrogen atmosphere with energy of 500mJ/cm^2. The thickness of LCP was approximately 100nms. Mixture of glue with glass rod spacers with appropriate thickness was prepared; the prepared substrates were glued using this mixture in *anti parallel* manner i.e. the polarisation directions in substrate one and substrate two were kept in opposite direction. Any commercially available nematic liquid crystal can be filled in this cell above isotropic temperature of the nematic liquid crystal. When cooled down planar alignment of nematic liquid crystal is obtained. It was observed if only LPP was used without further deposition of LCP, the alignment was homeotropic. It is worth noting that the norms for heat treatment for LCP must be followed in order to achieve perfect alignment. Pre-tilt angle adjustments can be done by exposing the LPP substrates in a slanting position rather than in horizontal. Please note that the pretilt angle is independent of slanting angle and it is only decided by adjusting the exposure energy (further details about pretilt angle generation can be found in LPP datasheet). Fabrication of twisted cells is possible by changing the angle of polarisation by appropriate value. Following diagram represents schematically the protocol for photo-alignment. UV filter is used during the first exposure in order to remove unwanted UV wavelengths. The anchoring energy to nematic liquid crystal molecules is provided by the LCP molecules as they themselves have undergone a planar alignment. The twisted nematic cells can be obtained by rotating the substrates only by 90° than by 180°. High contrast ratio can be observed as the extinction of light in OFF state is very good.

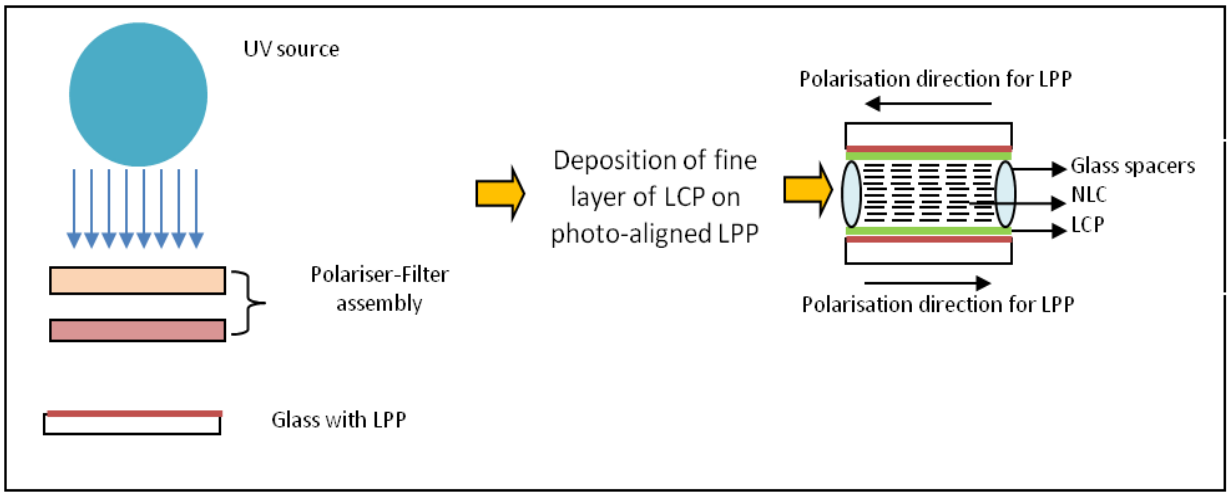

FIGURE 2- 5: PROTOCOL FOR ALIGNING THE NEMATIC LIQUID CRYSTALS

2.3.2 Photo-alignment of Cholesteric Liquid Crystal

Cholesteric liquid crystals can be considered as the layers of nematic liquid crystal in helical shape where the director in each layer traces out 360^0 with a finite pitch. Therefore, one can easily say that cholesteric liquid crystals have similar physical properties as that of nematics; moreover, it can be said that the nematics are special case of cholesteric liquid crystals with pitch value of the helix tending to infinity [1]. This peculiar helical structure gives rise to some interesting properties from propagation and reflection of light point of view. Since cholesteric liquid crystal and nematic liquid crystal have similar properties one can assume that the alignment techniques used for cholesterics are similar to those of nematics. Therefore, to align cholesterics we followed similar protocol like that for nematics in order to achieve homogeneous planar structure. Due to helical shape of the cholesterics light is either right or left circularly polarised depending on the handedness of the helix. Following photo is taken under microscope between two crossed polarisers; it represents the homogenous planar structure. The lines represent the defect lines or "oily streaks" peculiar to cholesterics, also it can be observed that the step like structure, which is due to the lack parallelism between the two substrates while fabricating the cell. The pitch of the cholesterics can be tailored by addition nematic liquid crystal i.e. addition of nematic can allow to increase the pitch to higher wavelengths. Later in this chapter we will try to exploit few of the structural properties of cholesterics and fabrication of an optical device based on these properties. The device is fabricated using the polymer stabilised cholesteric liquid crystal. Importance of adding a polymer and preparation of cholesteric mixture is also detailed in following sections.

FIGURE 2- 6: GRANDJEAN STRUCTURE IN CHOLESTERICS WITH OILY STREAKS

Photo-alignment of smectic liquid crystals is discussed in a separate chapter.

Chapter 3: Liquid crystal for wavelength selective devices

3.1 Devices based on choice of Alignment Technique

Previous chapter we have seen the alignment of different liquid crystals using different alignment techniques. Now, we will try to exploit those techniques to fabricate some devices. Here, we will be exploiting few of the interesting properties of the liquid crystals. As mentioned in the previous chapter the structure of cholesteric liquid crystals presents some interesting properties with respect to reflection of light. We will be discussing the fabrication of Bragg mirror using these structural properties of cholesterics. We will be also focussing on the fabrication of tunable Fabry-Perot using these Bragg mirrors. Tunability is based on the variation of the cholesteric pitch with respect to the applied electric voltage and the temperature. We have fabricated a tunable isotropic nematic cavity.

3.1.1 Light reflection based on Structural Properties of Cholesteric Liquid Crystals

The structure of cholesteric liquid crystals is characterized by a helix structure of the director. The helix axis is orthogonal to the director. The length of this helical period is called as pitch of the cholesterics. These liquid crystals have very attractive optical properties: The periodic structure of the director induces a periodic birefringence modulation and causes a selective reflection of a circularly polarised light. This structure offers continuous variation in dielectric tensor in a helical structure. When light beam is propagating along the helical axis Bragg reflection occurs in following wavelength range [46, 47],

$$n_o P \leq \lambda \leq n_e P \qquad (3\text{-}1)$$

Where P is the pitch of the cholesteric liquid crystal and n_o and n_e are ordinary and extra-ordinary indices of the liquid crystal. When a left circularly polarised light is incident on the right handed cholesteric liquid crystal it passes through without any reflection and vice versa. On the other hand, if left circularly polarised light is incident on left handed cholesteric liquid crystal it gets completely reflected. Exact solutions for normal incidence can be found in [47]. The circularly polarised light with same handedness as that of cholesteric is completely reflected. This reflection however, differs from the metallic or dielectric mirror reflection where the handedness is reversed but in case of cholesteric mirrors the handedness is preserved. The reflection band has a finite value and is function of optical anisotropy of the medium. The reflection coefficient versus wavelength is an even function with sharp cut-off and side-lobes. The spectral range is given by,

$$\Delta\lambda = \Delta nP \tag{3-2}$$

Where, Δn is optical anisotropy of the medium and P is the cholesteric pitch. The central wavelength of the Bragg reflection is given by,

$$\lambda_0 = \langle n \rangle P \tag{3-3}$$

Where, ‹n› is the average refractive index of cholesteric layers, P is the helical pitch length and Δn is the difference between the ordinary and the extraordinary refractive indices. There are number of assumptions which are taken into consideration before coming to above equations. The propagation of the wave is considered to be in along the helical path of the cholesteric liquid crystal. The helix is considered to be semi infinite with the border at the front plane and the reflection from the front plane is considered to be negligible. The optical anisotropy is considered small i.e. Δn is considered much smaller than the average refractive index of the cholesteric. Finally, wavevectors of incident light and cholesteric helix have the same amplitude.

The fabrication of the Bragg mirror was made by making a cell with cholesteric liquid crystal having a quarter waveplate deposited on one of the substrates of the cell. This quarter waveplate convert linear polarization into circular one. The cell was aligned by using photo-alignment technique and deposition of the quarter waveplate was also done by using the ROLIC LPP and LCP materials. The quarter waveplate served as an alignment layer on one side, while on the substrate a fine layer of diluted LCP on a photo-aligned LPP was deposited.

The Bragg mirror was realised by using pure cholesterics as well as using polymer stabilised cholesterics. Another important point of consideration is that the pitch of the cholesteric can be adjusted for different wavelengths and this can be done by using nematic liquid crystal as a dopant in order to vary the pitch length. Therefore, before proceeding with fabrication of the Bragg mirror we will show the preparation of “cholesteric mixture” and also the preparation of polymer stabilised cholesteric mixture.

3.1.1.1 Preparation of “Cholesteric Mixture” and Polymer Stabilised Cholesterics

We used a nematic liquid crystal to add to the cholesteric liquid crystal to get a pitch at appropriate wavelength in visible range. MDA-00-1445 from Merck was the cholesteric liquid crystal and MDA-00-1444 from Merck was the nematic liquid crystal involved in making of the mixture. The concentration giving reflection in visible range is: 80/20; MDA-00-1445 / MDA-00-1444. Different percentage of RM257 are tested (mesogenic polymer

from Merck) in the above cholesteric mixture in order to optimize both switching and optical reflection. The optical indices of this material are n_o=1.508, n_e=1.687. The melting and clearing points for RM257 are 66°C and 127°C, respectively and it has a very good miscibility with the host liquid crystal when mixed at higher temperatures. We added 0.1% of Igracure 651 photoinitiator to trigger the polymerisation reaction. The need for using polymer in the cholesteric reduces the defects like focal conics in the cholesteric structure. Improved response time is another advantage associated with the use of polymer which will justify later on in the article.

Similar fabrication procedure can be followed using polymer stabilised cholesteric liquid crystals with the PSCLC will be filled in the cell gap. The number of layers for having a good reflectivity was decided using the measurements performed earlier [48]; therefore we made a cell with 30 layers of cholesterics equivalent to 12 microns of cell thickness. When the plane polarised light within the stop band of cholesterics enters the cell through the quarter waveplate, the plane polarised light gets converted into the circular polarised light with handedness similar to cholesteric liquid crystals as the axis of quarter waveplate is adjusted so as to match the handedness of the cholesteric, which eventually reflects the circular mode completely conserving the handedness of the reflected mode. It was observed that the alignment of cholesteric was not perfect after filling the cell and hence we used the technique of shear alignment i.e. making slight displacement of the substrates after filling in opposite direction to remove the defect lines. It was observed that the defects did disappear after the shear alignment. If one has to displace the substrates slightly after the filling it means that the cell walls were not polymerised before filling. They were polymerised only after the defect lines were removed. The shear alignment was used only if the cell had many defect lines. The filling of the cell was made in nematic phase. The reason for not filling at isotropic phase was the photoinitiator may have triggered the polymerisation reaction at higher temperature and the liquid crystal would have got polymerised before completing the filling.

It was necessary to see the behaviour of the polymer stabilised cholesteric cells with respect to the applied electric field at different polymer concentrations. Therefore, we prepared PSCLC for 4 different polymer concentrations 1%, 3%, 5% and 10% of polymer (RM257) in pure cholesteric mixtures. It should be noted that the reflection band of the cholesteric Bragg mirror was still in the visible range. The fabrication of the cholesteric cell remains same mentioned in Figure 3-1. Based on the behaviour of these cells it was decided which concentration of polymer will be used for making the Fabry-Perot.

3.1.1.2 Fabrication of Bragg mirrors using Cholesterics

The mirror realised using cholesteric liquid crystals was made for wavelengths in visible range. It should be noted that the cell with cholesteric liquid crystal will behave as the Bragg mirror for the stop band of the cholesteric liquid crystal. Therefore, the reflectivity of the mirror will be the highest for the wavelengths in the stop band only, for other wavelengths the reflectivity will be very less, this particular property we have tried to exploit by making a Fabry-Perot at desired wavelengths. The reflectivity of the mirror depends not only upon the wavelength of incident light but also the polarisation of the incident light. Linearly polarised incident light will be converted into circularly polarised light of same handedness of that of cholesteric liquid crystal using quarter waveplate; this light will be ideally reflected with the reflectivity of 100%. However, this value is affected by transmission losses, scattering, the defect lines of cholesterics, etc.

The objectives are to characterize the optical properties of both the cholesteric liquid crystal and the quarter waveplate. This half-cavity is the first step toward the switchable Fabry-Perot Cavity. This structure is polarization sensitive as the input polarised light should enter at 45° with respect to the quarter waveplate. The reflection band is intrinsically restricted to the band gap of cholesteric structure but the quarter waveplate, , has an intrinsic sensitivity versus the wavelength. However, straightforward calculations indicate that waveplate sensitivity can be neglected: For 10% of optical intensity losses due to wavelength compression in polarization conversion, we obtain a ratio $\Delta\lambda / \lambda_0 \cong 0.4$ where λ_0 is the central wavelength giving the exact phase shift of 90°. For simplicity, we test our device in visible range knowing that shifted the device to the infrared range can be easily processed.

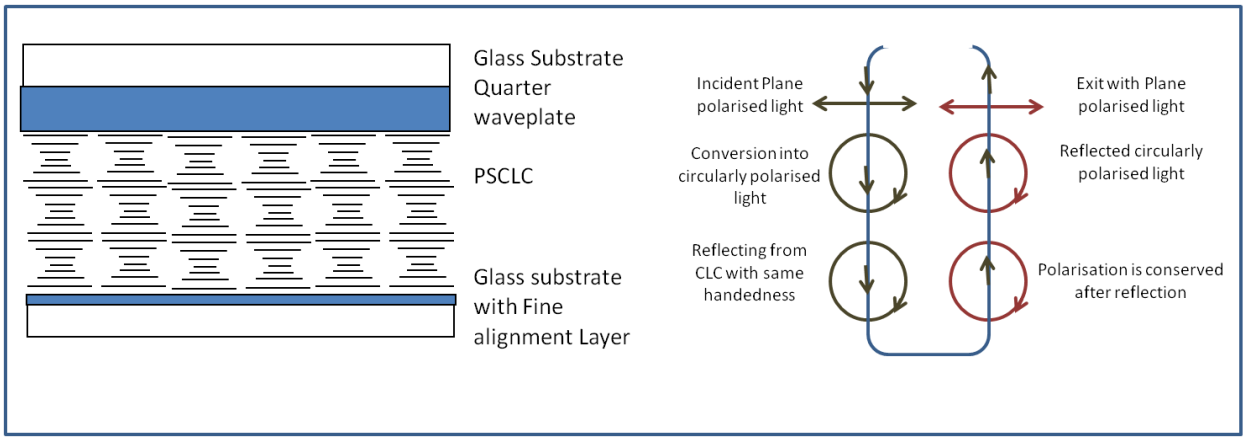

FIGURE 3- 1: FABRICATION OF BRAGG MIRRORS USING CHOLESTERIC LIQUID CRYSTALS

Above figure illustrates the fabrication of mirrors. One can notice the path of light with linearly polarised mode entering at 45° orientation with respect to quarter waveplate.

3.1.2 Fabrication of Quarter Waveplates

A waveplate is an optical component which alters the state of light polarisation. This alteration is normally the phase change between two perpendicular polarisation components of a light wave. In the case of quarter waveplate, the phase change is π/2. Quarter waveplate transforms the linearly polarised light into circularly polarised light and vice versa. This can be achieved by adjusting the neutral axis of the birefrigent material at 45° to the polarization axis of incident light. Reactive liquid crystals are intrinsically birefrigent material and are ideal to make such optical retarders. The combination of commercially available LPP and LCP from ROLIC is ideal for manufacturing such waveplates. The phase change is given by,

$$\Delta\varphi = \frac{2n}{\lambda}\Delta n \,.\, \mathbf{e} \qquad \textbf{(3- 4)}$$

Since the phase change (in this case it is π/2) is wavelength dependent and Δn i.e. the birefringence of liquid crystal used (in this case it is LCP with birefringence of **0.18**) for chosen products is also constant. Hence the thickness of the waveplate should be carefully chosen in order to observe the right phase shift. Quarter waveplates at wavelengths ranging from visible to infrared were realised by modifying the spin coating parameters for coating LCP. Similar procedure was followed to prepare photo-aligned LPP substrates, which served as the alignment layer for further LCP deposition. Following table represents the spin coating parameters and thickness of the LCP film at given wavelengths. For quarter waveplate at 1550nm the thickness of the LCP film required was quite high and it was difficult to attain that value in single spin coating as the homogeneity of the film was being hampered at lower RPMs. Therefore, this particular quarter waveplate was realised by making the two step spin coating, i.e. the first layer of LCP at higher speed was deposited and polymerised followed by second layer of LCP on the first layer was deposited allowing in increased thickness with homogeneity of film. The optical retardation of the fabricated films was measured by using the Berek compensator.

Wavelength nm	Thickness in microns	Compensator Reading in degrees
630	1.1	14.8
850	1.8	17.4
1330	2.5	21.6
1550	3.44	23.8

TABLE 3- 1: THICKNESS OF LCP FOR QUARTER WAVEPLATES AT DIFFERENT WAVELENGTHS

Above table shows the thickness values and retardation values for quarter waveplates at different wavelengths. We have successfully fabricated quarter waveplates for wavelengths from visible range to wavelengths in C band of optical communications. Hence one can fabricate the Bragg mirrors using cholesteric liquid crystals for different wavelengths.

3.1.3 Fundamentals of Fabry-Perot cavity

Conventional Fabry-Perot cavity consists of 2 partially reflecting mirrors with a dielectric medium in between them [49]. The fundamental application of such a cavity is fabrication of the laser with the gain medium in between these 2 partially reflecting mirrors. The transmission spectrum as a function of wavelength of such cavity exhibits transmission peaks at the resonant wavelength. This particular cavity is nothing but the interferometer where the reflecting beams interfere with each other. When the reflecting beams are out of phase they undergo destructive interference while when these beams interact each other in phase constructive interference takes place [50]. The transmission peaks are high for constructive interference, which is nothing but the condition of resonance.

Authors at this point do not intend into rigorous mathematical analysis of the Fabry-Perot cavity, however, we would like to give some fundamental and few important parameters which govern the behaviour of the Fabry-Perot. Let us therefore consider cavity using two mirrors with reflectivity R_1 and R_2 separated by distance d and index of refraction n; the phase after completion of one round trip in the Fabry-Perot cavity is given by;

$$\delta = \frac{4\pi nd}{\lambda} \qquad (3\text{- }5)$$

Where, λ is the wavelength of the light incident and incident angle is considered to be normal to the substrate. Another important property related with the Fabry-Perot cavity is free spectral range (FSR) which can be defined as the separation of the two maxima in the transmission function and it is given by;

$$FSR = \frac{\lambda_0^2}{2nd} \quad (3\text{-}6)$$

Where λ_0 is the central wavelength of Fabry-Perot cavity and n is the average refractive index of the cavity and d is the thickness of the cavity.

In our case one of the mirrors are made up of cholesteric liquid crystal based on the property of selective reflection of these liquid crystals. The other mirror is made up of Gold with high coefficient of reflectivity. The transmission function of the Fabry-Perot is given by;

$$T = \frac{1}{1+F\sin^2(\delta/2)} \quad (3\text{-}7)$$

Where F is the finesse of the Fabry-Perot cavity which is given by;

$$F = \frac{\pi(R_1R_2)^{1/4}}{(1-\sqrt{R_1R_2})} \quad (3\text{-}8)$$

Finesse is defined as the quantification of the shape of the transmission peak [51]. To obtain higher finesse it is necessary to improve the reflectivity of the Fabry-Perot mirrors. It should be noted that the above equations hold good for ideal Fabry-Perot. In real Fabry-Perot systems, finesse is dependent on number different parameters like the absorption losses in the cavity, the parallelism of the surfaces, the curvature of the mirror surface, the divergence of the incident beam and finally on any diffraction related effects occurring inside the cavity.

3.1.4 Principle of asymmetrical Fabry-Perot cavity

Conventional Fabry-Perot consists of two highly reflective mirrors separated by a medium having an optical index n. Here we have realised a Fabry-Perot using a cholesteric Bragg mirror and conventional metallic mirror. The idea of making the Fabry-Perot using Bragg mirrors using cholesteric liquid crystal was to use these liquid crystals as a means of tunable medium so that the cavity can be tuned or switched with respect to applied electric field or temperature.

Previously the fabrication of the symmetric Fabry-Perot cavity using cholesteric as Bragg mirror was made [52]; however in that particular Fabry-Perot they have made both the mirrors using the left handed cholesteric liquid crystals. These two mirrors are separated by an index matching fluid. Hence this structure worked as a Fabry-Perot structure only for the left circularly polarised light as an input.

The monolithic fabrication and the presence of quarter waveplate inside the cavity make it a novel technique of Fabry-Perot fabrication. We tried to achieve the tunability by testing both the temperature and also the electric field. The tunable medium in this Fabry-Perot was the Bragg mirror, which changes the reflectivity with respect to applied electric field and temperature as the pitch begins to unwind with increasing temperature while application of election field creates the focal conics and eventually structure reaches the homeotropic alignment. Hence for temperature the tunability should be seen towards higher wavelengths and for electric field the tunability should be seen towards smaller wavelengths. The cholesteric Bragg mirror had similar design mentioned in 3.1.1.2 with only difference is that the quarter waveplate was deposited on an isotropic region made of up polymer glue (NOA 63), which was deposited on the metallic mirror deposited on substrate with ITO electrode. Although, the gold mirror could have served as an electrode, we still used ITO electrode as gold is very brittle and can be scratched off easily. The quarter waveplate converted in a round-trip the circularly polarised modes into the other of same handedness as that of cholesteric.

3.1.5 Fabrication of Tunable Fabry Perot using photo-alignment

Gold mirror was deposited as a metallic mirror on one of the substrates. An isotropic region was added in order to have sufficient free spectral range in the cavity. Therefore, the Fabry-Perot was made in a cell filled with the polymer stabilised cholesteric liquid crystal. The filling of the cell was made in nematic phase. The technique of shear alignment was used if required. The defect lines will affect the reflectivity and also can cause the scattering of the light. Following diagram shows the schematic of the Fabry-Perot device.

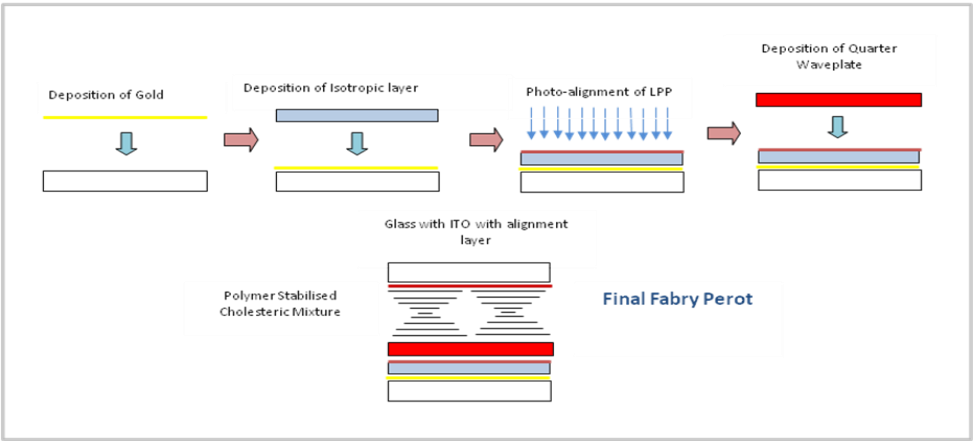

FIGURE 3- 2: TUNABLE FABRY-PEROT USING PHOTO-ALIGNMENT

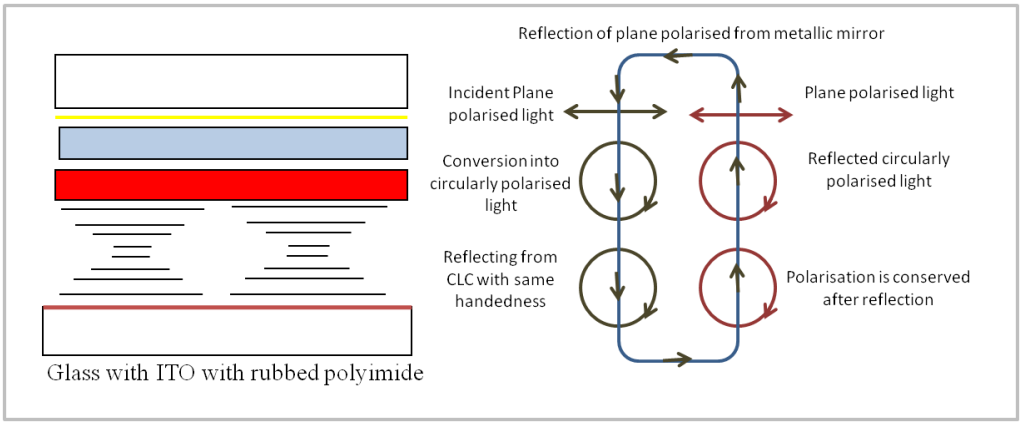

FIGURE 3- 3: TRAJECTORY OF A MODE INSIDE THE CAVITY

In the Figure 3- 2 one can see how the final Fabry Perot looks like. It can be easily noticed the asymmetric structure of it. The total thickness of the cell was approximately 20 microns, with cholesteric thickness of 12 microns. While in Figure 3- 3 one can see how the mode propagates inside the cavity with the polarisation alteration due to the quarter waveplate.

3.1.6 Fabry-Perot using traditional alignment method of rubbing

Metallic mirror:
The gold mirror deposition was the same as in 3.1.5 section with a reflectivity more than 90%.

Isotropic region:
NOA 63 from Norlands still served as the isotropic layer, which was used as another alignment layer. That is to say the polymerised NOA 63 layer was rubbed using a velvet cloth with similar anchoring parameters as that of the polyimide.

Alignment Layer:
The alignment layer on one of the substrates was the polyimide SUNEVER 410 from Nissan. The isotropic region served as an alignment layer for the deposition of the quarter waveplate.

Quarter Wave plate:
Another important observation from the point of view of fabrication is that the adhesion of RMS 03-001C is poor even on clean glass surface causing the dewetting of the coated film immediately after spin coating i.e. the film begins to shrink with increasing time. The dewetting is worse on polymer surfaces, in this case NOA 63 or polyimide. Therefore, to

improve the adhesion of the RMS 03-001C on the polymer surface we used plasma oxygen treatment to modify the surface of the polymer for few minutes so that the reactive mesogen film does not shrink before it is polymerised. The polymer surface was treated with plasma oxygen for 4 min to ensure the adhesion was good even at high temperature. The importance of maintaining the film quality even at high temperature was due to the fact that this particular reactive mesogen needs to go undergo heat treatment to remove any possible defects (thread like defects related to nematic liquid crystals), which are common to liquid crystal films. Therefore, most of the reactive mesogens undergo heat treatment to remove these defects. RMS 03-001C was kept at 60^0 C for 2-3 min so as to remove most of the defects. This particular reactive mesogen according to manufacturer's advice should be kept in $15\text{-}25^0$ (Refer Merck datasheet for this product); we had preserved it in a refrigerator to avoid any possible polymerisation and also any untimely exposure to UV light. Since the solution was at low temperature for long time, it had partially crystallised. Therefore, again according to manufacturer's advice the material was decrystallised at 50^0 C by constantly agitating it using magnetic agitator for couple of hours. The solution had become clear after this process was carried out; thereafter the solution was spin coated to verify the quality. It was observed that there were several anisotropic defects, which were not been able to remove even after the heat treatment. These defects were probably the small crystals which remained during the decrystallisation process. To overcome such defects we filtered the solution using 0.5 microns PTFE filters and subsequently coated the filtered solution. After this process, the observed density of defects is reduced but we failed to remove these defects entirely

Cholesteric liquid crystal layer

This layer was made by using the same mixture mentioned in 3.1.1.1 section.

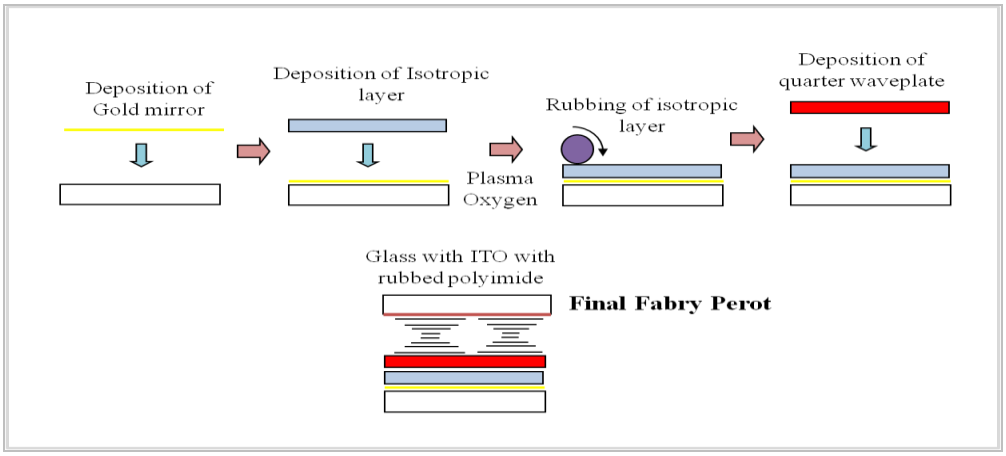

FIGURE 3- 4: FABRY-PEROT USING RMS-03-001C FOR QUARTER WAVEPLATE AND RUBBING AS AN ALIGNMENT METHOD

In Figure 3- 5 we can notice the thickness and the refractive index profile of each of the layer used in making the cavity. The thickness of the gold mirror is approximately 20 nm hence it is counted in cavity length.

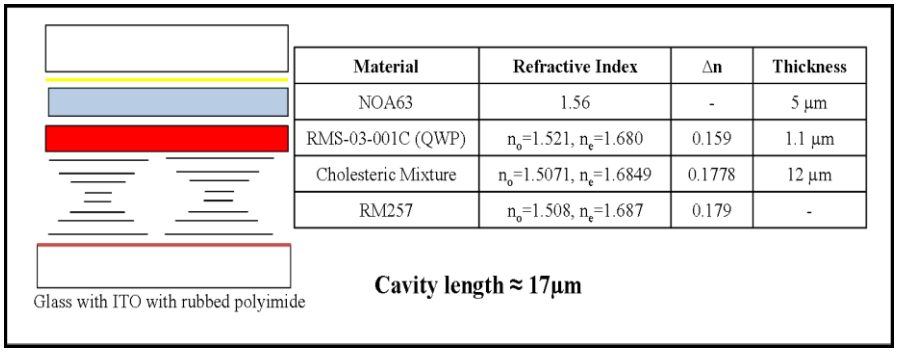

Material	Refractive Index	Δn	Thickness
NOA63	1.56	-	5 µm
RMS-03-001C (QWP)	n_o=1.521, n_e=1.680	0.159	1.1 µm
Cholesteric Mixture	n_o=1.5071, n_e=1.6849	0.1778	12 µm
RM257	n_o=1.508, n_e=1.687	0.179	-

FIGURE 3- 5: STRUCTURE AND REFRACTIVE INDEX PROFILE OF THE FABRY-PEROT

The stop band of cholesteric was still kept in the visible range. The idea of fabricating entirely using entirely new alignment methods and also few changes in the material was to show that such a monolithic fabrication can be achieved by different alignment methods as well. The experiment of tunability using the electric field was also attempted. The polymer concentration used was 10% in the previously mentioned cholesteric mixture.

3.1.5 Fabrication of Tunable Fabry-Perot using conducting polymer

The fabrication of this method was envisaged because the electric field applied was to entire cell and not just to the cholesteric stack. This fabrication method allowed the application of electric field only to the cholesteric stack. As one can see in the figure 3-2 the position of one of the electrodes is quite far from the cholesteric stack. Therefore, if at all the voltage is applied it will be applied over the entire and not just on the cholesteric stack causing the considerable reduction in the electric field on the cholesteric stack. Hence, we came up with another interesting idea of having displaceable electrode i.e. the position of the electrode can be adjusted according to the need. Therefore, we deposited the layer of conducting polymer on top of the quarter waveplate in order to apply the field exactly on cholesteric liquid crystal. Previously, compatibility of this polymer with liquid crystal was demonstrated [53]. Highly transparent electrode makes it interesting from the fabrication point of view. The structure of the cholesteric remains more or less except the presence of the conducting polymer on quarter waveplate.

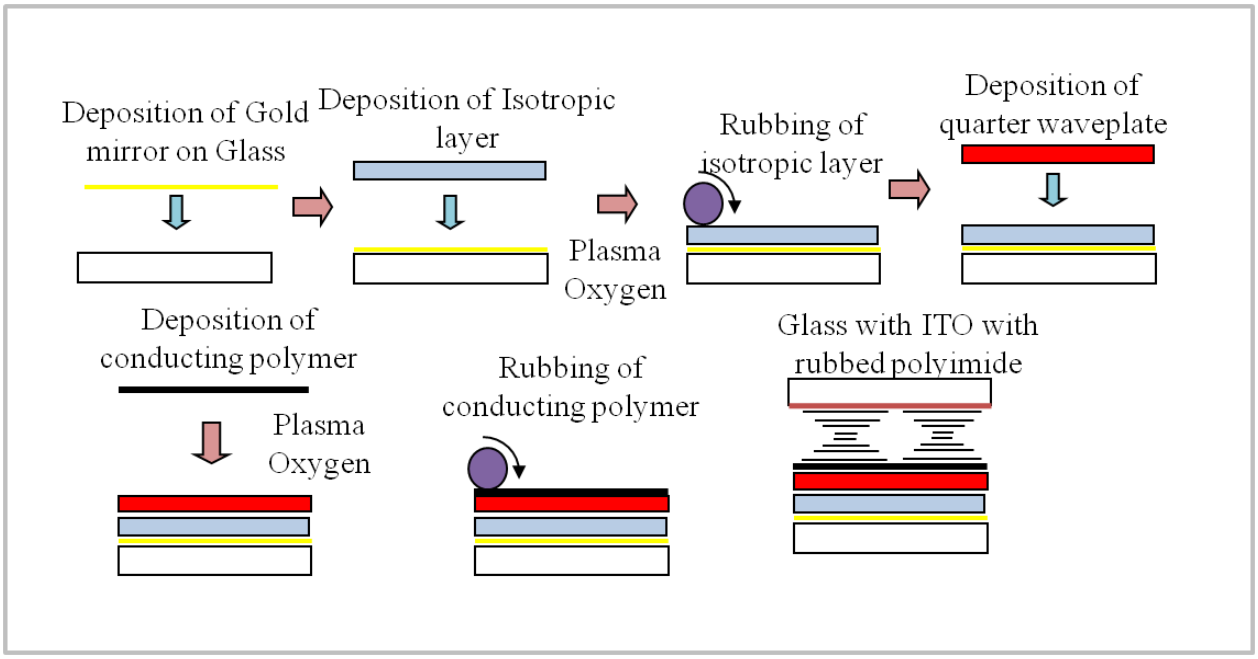

FIGURE 3- 6: TUNABLE FABRY-PEROT WITH CONDUCTING POLYMER

The above diagram explains the fabrication of the Fabry-Perot using conducting polymer. One can notice now that the electrode position gives the advantage of applying the electric field directly to cholesteric stack. Another important point of consideration is that the electrode with conducting polymer also serves as an alignment layer to the cholesteric stack. Rubbing of the electrode is sufficient to have good quality of alignment. The need of having plasma oxygen is to have the good quality of deposition for conducting polymer. We used Baytron PEDOT/PSS water based solution to make the conducting polymer film. This polymer is dissolved in water at 1-3% solution. This solution was then dissolved in 90-10% of Ethylene glycol. Then diluted PVA (polyvinyl alcohol) was added to this solution. The deposition of entire mixture was carried out 3000RPM during 30 seconds and then dried 120-130°C for 5 min to remove the excess solvent. Another important characteristic with this polymer is that the resistivity of the conducting layer can be modulated. The cholesteric mixture used was similar as the one mentioned in previous section. The cholesteric stack was polymer stabilised to have mechanical strength the mirror. The concentration of the polymer (RM257) used in the cholesteric mixture was 10%. The Fabry-Perot was made for the visible wavelengths.

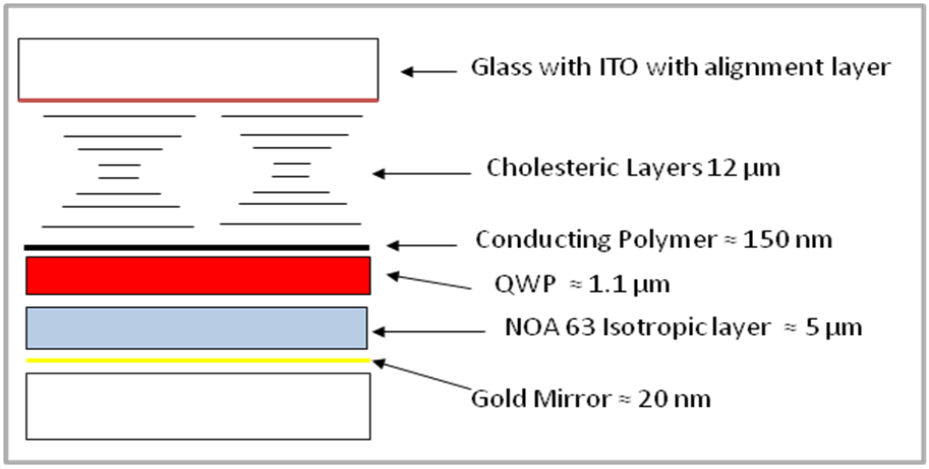

FIGURE 3- 7: FP WITH CONDUCTING POLYMER

Above diagram details the thickness profile and the structure of the Fabry-Perot with conducting polymer.

3.1.6 Fabrication of Isotropic Nematic Cavity

We also realised the fabrication of tunable isotropic nematic cavity. Previously, such cavity was successfully realised by [54, 55] It is well known that many devices in optical communication industry suffer from the problem of polarisation i.e. they are sensitive to input polarisation. The present Fabry-Perot offers the solution of being independent for input polarisation hence such cavity has many technological advantages. The Fabry-Perot cavity is isotropic because the output of the Fabry-Perot remains the same for any input linear polarisation state. We used the photo-alignment technique to make the cell. The fabrication is as follows. We took two glass substrates with ITO and we deposited a thin layer of gold on both these substrates, which are used as the mirrors in the Fabry-Perot design. On each of these two substrates we deposited quarter wave plates using ROLIC LPP and LCP products (the deposition of quarter waveplate is already mentioned in detail in previous chapter). The quarter waveplates make angle of 45° with respect to edge of the surface. Then, a layer of SiO_2 was deposited followed by the thin layer of LPP-LCP pair for nematic alignment. The SiO_2 gave the possibility to have the alignment of nematic liquid crystal filled in the cell at 45° with respect to the quarter waveplates i.e. the alignment was conventional anti parallel alignment. Following is the schematic diagram of the isotropic nematic cavity.

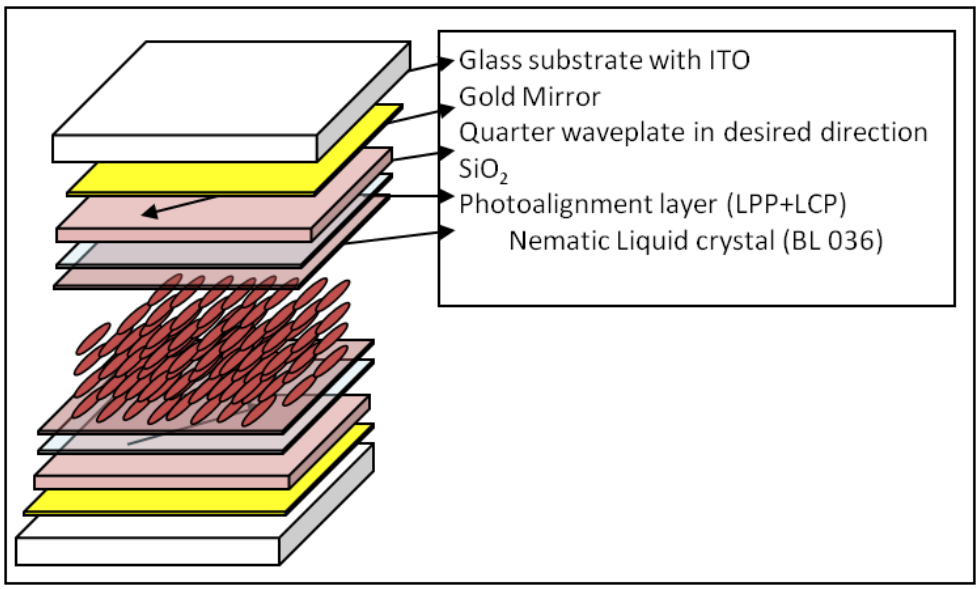

FIGURE 3- 8: ISOTROPIC NEMATIC CAVITY

Above diagram illustrates isotropic nematic cavity. The nematic liquid crystal filled inside the cell was BL036 with Δn of 0.22. The cell was made using 5 micrometer thick glass rod spacers

We will now justify the isotropic behaviour based on Jones' matrix form. Where, J_{tf} is the Jones matrix for 'to and fro' of the mode inside the cavity and X is a phase shift of π/2 due to quarter waveplate.

One Way Return

Mirror Quarter waveplate Nematic Quarter waveplate Mirror Quarter waveplate Nematic Quarter waveplate

$$J_{tf} = \begin{bmatrix}1 & 0\\ 0 & -1\end{bmatrix}\begin{bmatrix}\cos\frac{1}{2}X & i\sin\frac{1}{2}X\\ i\sin\frac{1}{2}X & \cos\frac{1}{2}X\end{bmatrix}\begin{bmatrix}e^{i\beta} & 0\\ 0 & e^{-i\beta}\end{bmatrix}\begin{bmatrix}\cos\frac{1}{2}X & -i\sin\frac{1}{2}X\\ -i\sin\frac{1}{2}X & \cos\frac{1}{2}X\end{bmatrix}\begin{bmatrix}1 & 0\\ 0 & -1\end{bmatrix}\begin{bmatrix}\cos\frac{1}{2}X & i\sin\frac{1}{2}X\\ i\sin\frac{1}{2}X & \cos\frac{1}{2}X\end{bmatrix}\begin{bmatrix}e^{i\beta} & 0\\ 0 & e^{-i\beta}\end{bmatrix}\begin{bmatrix}\cos\frac{1}{2}X & -i\sin\frac{1}{2}X\\ -i\sin\frac{1}{2}X & \cos\frac{1}{2}X\end{bmatrix}$$

$$J_{tf} = \begin{bmatrix}1 & 0\\ 0 & 1\end{bmatrix}e^{2i\beta} \qquad (3\text{- }9)$$

We have put the Jones matrix for individual component inside the cavity and the product comes out to be the singular matrix confirming the conservation of polarisation inside the cavity.

3.2 Results and Discussion for different devices: Mirror and Fabry-Perot Cavities

In this section we will discuss the results of the experiments discussed above. To begin with we will see the transmission spectrum of pure cholesteric mixture at few wavelengths. Then we will speak about the transmission spectrum of the polymer stabilised cholesteric liquid crystal sample. Transmission spectrum of the Fabry-Perot with metallic mirror and tunability with temperature and electric field of the same will be discussed later on. We will then move on the transmission spectrum of the Fabry Perot with dielectric mirror. Finally, the response time and contrast ratio for glasses for 3D cinema along with the scattering analysis from the point of view of spectators will be done.

3.2.1 Transmission spectrum based on polymer concentration

In order to measure the reflection of cholesteric stack we measured the transmission spectrum of the cholesteric cell with built-in quarter waveplate using a spectrometer. The input polarisation of the light was controlled at 45° with respect to the polarisation so that the linear modes will get converted into perfectly circular modes, failing to do so the linear modes will be converted into the elliptical modes and the reflection from the cholesteric liquid crystal will not be 100%. It should be noted that we measured the transmission spectrum and not the reflection spectrum; in order to get the reflection spectrum we assumed that the absorption of the light during recording the intensities is negligibly small and hence was neglected.

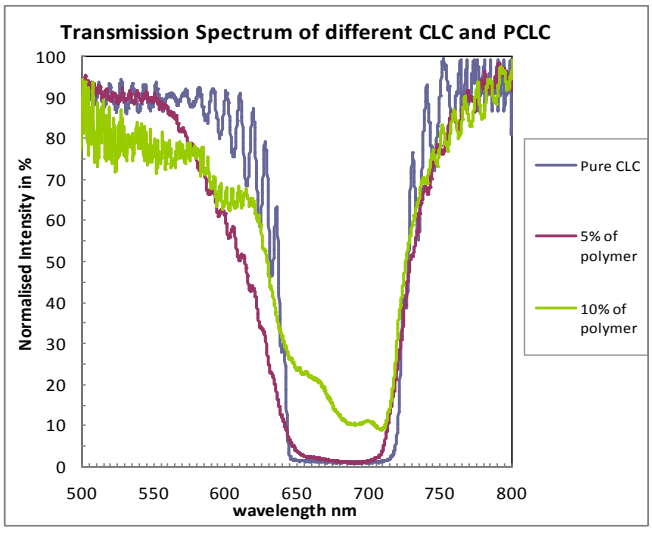

GRAPH 3- 1: TRANSMISSION SPECTRA FOR DIFFERENT POLYMER CONCENTRATIONS

The photonic bandgap of the cholesteric is also broadened in the polymer stabilised cholesterics. The Δn of the entire cell is modified by addition of polymer. The reflectivity is reduced as the polymer concentration is increased. The reflectivity of above 99% was observed using pure cholesteric mixture without any polymer. All the mixtures used in these measurements are same as mentioned in section 3.1.1.1**.** Detailed discussion about dependency of polymer on cholesteric liquid crystals can be found in [56]. It is obvious that the reflectivity and the quality of the mirror are much better in case of pure cholesteric Bragg mirror than with polymer stabilised cholesteric Bragg mirror. However, it would be advisable to verify the response with respect to the applied electric field for different polymer concentrations in order to decide which concentration would be ideal to fabricate a Fabry-Perot cavity.

3.2.2 Electric field dependence on Cholesteric Bragg mirror for different polymer concentrations

As discussed earlier we tested different polymer concentrations and their dependence on applied electric field. The behaviour of the Bragg mirrors using PSCLCs with respect to the applied electric field at different concentrations of polymer is shown in the following spectra. It was observed that polymer concentrations are below 5% are not enough to stabilise the cholesteric cell as after application of the electric field the helix was unwound; however, the cells failed to come back to original position. This clearly suggests that the polymer concentration is too low in order for the cell to come back to original position. It should be noted that the electric field values required to tune and eventually switch the pure CLC (0% polymer) Bragg mirror are small. Although the switching speeds are quite fast for cholesterics the relaxation time for pure CLC to come back in the planar orientation after removal of the electric field is extremely slow (See Table 3- 2 for more details). Improved relaxation speeds were observed for cholesteric mirrors with 5% and 10% of polymer but by increasing the electric field. We applied a bipolar square pulse with ON-OFF state. Table below indicates the switching behaviour of the cholesterics with different polymer concentrations.

Polymer Concentration %	Switching Speed µs	Relaxation Time	Voltage in Volts
0	400	>10 sec	10
5	350	50 ms	50
10	300	30 ms	100

TABLE 3- 2: SWITCHING AND RELAXATION TIMES FOR CHOLESTERICS WITH DIFFERENT POLYMER CONCENTRATIONS

The cholesteric mirror with 10% of polymer shows a poor reflectivity curve as compared to pure cholesterics, whereas the Bragg mirror with 5% of polymer seems to be good trade-off as it shows good reflectivity and also it sustains larger electric fields as compared to pure cholesterics. Moreover, the cholesteric mirror with 5% of polymer shows much better relaxation time than the pure CLC. Therefore, we built the Fabry-Perot using 5% of polymer.

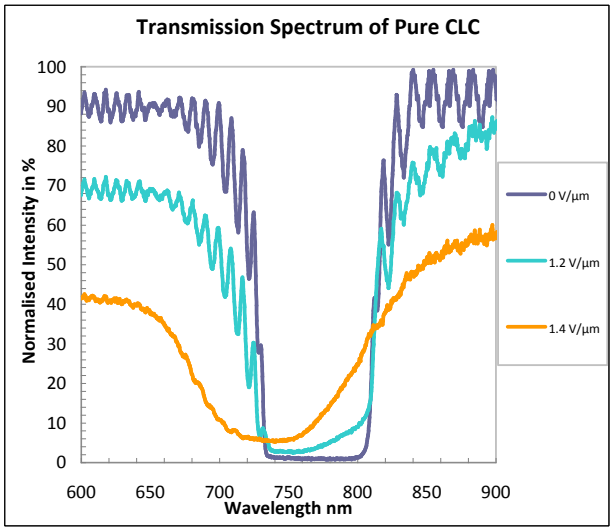

GRAPH 3- 2: ELECTRIC FIELD DEPENDENCE OF PURE CHOLESTERICS

Above graph clearly suggests that the electric field required for changing the planar alignment to focal conics and focal conics to homeotropic alignment. Therefore, we fabricated the Bragg mirrors at 5% and 10% of polymer concentration. Below are the graphs which represent the behaviour of the cholesteric cells for applied electric field for 5% and 10% of polymer concentration. The samples prepared for these analyses are prepared from the liquid crystals as mentioned in section 3.1.1.1. These samples contained the quarter waveplate and the input polarisation was adjusted to be 45° with respect to the quarter waveplate.

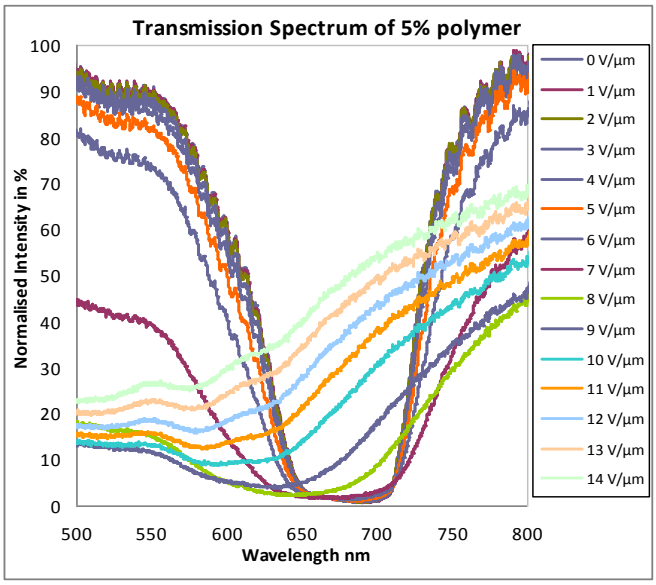

GRAPH 3- 3: TRANSMISSION SPECTRUM OF THE CHOLESTERIC BRAGG MIRROR WITH 5% OF RM257

Above graph suggests that there has been blue shift in the Bragg mirror as the electric field increases. This causes due to the focal conical structure appearing at higher electric fields. As the electric field increases the stop band completely disappears and the mirror has completely switched from being highly reflective to being transmissive. Therefore, it can be safely said that the Bragg mirror acts as a tunable and eventually switchable mirror for applied electric field. The switching speed is of the order of few milliseconds. Once the electric field is removed the mirror comes back to original state.

The maximum reflectivity of the cholesteric mirror is calculated from following formula

$$R = tanh^2\left(\frac{\Delta n \pi h}{\bar{n} p}\right) \qquad \textbf{(3- 10)}$$

Where, h is the thickness of the cholesteric stack, Δn is the birefringence of the liquid crystal, $\bar{n}$ is the average refractive index of the entire stack and p is the pitch of the cholesteric at 650 nm. By substituting the values for the cholesteric mixture mentioned in section 3.1.1.1 we obtain the reflectivity of **99.91%.** The values are Δn= 0.1778, h= 12µm, p=1µm, $\bar{n}$=1.59. It is proves that one can fabricate highly reflective mirrors for a given wavelength using cholesteric liquid crystals.

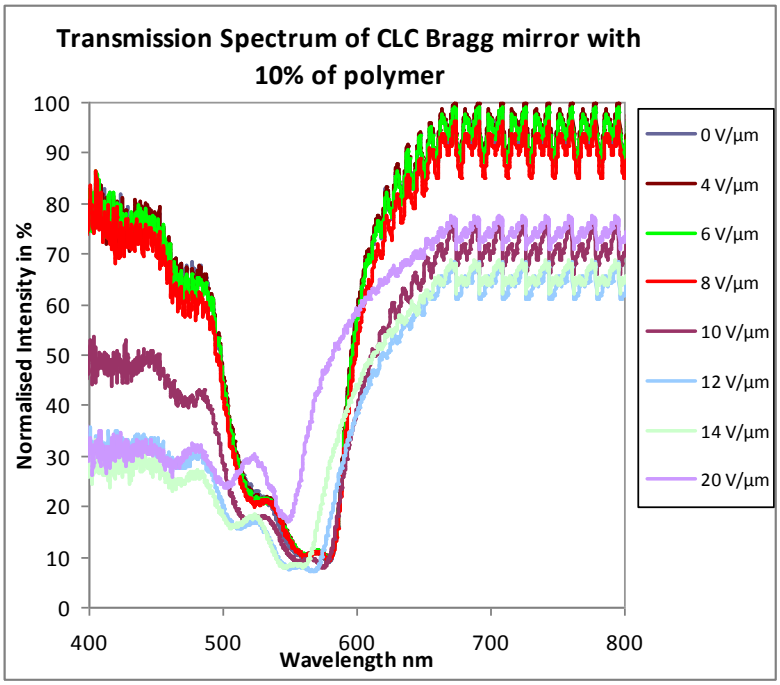

GRAPH 3- 4: TRANSMISSION SPECTRUM AT DIFFERENT VOLTAGES OF PSCLC AT 10% OF RM257

Above graph clearly suggests that the cell with 10% polymer in the cholesteric mixture sustains higher electric fields and also the cholesteric structure is retained after removal of the electric field. The reflectivity of the Bragg mirror has suffered as compared to the cell with 5% of polymer. It can be observed that the mirror is acting as a tunable mirror and after certain voltage it is completely switched

The concentrations below 5% were not enough to hold the cholesteric structure together. The structure collapsed because there was not enough cross linking of the polymer chain to form dense enough polymer network to hold the cholesteric structure. Therefore, when the electric field was applied the transmittance changed; however, the removal of the electric field did not bring the cholesteric structure to original state or it brought it to original state really slowly. The cell with 5% of polymer showed resilience to electric fields up to 10 Volt/ micron. In case of the cell with 10% of polymer concentration it survived the fields as big as 40 Volt/ micron without causing any damage to the structure or to the cell. However, the cell with 5% showed a very good reflectivity as compared to 10% and also the switching performance was much better than the pure cholesterics. Hence it was a good trade-off to fabricate the Fabry-Perot.

3.2.3 Transmission Spectrum of Tunable Fabry-Perot

In this section we will discuss the tunability of the Fabry-Perot with cholesteric mirror. The idea behind the tunability using the temperature is that the pitch of the cholesteric liquid crystal is temperature dependent i.e. as the temperature applied to Fabry-Perot increases the pitch begins to unwind causing the red shift. However, if the temperature passes the clearing point of the cholesteric i.e. the nematic-isotropic transition; then the helix structure will collapse. To measure the transmission spectrum of the Fabry-Perot, we used an optical spectrum analyser from Ocean Optics HR 4000. The source was an unpolarised white light, whose light was later on polarised using a linear polariser. The input polarisation was controlled in such a way that it will meet the quarter the waveplate in 45^0 to convert the linear modes in circular modes.

3.2.3.1 Tunability using temperature

The light was injected through the gold mirror with reflectivity close to 90%. The output of the Fabry Perot was given to the optical spectrum analyser, which had a multi mode fibre to as an input to itself. The output of the spectrum analyser was connected to the laptop computer. Following are the graphs showing the Fabry Perot behaviour for different temperatures.

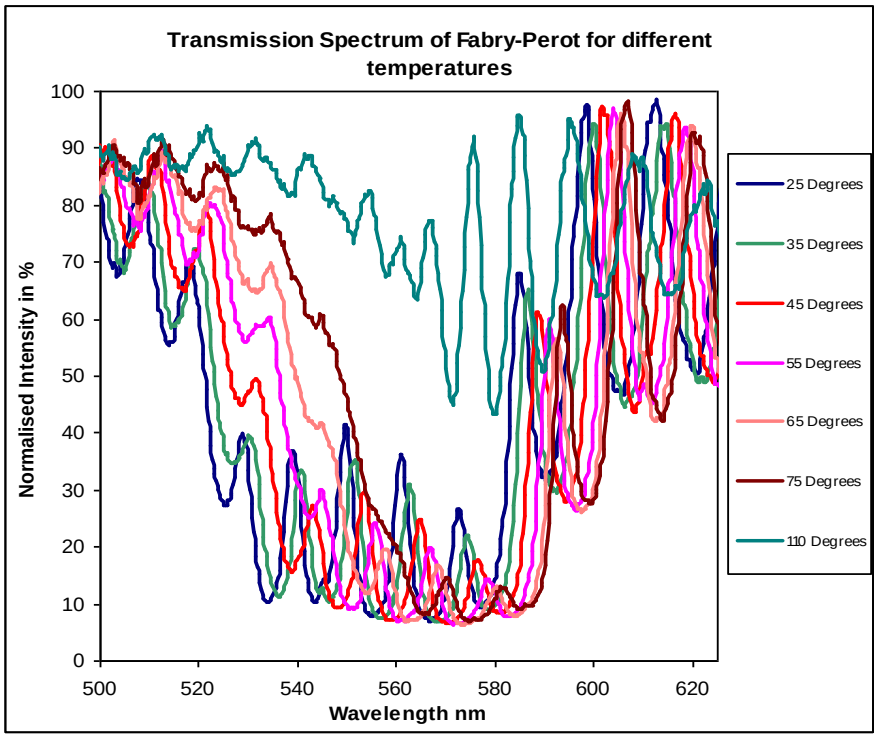

GRAPH 3- 5: TRANSMISSION SPECTRUM OF FABRY-PEROT INTERFEROMETER FOR DIFFERENT TEMPERATURES

The spectrum in Graph 3- 5 illustrates the red shift caused by the application of temperature. The pitch of the cholesteric liquid crystal depends upon the temperature [4]. We have analyzed the dp/dT for this particular cholesteric sample. The shift for this particular cholesteric mixture is positive. We have obtained it to be equal to 0.0914nm/°C. At temperature below isotropic temperature the cholesteric stop band is conserved as it undergoes red shift with a reduction of the stop band width linked to the birefringence decrease. Above the nematic-isotropic transition the cholesteric structure collapses and the stop band disappears. The width of Fabry-Perot peaks in approximately 3 nm and the FSR is about 16 nm. The total shift of FP peaks observed over the range of nematic phase was 8 nm. This FP tunability results mainly of the optical birefringence variation of cholesteric liquid crystal. The Δn of cholesteric liquid crystal is temperature sensitive and decrease when increasing temperature. The birefringence is Δn = 0.17. Where e is the penetration length of cholesteric mirror and cavity is given by

$$\frac{\Delta\lambda}{\lambda} = \frac{\Delta n}{n}\left(\frac{e}{L_{eff}}\right) \qquad \textbf{(3- 11)}$$

L_{eff} is the effective length of FP cavity. This length corresponds to the concatenation of the quarter waveplate, the NOA63 film and penetration length in cholesteric mirror. The ratio $\left(\frac{e}{L_{eff}}\right)$= 0.15 gives a penetration length of about 1 µm. This estimated penetration length is very small compare to the total thickness of CLC, however to obtain a satisfying Finesse of the FP cavity, maintaining a high reflectivity (a large thickness) of CLC mirror is essential.

We have successfully demonstrated the tunability and switchability using temperature. The temperatures involved in this system are quite high and are not ideal from the point of view of industry. However, the system can be deployed using high precision temperature control systems to be able to use over longer period of time. This solution is not cost effective and hence we need to envisage electrical addressing for tuning and switching the Fabry-Perot.

3.2.3.2 Response using Applied Electric Field

The dependence of electric field on the cholesteric liquid crystal is given by following equation;

$$E_{CN} = (\pi^2/p)(K_{22}/\varepsilon_0\Delta\varepsilon)^{1/2} \qquad \textbf{(3- 12)}$$

Where ε_0 is permittivity of free space, $\Delta\varepsilon$ is dielectric anisotropy K_{22} is the twist elastic constant and p is the pitch of the cholesteric. The behaviour of the cholesteric liquid crystal for the applied electric field is a complex issue as there are various different parameters like dielectric anisotropy, the thickness to pitch ratio, the helical pitch, the frequency of the electric field, the direction of the electric field and the boundary conditions of the cholesteric geometry i.e. the alignment conditions given to the cholesterics. In our case we have a short pitch cholesteric with positive dielectric anisotropy aligned in planar direction. When the applied electric field is perpendicular to cholesteric helix and also less than the above mentioned critical field ($0<E<E_{CN}$) then the cholesteric helix begins to unwind causing increase in pitch eventually causing the red shift of the central wavelength of the Bragg reflection. At the electric field equal to the critical electric field ($E= E_{CN}$) the cholesteric – nematic transition is observed [57]. If the initial texture of the cholesteric liquid crystal is planar and the electric field applied is parallel to the helix then the situation becomes slightly complicated [58]. In this case, the conical-helical perturbations result in tilt in the helix and various irregular domains are formed. The parameters like thickness of the cholesteric i.e. the cell thickness and the pitch govern the various effects arising in the structure. If the pitch has comparable value with the wavelength (the case of cholesteric mixture we used) the maximum of the selective reflection will undergo the blue shift. However, this blue shift is not caused by the "compression of the helix" but by different focal conics inside the cell geometry i.e. destruction of the structure. It is also possible to observe the gradient in helix-pitch causing the blue shift of the central wavelength in the stop band of the cholesterics. In any case the increasing electric field will cause the focal conics and eventually the homeotropic alignment of the cholesterics. Therefore, to analyse the situation of the cholesteric mixture used in experiments we had applied the electric field parallel to the helix.

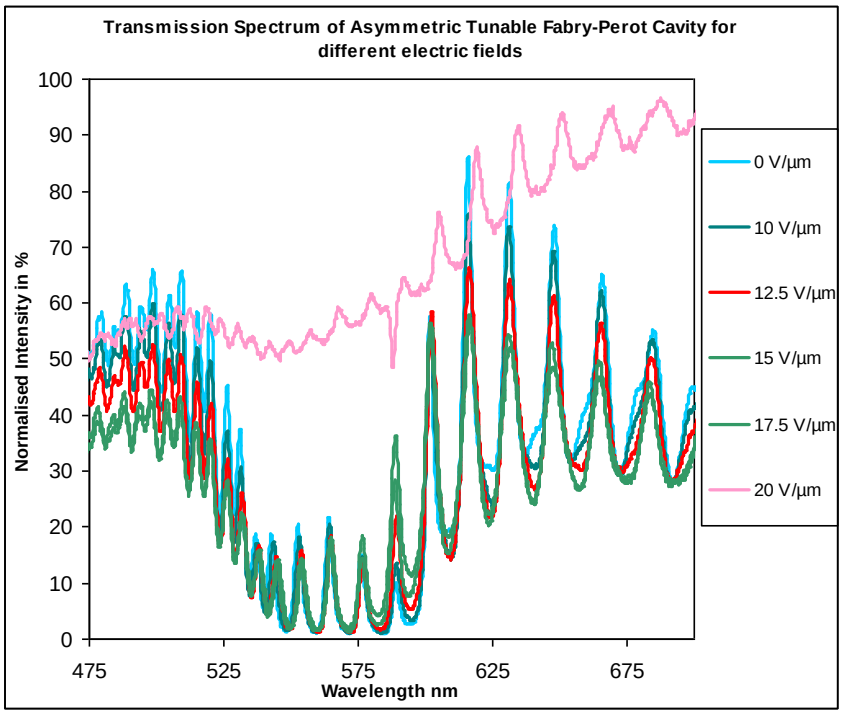

GRAPH 3- 6: TRANSMISSION SPECTRUM OF FABRY-PEROT FOR DIFFERENT ELECTRIC FIELDS

Above graph shows the behaviour of the cholesteric Fabry-Perot interferometer with respect to the applied electric field. It can be easily observed that hardly any tunability or any blue shift was observed before the Fabry-Perot cavity was completely switched off i.e. the homeotropic state. This can be due to the fact the entire cell was 20 microns thick (that does not necessarily indicate that the cavity length was 20 microns) and the field applied over that thick size might not have been enough to cause any kind of shift. One more interesting point from the geometry of the Fabry-Perot is that if one observes carefully one of the electrodes is 7 microns far from the liquid crystal i.e. the liquid crystal is not exactly in contact with one of the electrodes. This may cause considerable amount of reduction in applied electric field than actual electric field mentioned in the graph below. This may be the reason why no apparent shift was observed when the electric field was applied.

Let us now measure the free spectral range and the finesse of the Fabry-Perot cavity. To measure these values we will make use of the equations mentioned in the section. The measured values of the reflectivities of the two mirrors are 80% and 97% for metallic and for cholesteric mirror respectively. By making appropriate substitutions in equation for finesse we obtain the theoretical value of **finesse of the Fabry-Perot as 24.85.** The **theoretical free spectral range** was found to be **16.071nm** for given refractive index i.e. an average refractive index of the entire cavity (≈1.6 in our case) and the thickness of the cavity (≈7 microns). The average refractive index was measured by taking the average of

the ordinary and the extraordinary refractive index of the cavity. These values are different from the experimentally found values of FSR and finesse. Considering the Fabry-Perot peaks inside the stop band of cholesteric and the FSR was observed to be **14 nm.** The experimental value of the It can be clearly seen from the geometry of the Fabry-Perot that the cavity is made up of many different materials viz. the liquid crystal polymer for quarter waveplate fabrication. It may be possible since these materials have slightly different refractive indices and index matching was not accurate which may have given rise to multi cavities inside the same cavity.

We have successfully demonstrated Fabry-Perot using rubbing as well as photo-alignment method. Presence of isotropic area in Fabry-Perot using both the alignment methods ensured the possibility of having more than one peak in the stop band of the cholesteric liquid crystal.

The switching principle can be either by electric field or by thermal change. The tunability has been observed only in case of temperature. In case of electrical addressing no tunability is observed but the cholesteric mirror can be completely switched OFF using electric field. The first design requires very high voltages to switch; hence it is not interesting from the application point of view. The second design allows in contrast, a considerable reduction in electric field values to switch the FP completely. In case of temperature control, a tunability of around 8 nm has been obtained. In case of electric field control the reason for no tunability is probably due to absence of director reorientation with respect to applied electric field or the focal conical defects. Therefore, the electric addressing cannot be used in such an arrangement to tune the FP but can be used to switch it. The drawbacks of these filters is that the input polarization should be controlled, which can be achieved by for instance by including a polarisation diversity system for applications in optical telecommunication.

3.2.4 Transmission Spectrum of Fabry-Perot with conducting polymer

It was observed that the flexibility in positioning the electrode led to many advantages. The first advantage being the voltage applied was only on the cholesteric stack and not over the entire cell. The presence of electrode right next to cholesteric stack reduces the field required to make the complete switching of the cholesteric mirror because in principle cholesteric will transform from planar to focal conics and focal conics to homeotropic state as the applied field increases. We observed such a transition in this case; however, tunability is still not apparent before the mirror was completely switched.

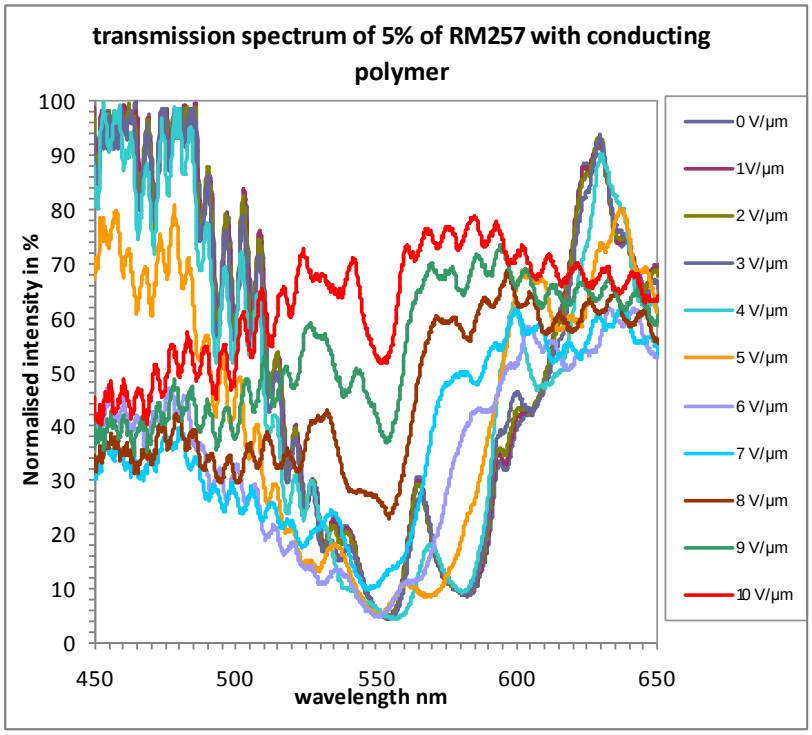

GRAPH 3- 7: BEHAVIOUR OF FABRY-PEROT WITH CONDUCTING POLYMER AT DIFFERENT VOLTAGES

The presence of conducting polymer definitely has enabled us to switch easily the FP by the voltage. However, tunability is still not observed; also the number of peaks inside the cavity has gone down. This can be due to the fact that the monolithic fabrication, which leads to multicavities i.e. different materials with index mismatch were deposited on top each other.

Material	Refractive Index (in visible region)	Δn
PEDOT-PSS	1.53	-
RMS-03-001C (Quarter waveplate)	n_o=1.521, n_e=1.680	0.159
NOA63 (Isotropic Region)	1.56	-
Cholesteric Mixture	n_o=1.5071, n_e=1.6849	0.1778
RM257	n_o=1.508, n_e=1.687	0.179

TABLE 3- 3: REFRACTIVE INDICES OF ALL THE MATERIALS USED SUCCESSIVELY IN THE FABRY-PEROT

Another possibility for reduction in peaks is the absorption of light inside the cavity. Therefore, improvements are possible in this current structure, perhaps first by reducing

the thickness of the conducting polymer (as compared to current thickness which is between 100 and 200 nm) and secondly by using electrodes with good index matching and low absorption. Another important point is that the number of peaks inside the cavity has gone down. This can be due to the fact that the monolithic fabrication leads to multicavities or even index mismatch which can be noticed in Table 3- 3. Thickness reduction of cholesteric stack to very small value like 5 microns will reduce the voltage required to achieve the tuning and the switching. Since the mirror reflectivities of both the mirrors have remained same, the finesse, a property depends upon the mirror reflectivities of Fabry-Perot, remains same.

The fabrication of Fabry-Perot with flexible position of electrode presented some problems and the technology seems to be trade-off between having the tunability, switching of the mirror and the quality of the Fabry-Peaks. However, there are possible improvements which can offer better solution in terms of electrical tunability and also the quality of Fabry-Perot peaks. The presence of an electrode next to the cholesteric stack allows direct application of voltage to the entire stack. This reduces the voltage required to tune and to switch the cholesteric mirrors. It is obvious that the Fabry-Perot peaks will be weakened after the application of electric field as the cholesteric will undergo transformation from the planar to finger print structure i.e. the polarisation states will not be conserved and the mirror reflectivity will go down. It is evident that the introduction of conducting polymer has possibly opened a door for monolithic fabrication of tunable Fabry-Perot but with the compromise on the quality. The reason for the poor quality may be because monolithic fabrication of many layers one on the other may have led to the multicavity structure. The resonance condition is no more satisfied in this case. As mentioned earlier, if the tunability and the quality are maintained then wide variety of applications can be envisaged like tunable laser for any wavelength range in optical band, filters to name few.

3.2.5 Transmission Spectrum of Isotropic Nematic Cavity

The measurement of the transmission was carried out using ocean optics spectrum analyser. In order to observe the effect of input polarisation we polarised the light and also made the measurements for different input polarisations. The spectrum below illustrates the behaviour of this particular cavity for different polarisations. It can be clearly observed that the cavity is not completely polarisation independent that is to say there is a shift in the Fabry-Perot peaks for each wavelength.

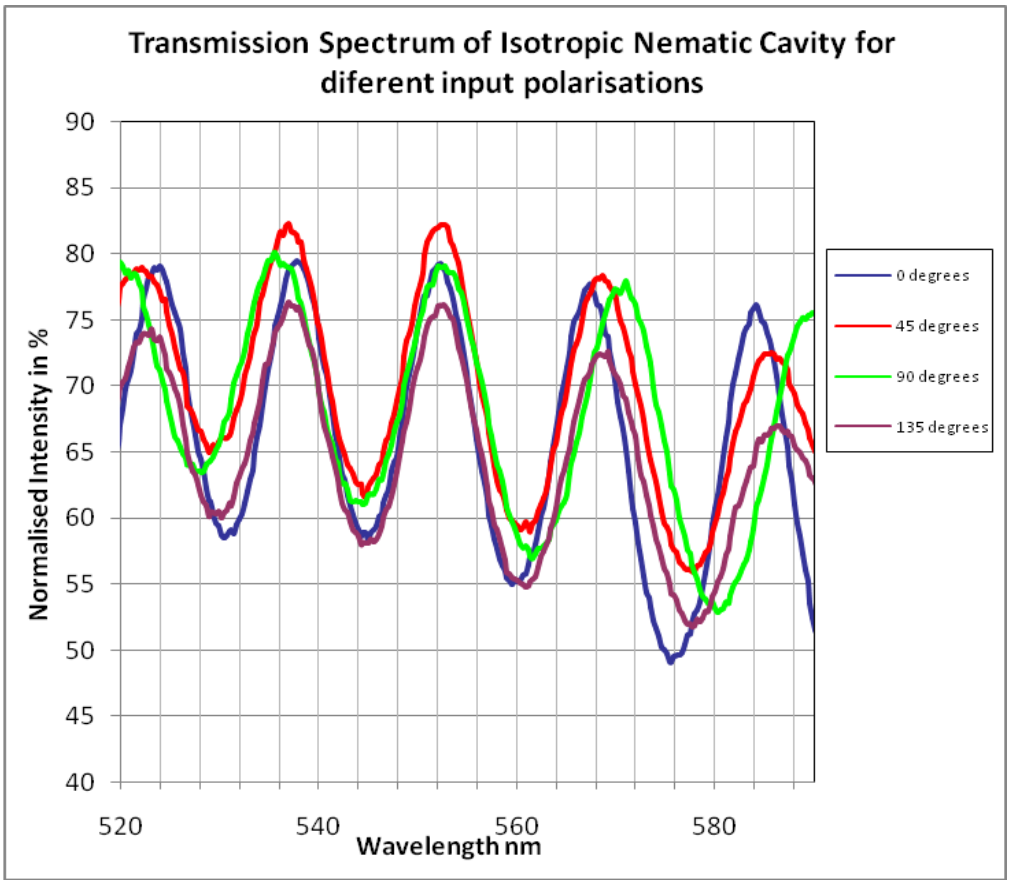

GRAPH 3- 8: POLARISATION DEPENDENCE OF ISOTROPIC NEMATIC CAVITY

Above graph shows the dependence of the output polarisation of the nematic cavity for changing input polarisation. It can be clearly observed that the isotropic nematic cavity is not isotropic for all the wavelengths in the visible region. The fabricated quarter waveplates are wavelength dependent and they were fabricated for the wavelength 550nm. It can be observed that the cavity behaves as an isotropic cavity in the vicinity of the 550nm in the 50nm window to be precise. The wavelengths beyond these wavelengths the quarter waveplate does not act as quarter waveplate causing the circular modes to become elliptical and there is slight deviation of the output peak for every change in the input linear polarisation.

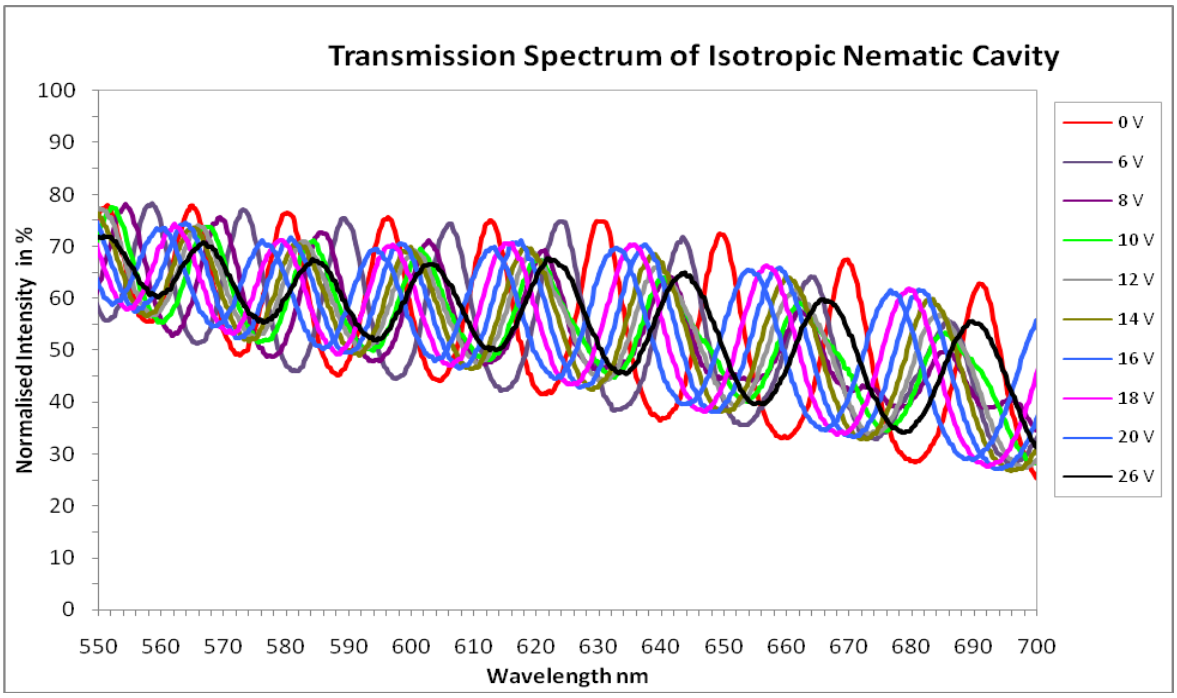

GRAPH 3- 9: VOLTAGE DEPENDENCY OF ISOTROPIC NEMATIC CAVITY

It is can be easily observed that there is a blue shift, which is obvious from the fact as the electric field is applied the Δn of the nematic will decrease as the molecules will start to orient from planar alignment to homeotropic alignment. Another important observation is that the last peak has shifted more than the free spectral range of the Fabry-Perot. Below graph indicates the shift of one single wavelength for applied voltage. It can be seen that the maximum of 29 nm wavelength shift has been observed.

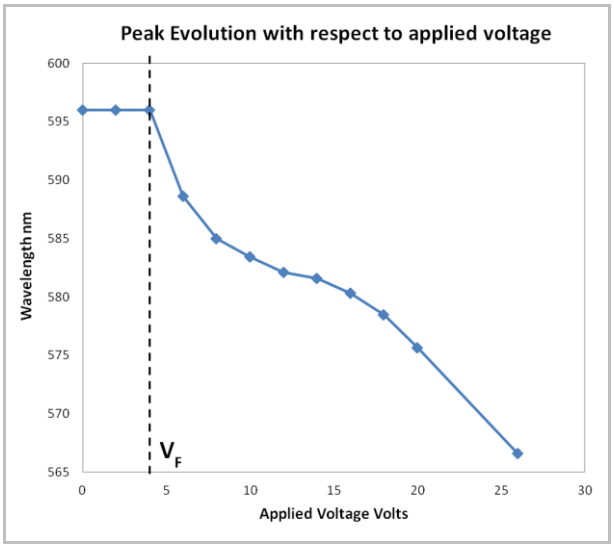

GRAPH 3- 10: EVOLUTION OF SINGLE PEAK OVER APPLIED VOLTAGE

It can be noticed that the Frederick's voltage was observed to be 4 volts. The free spectral range was measured experimentally and also was calculated experimentally. The **theoretical free spectral range** for this cavity is **13.52 nm** (considering **λ_0 at 550 nm, n_{avg} of BL036 = 1.66, while n_{avg} of LCP 1.625** as the quarter waveplates were fabricated for this particular wavelength). The **observed free spectral range** around this wavelength was observed to be **15.61 nm.**

We have successfully realised the fabrication of an isotropic nematic cavity with tunability around 30 nm. The isotropic behaviour of the cavity was observed only in 50 nm window. The wavelength dependence of the quarter waveplate is one of the principle problems for such behaviour. For the wavelengths apart from the ones in window the quarter waveplate did not behave exactly like quarter waveplate causing the formation of elliptical modes rather than circular modes has led to the shift in the Fabry-Perot peaks. However, if the cavity can behave as isotropic cavity only for 50 nm at λ=1550 nm, then there is possibility of investigating some applications in the C band of telecommunications.

3.3 Conclusions

The addition of a polymer in the Bragg mirror with cholesteric liquid crystal has given some obvious advantages like improved relaxation switching times and ability to sustain higher electric fields. The alignment of the cholesteric liquid crystal was made by using photo-alignment as well as the traditional rubbing

We demonstrated the feasibility to fabricate low cost wavelength selective switchable mirror using cholesteric liquid crystal structure either simple Bragg mirror or Fabry-Perot cavity tailored. The material is stabilised by anisotropic polymer network to obtain a reversible electrical switching. Moreover, the optical properties of this mirror can also be finely tailored by combining a mirror (metallic or dielectric) to a cholesteric mirror to fabricate a switchable asymmetrical Fabry-Perot cavity. The Bragg mirrors using pure cholesteric liquid crystals and also using polymer stabilised cholesteric liquid crystals had the reflectivity of above 98%, which is sufficient for numerous applications in optical field: optical notch filter, wavelength selective LASER mirror, etc.

We have successfully shown the tunability and the switchability using the temperature. Thermal addressing for tunability and the switchability of the Fabry-Perot peaks is not ideal as the temperatures involved are quite high hence it would require sophisticated thermal control system to monitor and to maintain the temperature. This would mean the system is no longer cost effective solution. Electrical addressing could have turned out to be an ideal solution but we observe no tunability using applied electric field. Moreover, the

electric field values required to switch the cavity completely are very quite high especially in absence of conducting polymer layer to switch just the cholesteric stack. The solution with conducting polymer does offer smaller values of switching but the quality of the Fabry-Perot is hampered.

It is necessary to assess the need for improving the device performances. There are several apparent solutions like reduction of oily streaks from cholesteric liquid crystals to improve the reflectivity of the mirror, use of dielectric mirror instead of a metallic mirror.

Further investigations concerning the improvement of such structures be incurred to realise, for example, switchable fibred mirrors for telecom applications for the diagnosis of dysfunction in optical networks access.

Chapter 4: Liquid Crystal Spatial Light Modulators

4.1 Introduction to 3D cinema

In this section we will take a brief overview of 3D cinema and the role of liquid crystal in this domain. The technique of creating an illusion of depth in an image by displaying two images separately for the left eye and for the right eye is called stereoscopy, in which users are required to wear a pair of specially made glasses in order to experience the phenomenon [59]. There are different ways to create an illusion of depth without using any kind of glasses, among which one is autostereoscopy. This technique however is not cost-effective and has not yet made its impact in the world of 3D [60]. This particular 3D image or the illusion of depth is a misapprehension, which in a way "cheats" with human brain to give the sensation of the 3D [60]. Normally, the illusion of 3 dimensions is created on a two dimensional surface like a cinema screen, by providing two different views of the same object each view for each eye; when the viewer wears specially made glasses combining these two views to form one single image that gives a sense of depth to it. The issue is how to code the pictures for right and left eyes. Several coding solution have been proposed: spectral, polarisations and times multiplexed. Spectral e.g. anaglyph and polarisations used passive glasses. The last one use active glasses with liquid crystal shutter [61]. Currently the main technologies are passive with polarising glasses and active with liquid crystal shutters; both of them almost share the market equally.

4.1.1 Passive 3D glasses

First we will consider the 3D effect using passive glasses. There are different kinds of passive glasses, which use different technique to create the sensation of 3D: Spectral and circularly polarised glasses.

The first type, the glasses use the red filter and the cyan filter for the left and right eye respectively. The stereoscopic image contains two different images with different colours, each image for each eye. When it is seen through these spectral glasses a viewer gets a sensation of 3D. These filters block the respective colours and therefore, each eye sees the perspective of it is supposed to see. In the second type, a stereoscopic motion picture sends the images with right and left circularly polarised respectively for each eye; the viewer wears glasses with circular polarisers with opposite handedness.

Following diagram represents the principle of working of 3D cinema using linearly polarised passive glasses. The two projectors are interlocked or only one projector with Z screen is used. These projectors send simultaneously the images with opposite polarisations and when the viewer sees these images using the glasses with orthogonal

circular polarisations adjusted for each eye, they get a sensation of 3D as there appears only one image on the screen.

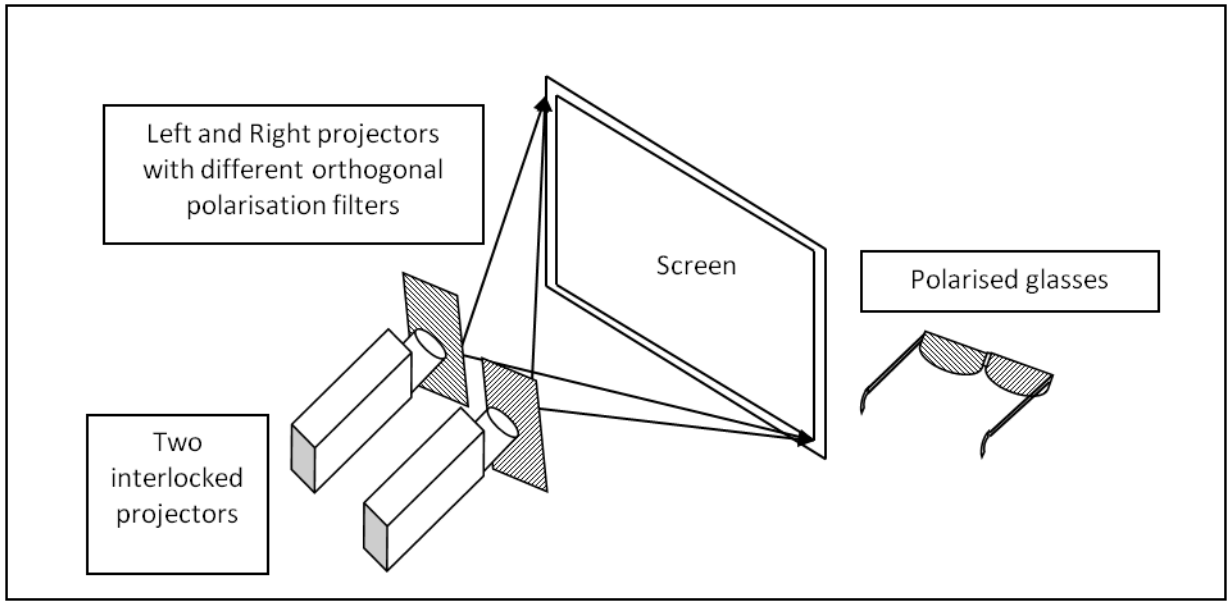

FIGURE 4- 1: PRINCIPLE OF 3D CINEMA USING POLARISED GLASSES. TWO SYSTEM ARE USED: THE FIRST TYPE USE TWO PROJECTOR ASSOCIATED WITH TWO CIRCULAR POLARISERS THAT LAUNCH SIMULTANEOUSLY LEFT AND RIGHT PICTURE ON THE SCREEN. THE SECOND ONE USE ONLY ONE PROJECTOR WITH A SWITCHABLE QUARTER WAVEPLATE TO LAUNCH ALTERNATE (RIGHT – LEFT) PICTURES

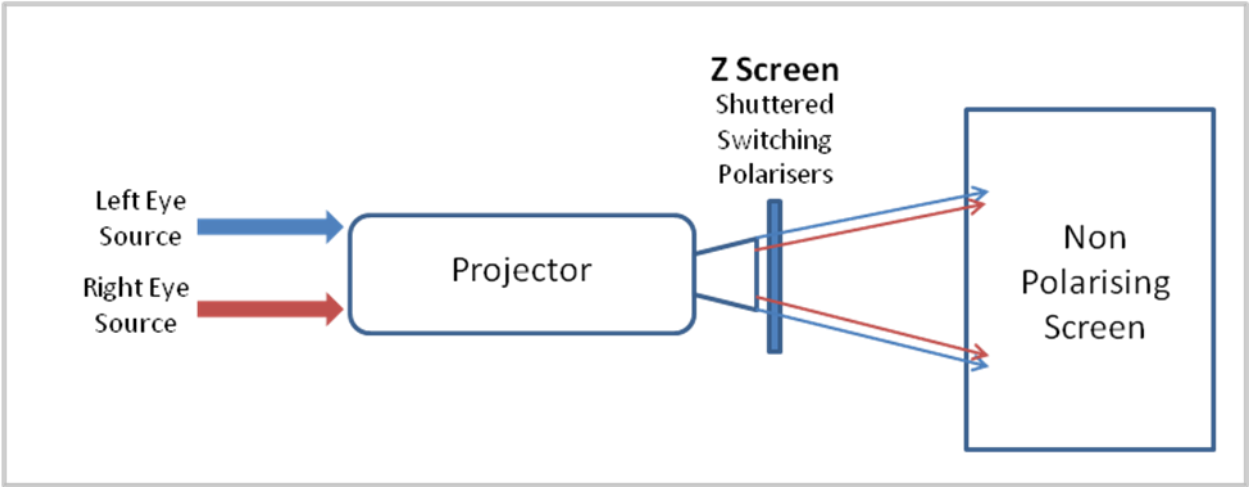

FIGURE 4- 2: Z SCREEN BASED 3D VIEWING

Above diagram shows the principle of behaviour of 3D viewing using the Z-Screen. The advantage of using Z-Screen is that it requires only 1 projector and the polarisation is switched between the left and the right circular polarisation using active shutter based polarisers.

4.1.2 Active 3D glasses

There has been tremendous development in all sectors of 3D world ranging from the quality of projectors or the quality of the movies produced etc. This created a need of providing the high quality experience for the viewers to enjoy the effect of 3D. As discussed in the earlier section passive glasses reduce the quality of the motion picture and also cause ghosting or crosstalk (although this effect can occur while viewing the active glasses but in passive glasses these effects are evident and affect the sensation of 3D severely). In fact it is required for the motion picture to undergo some *"ghost-busting"* technique before the movie is telecasted. This involves sophisticated image processing software and can be an expensive post production technique. Therefore, for better quality motion picture active glasses are ideal solution to enjoy the 3D cinema. The principle behind the active glasses is to project an image of the object with different perspectives for left eye and right eye. When these two perspectives are viewed alternatively at high speed using two optical shutters each for one eye, then the viewer gets the sensation of 3D. These two optical shutters have an alternate closing scheme. Infra-red sensor on the 3D glass triggers these shutters. The infrared radiations are sent from the projector are reflected from the screen and the sensor on the glass captures them to trigger the optical shutters to switch ON and OFF in tandem.

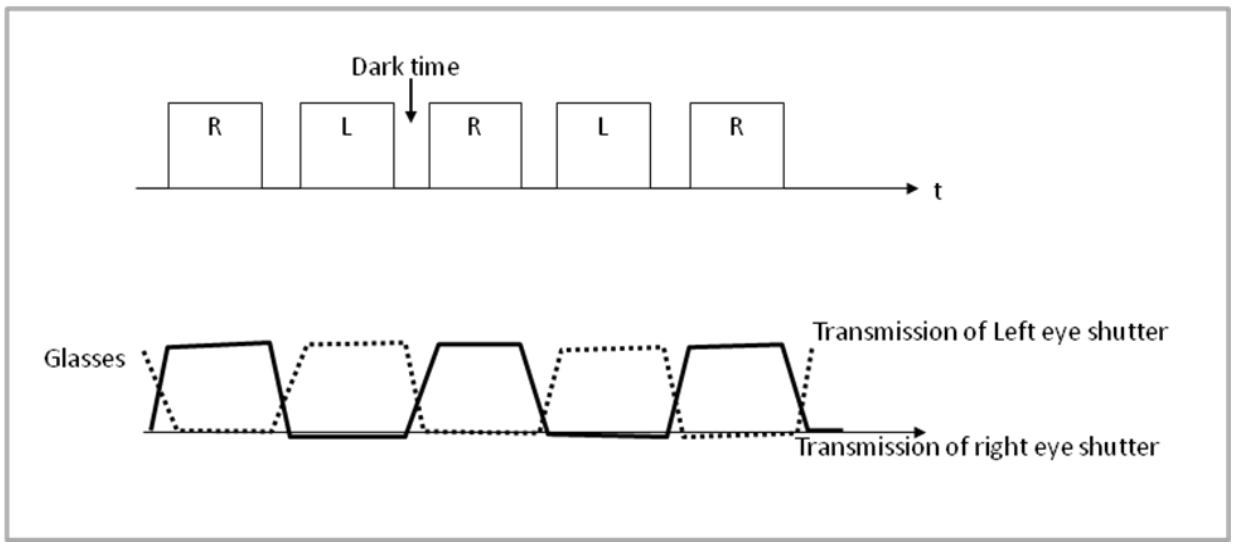

FIGURE 4- 3: CROSSTALK IN ACTIVE GLASSES

4.1.2.1 Colour banding and Ghosting effects

The use of passive glasses system causes a low polarising efficiency that can induce the perception of a "ghost" picture due a depolarization effect on the metallic screen. In particularly under the normal incidence the term *ghosting* is used in place of crosstalk, which is one of the major disadvantages in a stereoscopic motion picture. The appearance

is somewhat similar to that of double exposed image [62]. Crosstalk or ghosting is the leaking of an image to one eye, when it is intended exclusively for the other eye. In other words, it is the incomplete isolation of the left and right image channels so that one image leaks into the other. It happens with most stereoscopic displays and results in reduced image quality and difficulty of fusion if the crosstalk is large [63]. Many times ghosting can be termed as the perception of the crosstalk because that is how a viewer perceives to see two images at the same time instead of seeing only one. This causes leaking of an image from eye to another causing a loss in sensation of 3D. Passive glasses suffer severely from this problem. The only solution to circumvent this problem is the use of sophisticated "*ghost busting"* softwares to process the movie in post production.

In case of active glasses there are two different defects that arise. They can hamper the quality of the viewing. First being the colour banding and it is the inappropriate colour representation of the image. The image is coded according the primary colours. When the switching time of shutter is too long there is a risk of loss of information due to the incapability of displaying all the shades of a colour.

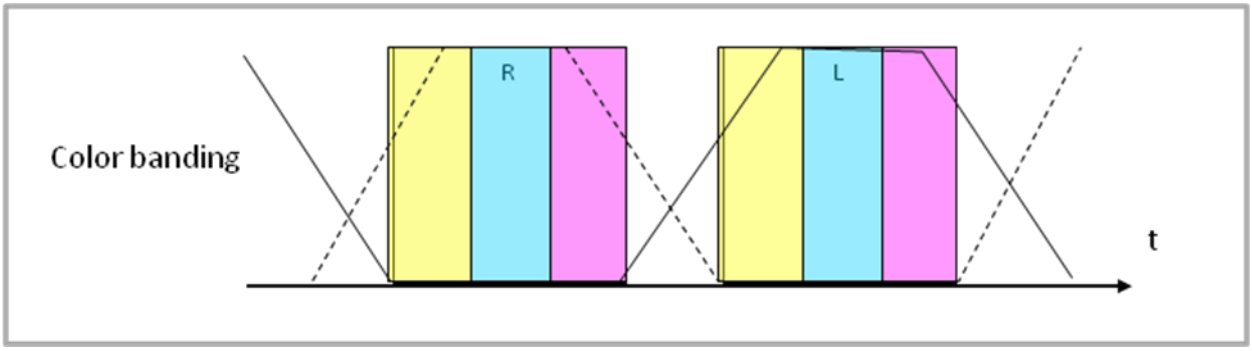

FIGURE 4- 4: COLOUR BANDING IN ACTIVE GLASSES

There is a risk of loss of information due to the incapability of displaying all the shades of a colour. Also, there is a possibility of abrupt changes in the shades of a colour.

Ghosting in case of active glasses results from a slow switching times or an incomplete isolation due to incomplete closure of the shutters or due to poor contrast. The diagram below gives the two different ways of arising of crosstalk.

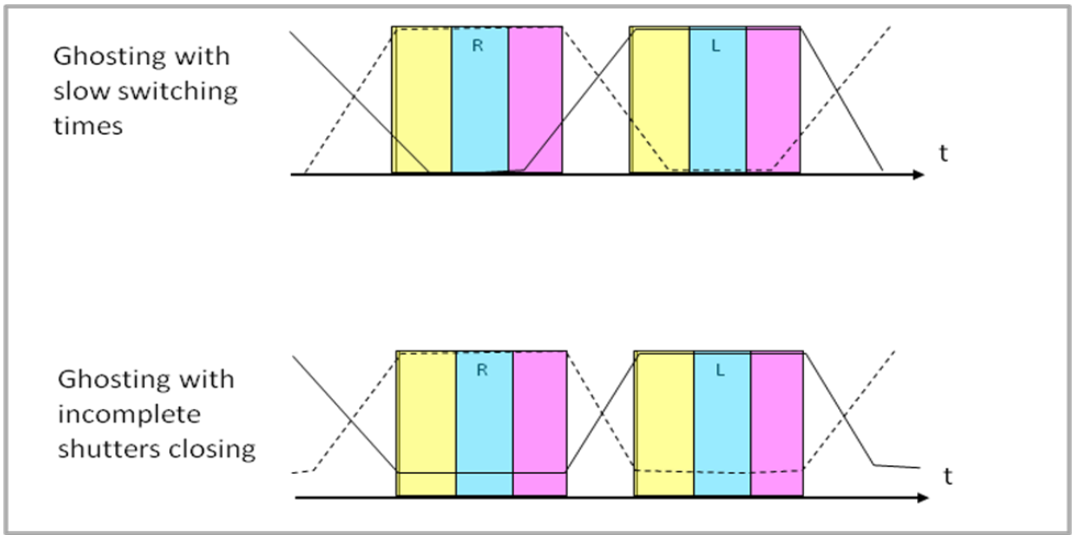

FIGURE 4- 5: GHOSTING DUE TO SLOW SHUTTERS OR INCOMPLETE CLOSURE OF THEM

These ghosting and colour banding effects affect the quality of the 3D viewing; also they cause eye strain to viewers if a viewer continues using the glasses for longer duration and if the system possesses these defects in large amount the sensation of 3D viewing can be completely lost.

4.1.2.2 Active glasses with liquid crystals in 3D cinema

Active glasses with liquid crystals do offer a solution to existing problems in 3D cinema and gives the sensation of 3D of the highest quality without any loss in information or colours provided the optical shutters are fabricated in such a way that they get rid of above mentioned problems. Liquid crystals play pivotal part in the fabrication of these glasses. Active glasses work on the battery operated optical shutters, which close and open with a speed equal to that of the video, whereas passive glasses do not require any power to function. The only disadvantage associated with active glasses is the cost due to the presence of electronics, switchable liquid crystal shutters and power supply. Moreover all these components make them much heavier than their traditional counterpart.

The main design parameters of liquid crystal shutter are switching times, contrast ratio and residual light [61]. We easily understand the constraint on the switching times to reduce the ghosting and the colour banding. This switching time is strongly linked to the dark times between two pictures. These dark times in different 3D system are between 1 and 2 ms. This dark time is obviously defined taking into account the parameters of existing active glasses switching. However, the reduction of this dark time can have another significant impact on the increasing of the brightness for a frame with duration of about 6ms. A switching time close to 1 millisecond (relaxation switching times) can be achieved

with the nematic liquid, whereas ferroelectric liquid crystals offer response time close to 100 microseconds and also symmetric switching. So using Ferroelectric liquid crystal can have a direct impact on both the brightness and ghosting. A particular attention should be taken on the quality of the contrast ratio to avoid any residual ghosting. The basic characteristic of any optical switch is that it should pass as much light as possible in ON state while should block everything in OFF state. The ratio of light passed in ON state to the light passed in OFF state is known as contrast ratio. The optical shutters with higher contrast ratio are preferred to offer better quality while watching the 3D movie.

4.1.2.3 Why Ferroelectric Liquid Crystal?

Now, we will concentrate on the fabrication of this liquid crystal optical shutter which is the heart of the active 3D glasses. Ferroelectric liquid crystals are one of the candidates to make high speed optical shutters. One can consider a fabrication of an optical shutter using pure ferroelectric liquid crystals i.e. without presence of any polymer in the liquid crystal. However, the susceptibility of these liquid crystals for pressure and also for the applied electric field for longer times will result into change in the ferroelectric texture causing the change in the electro-optic response. In a cinema the 3D glass will be used by many viewers over the period of time and obviously there will be mishandling or pressure applied on the glass, hence one has to make sure that the liquid crystal is not susceptible to applied pressure. The electric field may not damage the liquid crystal texture immediately; however, the longer usage of the same will definitely cause changes in the texture of the liquid crystal (transition from chevron texture to the stripe texture or quasi-bookshelf). To circumvent these problems a polymer stabilised liquid crystal was used. The presence of a polymer assures the stability and the required the robustness for the optical shutter. A polymer also makes sure that there is no deformation of the liquid crystal structure over the period of time. It was very important to decide the concentration of the polymer with respect to the liquid crystal. Another important aspect regarding the polymer stabilised ferroelectric liquid crystal is the scattering of the light due to the polymer network which causes blurring of the image. All these problems were addressed while making the optical shutter using liquid crystal. The response time of the smectic liquid crystal depends on the coupling between the spontaneous polarisation and the applied electric field. The coupling between the electric field and the director is continuous from one state to the other, that explains that no slow relaxation times appears in this dynamic [64]. We used a ferroelectric liquid crystal Felix 015/100 with RM257 as a polymer for stabilisation purpose and Igracure 651 as a photoinitiator. The polymer percentage we used was 13% as the robustness of the cell with that concentration was higher than at lower concentrations and also the cell with that polymer concentration could sustain higher voltages. We followed the cell fabrication technique of PSFLC cells mentioned in previous chapter. The cell was filled at a temperature above isotropic temperature and was slowly cooled down

till the nematic phase of the liquid crystal was achieved .The polymerisation of the cell was carried out at a temperature window representing the nematic phase of the liquid crystal. It is absolutely essential that the entire cell should be polymerised in nematic phase, if there are some domains which remain isotropic during polymerisation upon cooling those domains will show focal conical defects. It is very essential to get a defect-free cell in order to obtain the proper dark state so that no light escapes through the shutter during the OFF state. The size of the cells used was tailor made from the 3D glasses' purpose. The alignment layer was again polyimide rubbed where the alignment directions of both the substrates were parallel to each other. The thickness of the cell was 1.5 microns. The polymerisation energy supplied to the cell was 1.5 J/cm^2. The nematic window for this particular liquid crystal was found out to be between 70°C and 75°C; however, authors encourage the users to follow the actual conditions while finding out the actual temperature window. It may differ using the similar materials irrespective of the similarities in the process.

4.1.3 Alignment of FLC using Rubbing with twist and untwisted

Good alignment of these liquid crystals have always been difficult to attain because of several reasons; they possess translational order, which makes the structure very close from being a crystalline material and also they show the phenomenon of ferroelectricity, which means that smectics exhibit spontaneous electric polarisation without presence of external electric field. Former introduces defects called *Chevrons* which are typical for smectics in confined. Since smectic phase shows permanent polarisation without an application of electric field they qualify as the ferroelectric liquid crystals (FLC). Moreover the FLC is very sensitive to the nature of surface interaction and an inhomogeneous alignment film gives a large number of defects. As mentioned earlier another important aspect about smectic alignment is *Chevrons*, which causes the defects arising due to geometry of the smectics; recently it was shown that one of the two possible chevron defects i.e. either C1 or C2 can be overcome by making the cell in *parallel* fashion rather than following the traditional *anti parallel* way of making the cell [65]. This chevron structure can be irreversibly removed by applying low frequency electric field and quasi-bookshelf structure (stripe texture) is finally obtained. This non-stable structure of FLC remains a fundamental issue and a barrier for intensive use of this structure.

The alignment of smectic or ferroelectric liquid crystal was performed by preparing a cell in parallel orientation with two substrates coated with polyimide buffed in same direction. The filling of the smectic cell was carried out at temperature slightly above isotropic temperature (4-5°) and was cooled down at extremely slow cooling rate (approximately 0.2° per minute). This particular heat treatment is necessary in order to make sure that the

alignment is very good. Alignment of smectics can be susceptible to pressure and mishandling of the cell. To overcome these recurrent technological problems, a twisted structure of FLC induced by a tilt in rubbing direction on the two substrates is tested. It was proved that the spatial distortion of the director is coupled to the spatial distortion of the tilt of the smectic layers [66]. Moreover, with assumption that the normal of the layers is parallel to the median axis of both rubbing directions, the thickness of the layer is reduced, that could mitigate the chevron formation in the FLC bulk. The relative layer shrinkage is evaluated as: $\frac{\Delta l}{l} \cong \frac{\Psi^2}{8}$ where Ψ is the induced twist angle (in radians).

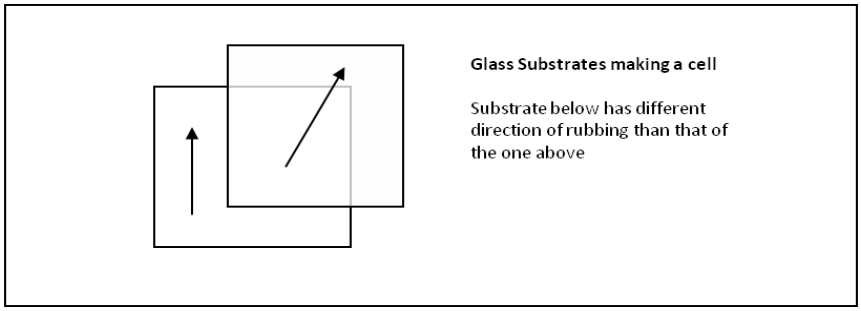

Figure 4- 6: Introduction of twist in cell formation

We will now explore experimentally, the influence of the induced twist of the director on the chevron structure.

The introduction of torque in the FLC geometry may constrain the possible appearance of chevron structure within the cell walls. The experiments were performed at various twist angles (starting from 5° to 45°) and also with different FLC samples with different tilt angle. Measurements for contrast ratio and response time were also performed. All the cells prepared had thickness of approximately 1.5μm. We will be tabulating the response time and contrast ratio for ferroelectric liquid crystal with respect to the applied twist. Therefore, the effect of twist will be scrutinised quantitatively. Following is the setup for measuring the contrast ratio and the response time of the ferroelectric cells. Experiments for the contrast ratio and the response time were performed using the He-Ne laser. The waveform applied was a square wave at 1 KHz frequency with 50% of duty cycle with voltage values mentioned are peak to peak hence ±20V.

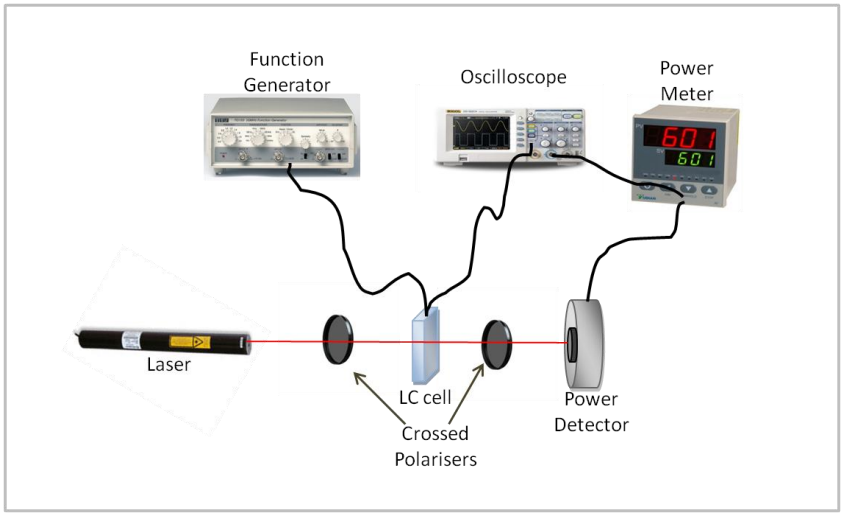

FIGURE 4- 7: SETUP FOR RESPONSE TIME AND CONTRAST RATIO MEASUREMENT

Following table represents the response time values for different twist angles for different ferroelectric liquid crystals.

	Time (µs)		
Twist in Degrees	**W206D**	**Felix 15/100**	**Felix 19/100**
0	260	37	32
5	250	32	30
10	220	72	33
15	300	35	30
20	266	37	36
25	425	35	35
30	315	40	33

TABLE 4- 1: RESPONSE TIME FOR DIFFERENT FERROELECTRIC LIQUID CRYSTAL AT DIFFERENT TWIST ANGLES

The twist angle has a very weak influence on the response times of FLC.

Following table represents the contrast ratio values for similar liquid crystals and also for similar twist angles as mentioned above.

	Contrast Ratio		
Degrees	**W206D**	**Felix 15/100**	**Felix 19/100**
0	973	967	1762
5	1138	916	2273
10	2727	2364	1149
15	2242	2080	1494
20	125	1531	2086
25	268	683	1653
30	72	141	1489

TABLE 4- 2: CONTRAST RATIO VALUES FOR DIFFERENT FERROELECTRIC LIQUID CRYSTALS AT DIFFERENT TWIST ANGLES

The idea behind choosing 3 different liquid crystals was to establish a relationship between the applied twist and the effective tilt angle of the ferroelectric liquid crystal. The twist was given in order to introduce the coupling between the director orientation and smectic layers tilt. The idea behind this coupling was to see the effect on chevron defects, also to see if such coupling helps in eradication or reduction of these defects.

Homogeneous alignment of ferroelectric liquid crystal was obtained by traditional alignment technique. The twist was given in order to introduce the coupling between the director orientation and smectic layers. The idea behind this coupling was to see the effect on chevron defects, also to see if such coupling helps in eradication or reduction of these defects. Although, the results on contrast measurement with a non zero twist angle exhibit higher contrast ratio due to a reduction in defects density, one cannot give definitive conclusions for the moment of the twist impact on the chevron structure. The reduction of defects density is not a relevant sign of a change in the chevron layers structure.

4.1.4 Alignment of PSFLC using rubbing

The experiments were performed by making a mixture of commercially available FLC (Felix-015/100) with commercially available liquid crystal based polymer (Merck-RM 257) and photoinitiator (Igracure 651). Different mixtures were prepared by changing the concentration (13%, 5% and 1%) of RM257. Photoinitiator actually ignites the polymerisation process, the concentration of which is roughly 0.1% by weight. The glass with ITO (Indium tin oxide – transparent electrode) substrates were coated with Nissan 410 polyimide and were buffed in the same direction as each other. The cell was fabricated by 1.5µm spacers and liquid crystal-polymer mixture was sandwiched between them. These cells were later on characterised for response time and contrast ratio. The matter of

detail as compared to pure FLC cells is that the filling of PSFLC cell is slightly different than the pure FLC cells. Although they are filled at temperature above isotropic temperature, they are not cooled slowly to room temperature; instead the polymerisation is carried out in the nematic phase i.e. the cell is cooled down till the temperature in the nematic phase of the liquid crystal is attained to undergo photopolymerisation in that temperature window. If the photopolymerisation begins during the isotropic phase of the liquid crystal, the alignment will eventually be destroyed and focal conical scattering texture will appear on the cell. Polymerisation energy supplied to the cell was consulted according to the datasheet of RM257.

As mentioned earlier the addition of polymer adds to several advantages in FLC structure. However, the alignment may be tricky as the polymerisation has to be carried out in proper temperature window. Different polymer concentrations were used to see the effect of polymer concentration on texture and also on electro-optical properties. All the pictures taken and printed in this work were taken by 10X objective under polarising microscope.

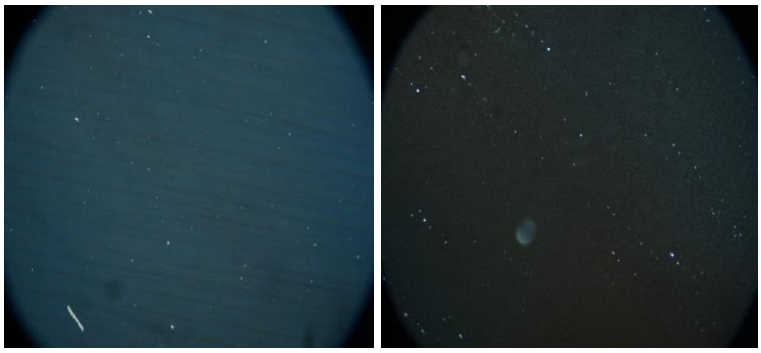

FIGURE 4- 8: PSFLC TEXTURE WITH 1% POLYMER (X10)

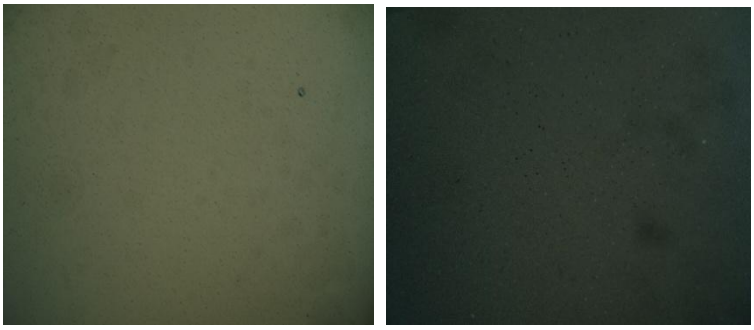

FIGURE 4- 9: PSFLC TEXTURE WITH 5% OF POLYMER (X10)

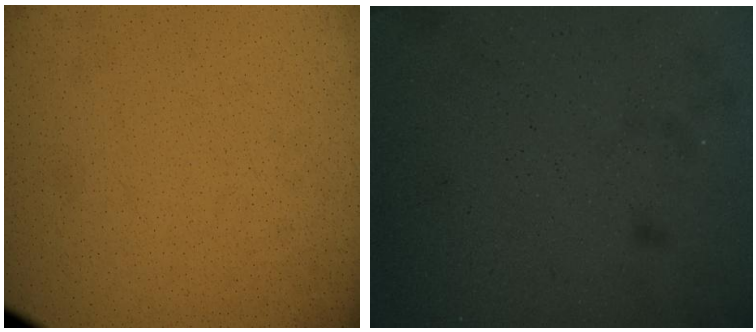

FIGURE 4- 10: PSFLC TEXTURE WITH 13% OF POLYMER (X10)

Above photographs are taken of the PSFLC cells after polymerisation. One can easily see the drastic change in bright state as well as dark state as the concentration of the polymer is reduced. Images on the left are bright state and the ones on right are dark states between crossed polarisers. The images were taken when no field was applied to the cell.

Polymer %	Contrast Ratio (With Laser)
13	685
5	342
1	967 (But too low concentration meant the contrast ratio was similar to FLC, hence causing defects)

TABLE 4- 3: PSFLC CONTRAST RATIO AT 10V PEAK TO PEAK

Homogeneous alignment of polymer stabilised ferroelectric liquid crystal (PSFLC) was successfully achieved using the traditional rubbing technique. The concentration of polymer plays an important role in alignment quality. One can observe the "stripes like" texture due to the polymer networks, oriented along the rubbing direction, appearing over the entire cell. The polymer network has a very interesting impact on the stabilisation of liquid crystal structure: resilience against shocks and stability with applying high electric field. However, as we will see in the 4.1.7 section, the induced stripe texture is scattering that lowering not only the contrast ratio but also the haze due to the increasing of the transmission level of the OFF state.

4.1.5 Substrate with Asymmetric Boundary Conditions

Another approach of FLC alignment which was investigated by buffing only one surface and by keeping the other surface in tact i.e. by providing asymmetric boundary conditions while making a cell. This was done in order to reduce the dislocation lines in the FLC structure. The downside of asymmetric cell can be that from the point of view of electro-optical properties, as for electro-optical operations bistability of the cell is essential.

Therefore, whether or not bistability of the cell has been sacrificed was also verified. The approach was similar to the one published in [67], where they had used the photo-alignment technique. The principle was similar to the one we have used i.e. there only one of the substrate underwent the photo-alignment process. No compromise in the bistability was observed hence similar approach was taken using the rubbing as an alignment method.

The results with the substrate whose only one side was buffed whilst the other side was kept without any alignment are mentioned below.

Voltage	Contrast	Time(µs)
2	5076	225
4	364	99
6	251	67
8	216	46
10	198	40

TABLE 4- 4: CONTRAST RATIO AND RESPONSE TIME OF SUBSTRATE WITH ASYMMETRIC BOUNDARY CONDITIONS

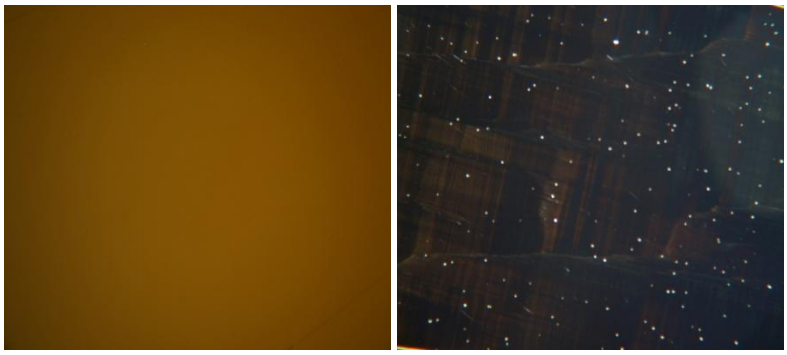

FIGURE 4- 11: BRIGHT AND DARK STATE OF THE SUBSTRATE WITH ASYMMETRIC BOUNDARY CONDITIONS (X10)

The spots seen on the bright state are the spacers, which were coated everywhere on the surface to improve parallelism of the cell. Asymmetric boundary conditions do prove to be successful in aligning the liquid crystal.

4.1.6 Photo-alignment of Smectic Liquid Crystal

Previous studies regarding photo-alignment of smectic liquid crystal have been detailed in [68]. Since smectics show high sensitivity to any non-uniformity and also damage to aligning layers, photo-alignment can be a promising way of aligning them [69]. The process of fabricating a photo-aligned smectic cell was similar to one with nematics, with changes in cell orientation in parallel manner and by increasing the anchoring energy, which was achieved by exposing LPP layer for much longer times than the one required for nematics. We chose the exposure time of 1 hour as compared to 15 minutes for nematics so as to

provide more anchoring energy. The filling of the smectic cell is also critical point in making sure that the quality of alignment is decent after filling as filled at temperature slightly above isotropic temperature and was cooled down at extremely slow cooling rate (approximately 0.2^0 per minute) in presence of small electric field (2V/μm) at high frequency (1 KHz). The application of electric field cancels effect due to spontaneous polarisation.

The higher anchoring energy required to align the ferroelectric liquid crystals was provided by illuminating the LPP substrate for longer time than for usual nematic liquid crystals. We had also prepared a cell with similar anchoring as that of nematic liquid crystal; however, the quality of alignment was poor in that case. It was thought that if the dose of the polarised UV is increased; higher anchoring will be provided and evidently the increase resulted into better alignment quality.

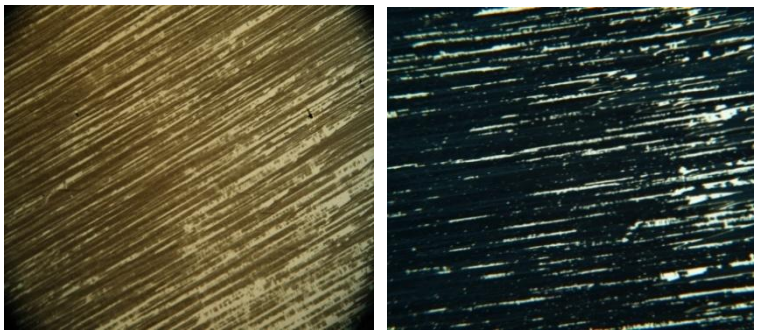

FIGURE 4- 12: BRIGHT AND DARK STATE AT UV EXPOSURE TIME OF 15 MIN (X10)

Increase in UV exposure time gave us following result.

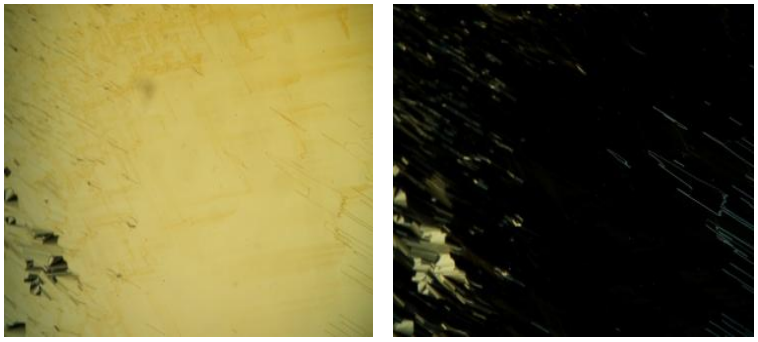

Figure 4- 13: Bright and Dark state at UV exposure time of 60 min (X10)

It can be easily noted that the increase in exposure time presents us with better alignment quality, although one can see the chevron structure but the alignment quality has definitely improved. Now we will discuss the effect of twist on alignment quality and also on the electro-optical properties.

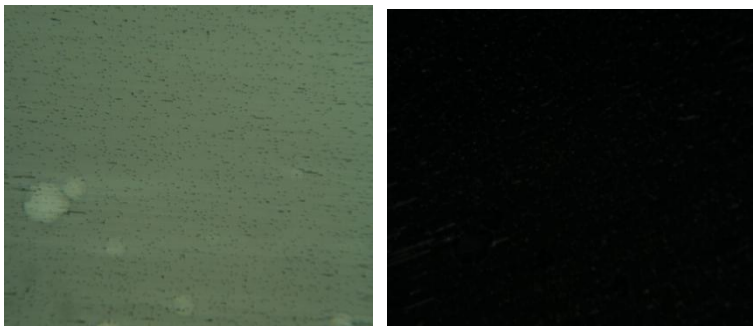

Figure 4- 14: Photo-alignment of Felix 015/100 with of twist of 10 degrees (X10)

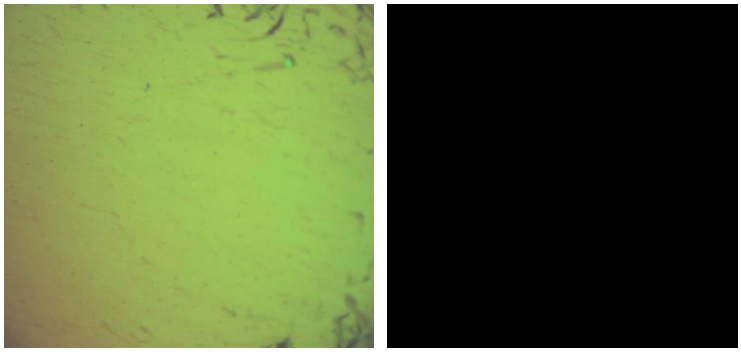

Figure 4- 15: Photo-alignment of Felix 015/100 with twist of 20 degrees (X10)

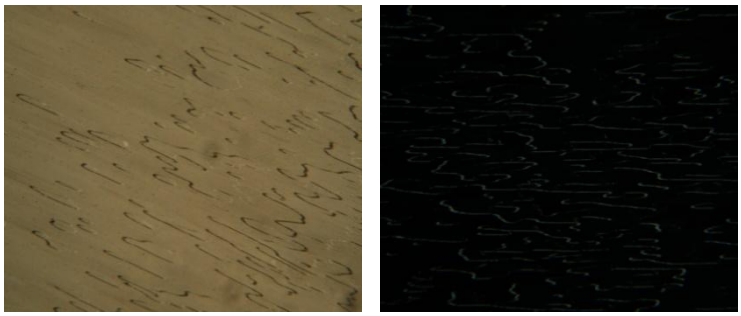

FIGURE 4- 16: PHOTO-ALIGNMENT OF FELIX 015/100 WITH TWIST OF 30 DEGREES (X10)

Twist Angle	Contrast Ratio	Response Time (µs)
0	259	73
10	418	45
20	93	86
30	9	160

TABLE 4- 5: RESPONSE TIME AND CONTRAST RATIO OF FLC CELLS WITH DIFFERENT TWIST ANGLES

It can be observed from the electro-optical measurements that the quality of alignment has been degraded at twist angles 20 and 30 degrees. However, the twist of 10 degrees shows the best results.

4.1.7 Electro-optic measurements of optical shutters for 3D glasses

The study about different types of shutters for 3D glasses has been detailed in [70]. The size of the liquid crystal cell used for making an optical shutter was much larger than the normal cell size we normally use during the characterisation. It was custom made to fabricate the glasses for 3D viewing with already aligned layer in on both the substrates. The optical properties relevant from the fabrication point of view are:

- Response time
- Contrast ratio
- Scattering of the light or haze
- Viewing angle & chromatic response

Previously, the optical shutters for 3D viewing using ferroelectric liquid crystals have been presented in [71]. The first property deals with the rise time and fall time of the shutter. From the point of view 3D viewing, it is essential that both the times should be more or less equal i.e. for a symmetric waveform of applied voltage the behaviour of the cell should be symmetric. Contrast ratio is the ratio between the luminosities of brightest white and the darkest black. The scattering of light affects the viewing as the light passes through the cell during the OFF state. It is important to have a good chromatic response in order to maintain the colour quality of the motion picture. It is also essential to achieve the same behaviour of the shutter irrespective of a seat occupied by a viewer in a cinema hall; therefore, it is necessary to maintain the viewing angle of the optical shutter. Since the size of the cells used were large it was necessary to maintain the flatness of the cell over the entire area. The cells were fabricated with a thickness of 1.5 µm.

The response time and contrast ratio measurements were carried out by He-Ne laser. However, for the contrast ratio measurements the use of He-Ne laser will not give the accurate reading as not the entire cell will be illuminated and if the cell has some damaged domain it will not give the accurate reading. Therefore, the measurements were carried out by ELDIM EZlite colorimeter with white light. The principle of the ELDIM contrast measurement is based on the use of Fourier optics: A lens collects the light emitted by a small surface and refocus rays of light on the Fourier plane at a position that depends on their incidence and azimuth angles. This system is able to measure the angular contrast.

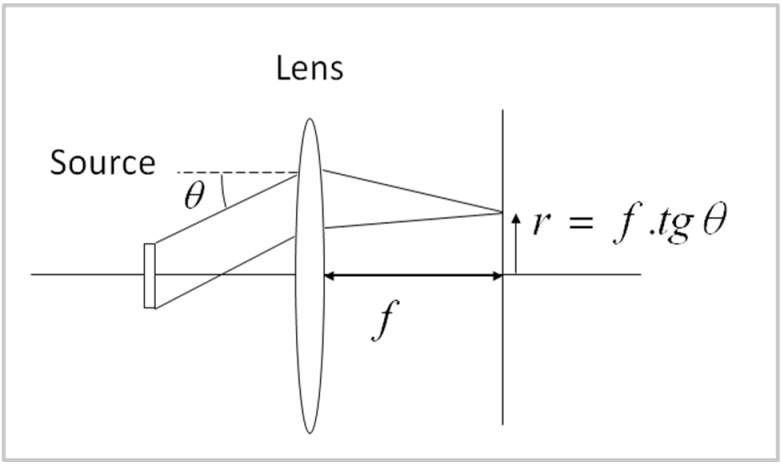

FIGURE 4- 17: PRINCIPLE OF THE ANGULAR CONTRAST MEASUREMENT

In order to have higher contrast ratio it is necessary to have a good dark state or OFF state i.e. most of the light should be blocked during the OFF state of the shutter. If the quality of the OFF state is not the viewers will suffer from the problems of ghosting and the effect of the 3D will be affected. Contrast ratio was measured by measuring the luminance of ON and OFF state. It should be noted that there are polarisers glued on side of the shutter in such a manner that the OFF state will pass minimum amount of light. Nematic liquid crystal normally posses the better OFF state than the smectic liquid crystal hence the measured contrast ratio is much higher for nematics than in case of smectics [64].

The scattering is an issue which needs to be addressed in assessment of the quality of the liquid crystal shutter. It is the amount of light leaked during the OFF state of the shutter. The scattering readings are essential in order to know whether any residual light is being leaked during the dark time of the shutter. Therefore we made scattering measurements for our glasses. Haze can be defined as the ratio of the percentage of the light scattered and percentage of the total light transmitted.

$$Haze(\%) = \left(\frac{T_d}{T_t}\right) \times 100 \qquad (4\text{- }1)$$

T_d = scattered transmitted light
T_t = total transmitted light

It can be caused due to the presence of any dust particles inside the cell; the polymer network also plays an important part in the scattering of the light. In the low polymer concentration regime (< 13%) the response time is improved but the there is a lot of scattering in the visible region [72]. If the domain size of the polymer network is much higher than the wavelength the light gets scattered; therefore, we decided to increase the polymer concentration in order to decrease the domain size of the polymer network. However, it was necessary to satisfy the conditions for the cell being qualified as polymer

stabilised liquid crystals in order to maintain the switching time requirements. Also, the voltage required for switching of the cell with higher polymer concentration is large and for glasses for 3D viewing one cannot have large voltage values on viewers' face!

Now we will see the measured the values of contrast ratio. Also we will have a look at the quality of alignment. Following are the photos of the ON state and OFF state taken in presence of electric field under polarising microscope with an objective of 5X.

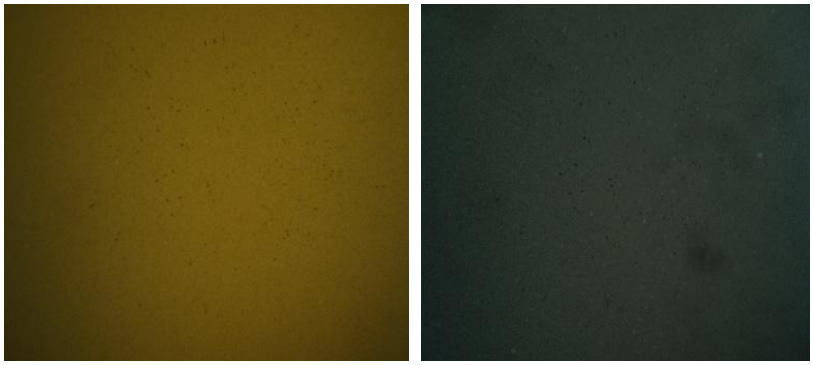

FIGURE 4- 18: ON AND OFF STATE OF THE OPTICAL SHUTTER UNDER POLARISING MICROSCOPE (13%)

Above photos show the ON state and the OFF state of the optical shutter. It can be noticed that the dark state of the liquid crystal when well aligned without any defects does not leak much light.

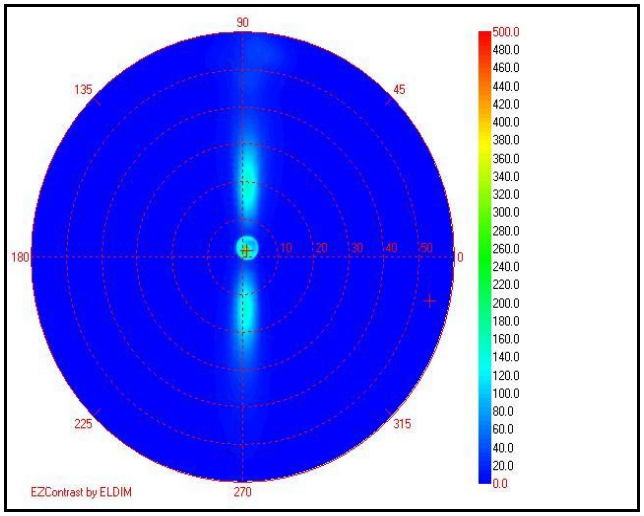

FIGURE 4- 19: MEASUREMENT OF SCATTERING I.E. LUMINANCE AT THE OFF STATE

The photo above shows the luminance of the optical shutter in the OFF state. The two side lobes which represent the scattering degradation the quality of the shutter. A white streak is clearly observed by an observer through the shutters. This is one problem we are still trying to overcome. There might be possible solutions to overcome this scattering which

comes from the polymer network. The increase in polymer concentration is possible solution but the applied voltage for complete switching of the cell will have to be increased as the polymer network will be resisting the liquid crystal molecules to move freely.

A planar aligned PSFLC normally suffer from the contrast ratio unlike a usual planar aligned nematic liquid crystal. This is the only trade off for higher response times with PSFLC. The contrast ratio was measured by taking the ratio of luminance of bright state and luminance dark state. The contrast ratio of 150:1 was recorded using the ELDIM colorimeter. It can be seen that uniformity over ±60° in x direction and ±30° in y direction was achieved.

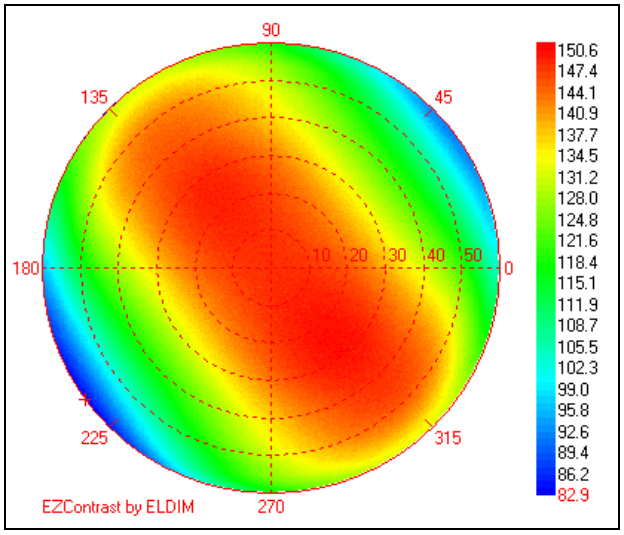

FIGURE 4- 20: CONTRAST RATIO OF THE PSFLC SHUTTER

The above diagram represents the division of the luminosities at ON state and OFF state. We also measured the contrast ratio using He-Ne laser and the contrast ratio we found out was 685:1; this huge value of the contrast ratio is due to the fact that the photodiode doesn't receive the scattered light and then the OFF state intensity is under evaluated.

The response time measurements were done for different voltage values. The voltage value we use for the switching the shutter in an actual 3D glass is 20 V peak to peak.

4.2 Conclusions and Perspectives

In case of the alignment of smectics using twist one can say that the amount of twist given during alignment has some correlation with the effective tilt angle of the ferroelectric liquid crystal, i.e. in case of Felix 015/100 the effective tilt angle was 20° and the cells with the twist above this value have shown drastic degradation in quality and also electro-optical response. The same can be observed with Felix 019/100; where the quality of alignment was poor if the twist above the effective tilt angle was given. In case of the W 206D the tilt angle was 45° but the effective tilt angle was only 13°; hence the alignment quality was poor if the twist above this value was given. However, author at this point would not want to claim that the alignment quality will definitely degrade if the twist above the effective tilt angle is provided. To support these preliminary experimental results we need a theoretical analysis and perhaps experiments like X-ray diffraction to observe the smectic layers with a director twist.

The similar can be said for the results concerning the photo-alignment of smectic liquid crystals. There are few parameters which can influence the alignment *viz.* azimuthal and polar anchoring energy, pre-tilt angle etc. In order to establish a possible correlation one has to perform experiments, in which one can control all these parameters. These studies emphasize the difficulties of implementation of FLC in shutters' technology. We demonstrate that with a splay structure we improve the contrast ratio; however, the lack of shocks resilience remains a weak point. The poor reproducibility of FLC texture quality (to compare to nematic liquid crystal) is also a drawback of this technology.

PSFLC seems to be a good candidate for 3D glasses: contrast ratio, response times etc. However, a particular effect should be investigated: the impact of anisotropic scattering on movie observation. In conclusion, we can summarize the main properties of both technologies with the following table:

Liquid crystal structure	Response times	Voltage for 1.5 µm cell	Defects	Defects impacts	Shutters	Contrast ratio
Ferroelectric Liquid Crystal	< 100 µs	10V	Zigzag defects & stripe defects - instable	Scattering with zigzag defect compared to PSFLC: loss of contrast. Anisotropic diffracting (stripe texture)	Shocks sensitivity	Good, with chevron structure without zigzag defects Low, with quasi-bookshelf structures
Polymer stabilised Ferroelectric liquid crystal	100 µs	20V	Stripe like-defects	Anisotropic scattering	Shocks resilience	Medium

TABLE 4- 6: COMPARISON OF PURE FLC AND POLYMER STABILISED FLC

Chapter 5: Liquid Crystal as Waveguides- Fundamentals and Theory

5.1 Polarisation Issues with Optical Waveguide Device

In this chapter we will speak about the fabrication of the waveguide which separates the two different polarisations in two different branches of the waveguide. We will also consider the important viewpoint from the design perspective. To begin with we will talk about the need of a polarisation separator and why liquid crystals are attractive candidates to serve the very purpose.

Polarisation sensitivity has been one of the more complex problems to treat for optical communications, since many years. For example, the polarisation mode dispersion PMD of polarisation due to cumulated differential group delay in optical fibres can create numerous issues that remain very difficult to mitigate. In optical telecommunication domain, the input polarization after propagation cannot be controlled and is totally unstable due to mechanical stresses on the optical fibre (these stresses, among other things, are responsible for the Polarization Mode Dispersion) [73]. Thus, these above optical functions can have an erratic behaviour due to the fluctuation of the input polarization and polarization sensitivity cancels all advantages of such high integrated waveguide devices.

Number of different optical wave guided devices use optical functions that are polarization sensitive (Bragg filter, MUX / DEMUX, coupler, etc.). This sensitivity mainly results from an induced birefringence in waveguides circuit. Requirements for polarization dependence (Telcordia GR1209) [74], specify that optical devices should fulfil the birefringence criterion: $\Delta n_{TE/TM} \leq 5.10^{-5}$ [75]. There are several sources of anisotropy which can be listed *viz.* geometrical origins as bend and asymmetrical section of the waveguide, technological origin with epitaxial growth or waveguide patterning techniques, photoelastic effect due to lattice mismatch between the guiding layer and the substrate [76-78]. Moreover, with both decreasing scale of optical devices and higher optical index contrast, practical design tolerances rapidly become difficult to meet. The coupling of light into and out of the devices is identified as a major engineering challenge and at the same times, polarization sensitivity and waveguide loss grow rapidly.

Several solutions have been proposed to reduce the polarization sensitivity: precise control of the geometric parameters of the waveguides [79], birefringence is balanced by the stress birefringence induced by a compressive cladding layer [80]. However, for tunable or reconfigurable function these solutions won't be easy to put into practice. The tunable and reconfigurable functions are requirements of the modern optical communication systems for better efficiency and control. To overcome this problem of polarisation sensitivity, a

polarization splitter is a key function, which treats separately two orthogonal polarisations and then recombines these orthogonal polarisations [75, 81-84]. Several technical designs have been already proposed to manage the polarization diversity. We will briefly describe these techniques. These techniques are based on anisotropic waveguide polarisation splitters, isotropic waveguide polarisation splitters, photonic crystal type splitter and Mach Zehnder based interferometers to separate the polarisations.

5.1.1 Anisotropic Waveguide Coupler Splitter

Our work is based on anisotropic nature of waveguides to handle the polarisation issues. In this work we propose an original solution to realize a polymer waveguide device that contains at the same time anisotropic and isotropic section. Polymer materials have undeniable qualities: They permit mass production at a low cost, and are easily integrated on a wide range of substrate materials, such as glass, silicon dioxide, and silicon. The anisotropic section is devoted to the polarization splitter and the isotropic section to the optical functions. The tested function can be for instance a wavelength filter. Moreover, we demonstrate the feasibility of this kind of device with a very simple technological process. However, before we start detailing our work it would be better to take a historical overview of the work done in this area.

The technique below is based on the coupling using asymmetric Y shaped coupler on the $LiNbO_3$ substrate using titanium indiffused waveguide channel [85], nickel indiffused waveguide channel and MgO induced lithium outdiffusion (MILO) waveguide. The principle of working is shown in following diagram

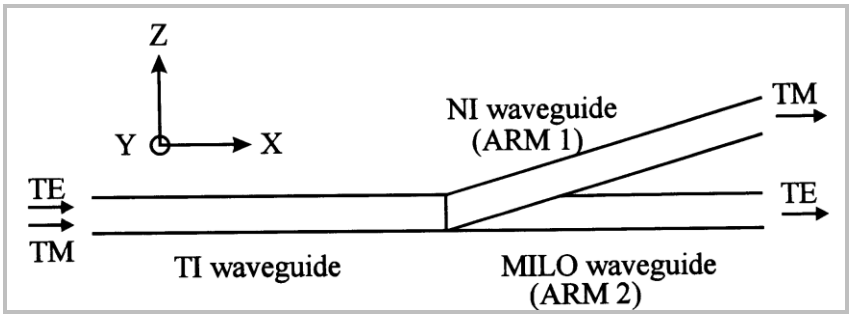

FIGURE 5- 1: TE-TM MODE SPLITTER ON LINBNO3 USING TI, NI, AND MGO DIFFUSIONS

This method offers the splitting of the two polarisation states, however, the extinction ratios for single mode operation are low and also the fabrication of this splitter is cumbersome.

Another method based on the anisotropic splitting uses the polymer waveguides to separate the polarisations [86]. The principle of working is shown below.

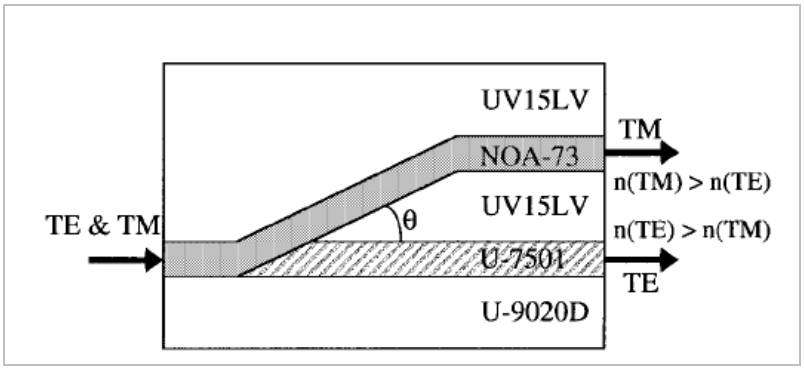

FIGURE 5- 2: VERTICALLY INTEGRATED WAVEGUIDE POLARIZATION SPLITTERS USING POLYMERS

The birefringence of a single waveguide channel as compared to the other is very small and this may be lead to higher coupling length.

5.1.2 Photonic Crystal Based Polarisation Separator

This type of splitter consists of a combination of multimode interference couplers and photonic crystal [81]. The photonic crystal is situated in the middle of the multimode interference coupler and is designed to be a polarisation sensitive based on the principle shown in [87]. The multimode interference works similar to multimode splitter; while the photonic crystal acts as a polarisation sensitive reflector. The photonic crystal prohibits TE mode to pass through while allowing the TM mode passes through. The TE mode is reflected back. The multimode interference coupler is designed to receive the reflected and transmitted polarisations at two different ports. The principle is shown in diagram below.

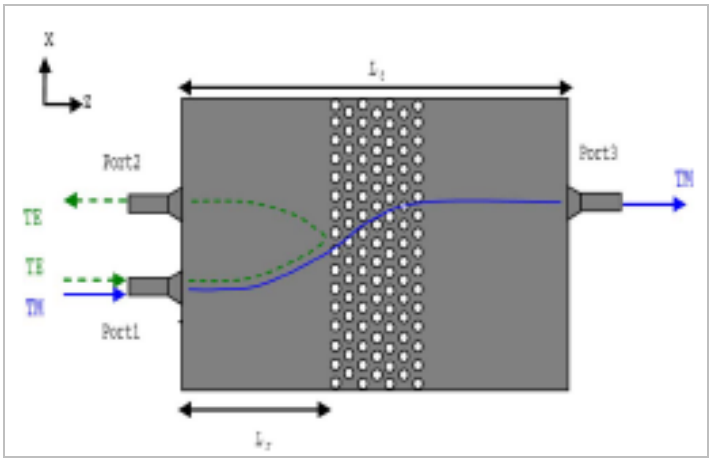

FIGURE 5- 3: POLARIZATION-BEAM SPLITTER BASED ON A PHOTONIC CRYSTAL

Another splitter based photonic crystal has been detailed in [88], where polarisation separation functionality is enabled by two mechanisms; photonic bandgap effect from TE polarisations and index-contrast effect TM polarisations.

5.1.3 Mach Zehnder Based Polarisation Splitters

This type of waveguide was fabricated on silicon substrates. To separate the polarisations it uses the principle of interferometer with anisotropic waveguide (the anisotropy is due to the geometry of waveguide) [89]. It comprises of two 3 dB multi Mode Interference couplers made in Mach Zehnder interferometer arrangement. In this type the TE polarisation does not suffer a phase shift or it has 0 phase shift while the TM polarisation suffers a phase shift of $\pi/2$ after the first 3 dB coupler. Once the light arrives at second coupler the TE polarisation will come out from one of the arms while the TM will suffer a phase of π in total and will come out from another arm. The principle of working is shown below.

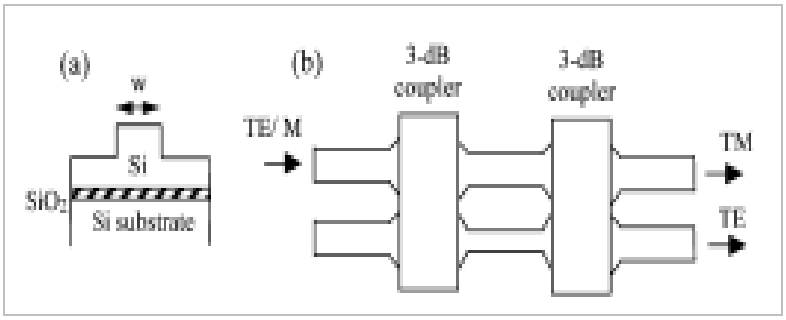

FIGURE 5- 4: MACH ZEHNDER BASED POLARISATION SPLITTER

These are few of the techniques to separate the polarisations. Our technique is based on liquid crystals, hence anisotropic waveguide splitters and has some advantages over these mentioned techniques like easy to fabricate and materialise. However, before entering the details of fabrication of the waveguides we will take overview of waveguides, coupled mode theory and principle of anisotropic coupling.

5.2 Introduction to waveguides Couplers

Optical waveguides can be considered as the dielectric solid state materials wherein the optical waves are confined along the path of the waveguide due to the phenomenon of total internal reflection [90]. The index of refraction of the guiding medium is larger than the outer mediums of the waveguide. We have introduced the waveguides thoroughly in Appendix IV.

5.2.1 Coupled Mode Theory

We have taken a brief overview of theory of waveguides, formation of TE and TM modes inside the waveguide in Appendix IV. For many practical applications it is necessary to have waves propagating in adjacent waveguides (co-directional) or waves propagating in opposite direction (contra-directional) in two different waveguides [91] [92]. In order to study the wave propagation in adjacent waveguides we will now consider the directional couplers and theory regarding the same. In the present research we have studied co-directional couplers. The energy transfer between the guided modes in two adjacent waveguides is known as directional coupling and to evaluate the equations for the power transfer and also for coupling coefficients we will now consider the coupled mode theory that deals with the interaction of such propagating modes with each other.

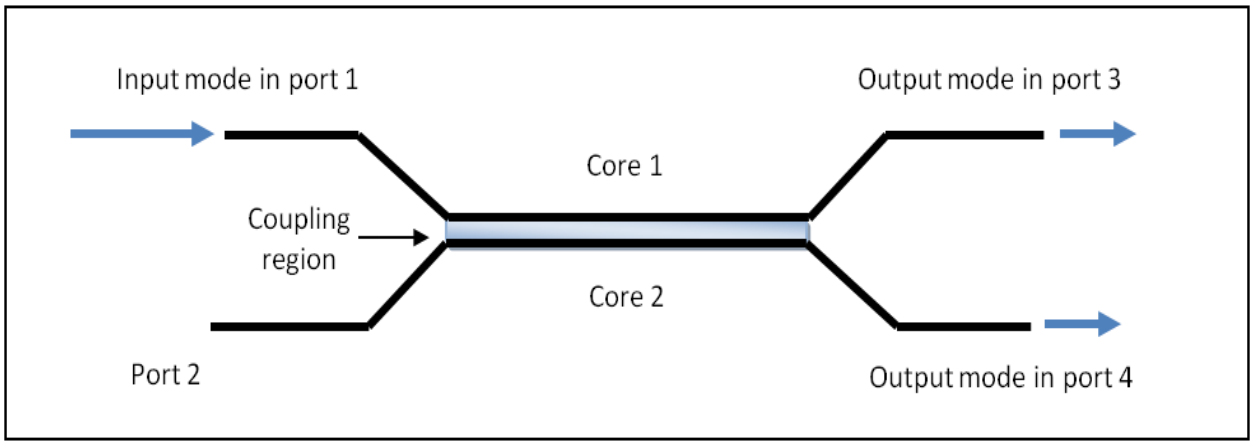

FIGURE 5- 5: PRINCIPLE OF DIRECTIONAL COUPLING

The directional coupler is composed of two or more parallel waveguides placed in close proximity. This new structure can be identified as a new “super waveguide” with two cores. The light mode is travelling or is injected through the port 1; the evanescent field coupling in two separate waveguides takes place. Hence the power is progressively transferred from core 1 to core 2 and this continues over the entire coupling region. This power transfer is the consequence of interference phenomenon between two “super-modes”. The output power in any port depends upon the length of the coupling region popularly known as the coupling length, is the length over which the light is completely coupled to adjacent waveguide.

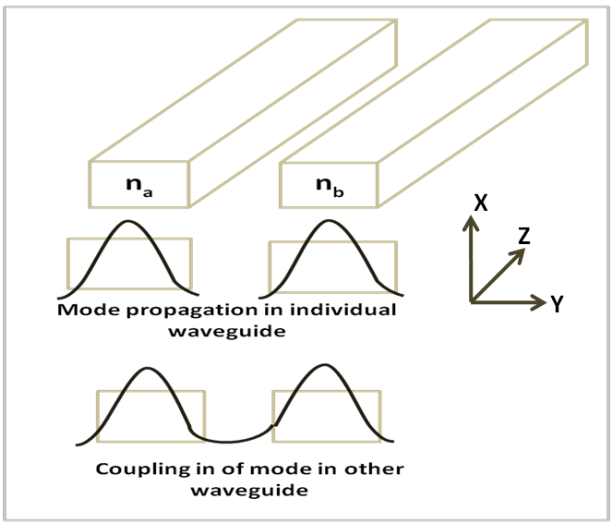

FIGURE 5- 6: COUPLING OF MODES IN ADJACENT WAVEGUIDES

Consider Figure 5- 6 where two single mode waveguides with refractive indices of cores n_a and n_b are parallel to each other. The refractive index surrounding these waveguides is considered to be constant as n_c. Now consider that in each of the waveguide there is a propagating mode and they are given by, $E_a(x,y)e^{-i(\omega t-\beta_a z)}$ and $E_b(x,y)e^{-i(\omega t-\beta_b z)}$. Where, β_a and β_b are the propagations constants in respective waveguides. Since these waveguides are separated by finite distance, the electric field of a general wave propagation in coupled waveguide structure can be approximated as [93],

$$E(x,y,z,t) = \frac{1}{2}\left(A(z)\,E_a(x,y)e^{-i(\omega t-\beta_a z)} + B(z)\,E_b(x,y)e^{-i(\omega t-\beta_b z)}\right) \quad (5\text{- }1)$$

The basic assumption here is that the waveguides are not too close from each other and also the modes are confined to the waveguides. If the distance between the two waveguides is infinite then the A(z) and B(z) will not depend upon the distance z and will be independent of each other. The presence of waveguide b will cause dielectric perturbation in mode propagating in waveguide 'a' and vice versa.

$$\left(\frac{\partial^2}{\partial x^2}+\frac{\partial^2}{\partial y^2}+\frac{\partial^2}{\partial z^2}+\frac{\omega^2}{c^2}\left[n_c^2(x,y)+\Delta n_a^2(x,y)+\Delta n_b^2(x,y)\right]\right)E = 0 \quad (5\text{- }2)$$

Where, $\Delta n_a^2(x,y)$ and $\Delta n_b^2(x,y)$ are distributions of refractive indices inside the waveguides and $n_c^2(x,y)$ is the distribution around the waveguide. By substituting equation 5-1 in equation 5-2 we have following equation,

$$-2i\beta_a \frac{dA}{dx} E_a(x,y)e^{-i(\omega t-\beta_a z)} - 2i\beta_b \frac{dB}{dx} E_b(x,y)e^{-i(\omega t-\beta_b z)} = \frac{\omega^2}{c^2}\Delta n_b^2(x,y)E_a(x,y)e^{-i(\omega t-\beta_a z)} - \frac{\omega^2}{c^2}\Delta n_a^2(x,y)E_b(x,y)e^{-i(\omega t-\beta_b z)} \quad (5\text{-}3)$$

By taking the scalar product with $E_a^*(x, y)$ and $E_b^*(x, y)$ with above equation and integrating over X-Y plane we obtain,

$$\frac{dA}{dx} = -i\kappa_{ab}Be^{-i\Delta\beta z} - i\kappa_{aa}A \quad (5\text{-}4)$$

$$\frac{dB}{dx} = -i\kappa_{ba}Ae^{-i\Delta\beta z} - i\kappa_{bb}B \quad (5\text{-}5)$$

However, the terms κ_{bb} and κ_{aa} result from the dielectric perturbations to one of the waveguides due to the other waveguide and are very small as compared to the propagation constants for both the waveguides and can be neglected. The terms κ_{ab} and κ_{ba} are related to the power transfer between two waveguides and in fact are complex conjugate of each other. Hence we have following equations. These equations are called coupling equations.

$$\frac{dA}{dz} = -i\kappa_{ab}Be^{-i\Delta\beta z} \quad (5\text{-}6)$$

$$\frac{dB}{dz} = -i\kappa_{ba}Ae^{+i\Delta\beta z} \quad (5\text{-}7)$$

Where, κ_{ba} and κ_{ab} are the coupling coefficients, which are determined by the physical conditions of the waveguide, $\Delta\beta$ is the phase mismatch constant depending on the propagation constants β_a and β_b and can be defined as $\Delta\beta = \beta_a - \beta_b$.

$$\kappa_{ab} = \frac{\omega}{4}\varepsilon_0 \int E_a^* \Delta n_b^2(x,y)E_b(x,y)\,dxdy \quad (5\text{-}8)$$

$$\kappa_{ba} = \frac{\omega}{4}\varepsilon_0 \int E_b^* \Delta n_a^2(x,y)E_a(x,y)\,dxdy \quad (5\text{-}9)$$

Since we are dealing with the case of co-directional coupling assuming that both the propagation constants are positive; the power flow in each waveguide can be defined as,

$$P_a(z) = \frac{|A(z)|^2}{|A(0)|^2} = 1 - F\sin^2(qz) \quad (5\text{-}10)$$

$$P_b(z) = \frac{|B(z)|^2}{|B(0)|^2} = F\sin^2(qz) \quad (5\text{-}11)$$

Where

$$q = \sqrt{\kappa^2 + \Delta\beta^2} \quad (5\text{-}12)$$

F is the maximum coupling efficiency will be observed at $\kappa_{ab}=\kappa_{ba}$, and is given by,

$$F = \left(\frac{\kappa}{q}\right)^2 = \frac{\kappa^2}{\kappa^2+\Delta\beta^2} \quad \text{(5- 13)}$$

The power coupling efficiency from waveguide a to waveguide b reaches maximum value at

$$z = \frac{\pi}{2q}(2m+1) \quad \text{(5- 14)}$$

Where m= 0, 1, 2, ...
The coupling length is defined as the length at which m=0; therefore, we have

$$L_c = \frac{\pi}{2q} = \frac{\pi}{2\sqrt{\kappa^2+\Delta\beta^2}}. \quad \text{(5- 15)}$$

If the two waveguides are identical then the 100% power transfer will occur at i.e. $\Delta\beta=0$, $\beta_a=\beta_b$ we have,

$$L_c = \frac{\pi}{2\kappa} \quad \text{(5- 16)}$$

When the two waveguides are symmetrically spaced like the ones shown in Figure 5- 6 the total structure is longitudinally invariant; however, it causes excitation of the fundamental mode in one of the waveguides results into excitation of two normal modes of the total structure which are popularly known as supermodes, each of these supermodes have different phase velocities and thus propagate along the two-waveguide structure that results in oscillation of light i.e. continuous transfer of power from one waveguide to the other. When a light beam is incident on guide 'a', it will excite both the supermodes i.e. even and odd, also denoted as symmetric and antisymmetric modes. For a travels distance equal to the coupling length a phase shift of π occurs between these supermodes and then almost all the power will transfer to waveguide 'b'. Hence the principle of a directional coupler is based on the phenomenon of interference between the two (or more for multiple waveguide coupling) supermodes [94]. The distance L_c is the coupling length as it equals the distance over which the guided power transfers from one of the individual guides into the other.

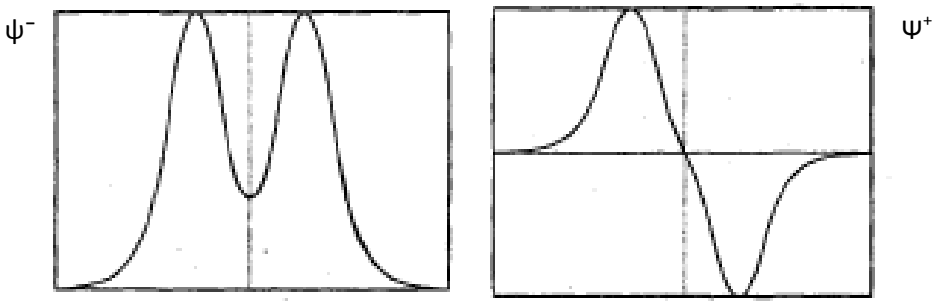

FIGURE 4- 21: MODAL ELECTRIC FIELDS FOR SYMMETRIC AND ANTISYMMETRIC SUPERMODE RESPECTIVELY

Above diagram shows the modal electric fields of the two lowest supermodes in an optical waveguide. One should bear in mind that the total power transfer from waveguide to another is strictly not possible because even and odd supermode cannot completely cancel each other in an individual guide because of their field distributions in a single guide.

Wavevectors in case of symmetric supermode and antisymmetric supermodes are given by.

$$\beta^{+} = \beta + \kappa \tag{5- 17}$$

$$\beta^{-} = \beta - \kappa \tag{5- 18}$$

$$\Delta = \beta^{+} - \beta^{-} = 2\kappa = \frac{2n}{\lambda}\Delta n_{eff} \tag{5- 19}$$

Now for the anisotropic section the core birefringence induces different index profiles for the TE and the TM modes (TE modes have polarization in the x direction, parallel to the substrate plane) and consequently the TE and TM modes have different propagation constants β_{TE} and β_{TM}. In the directional coupler the optical propagation can be expressed in term of two supermodes, even and odd, of the two waveguides system. $\Delta\beta_{TE}$ and $\Delta\beta_{TM}$ are the differences of the two supermodes for the quasi-TE and the quasi-TM modes. The coupling length is the length necessary to have a complete energy transfer. The coupling lengths for the quasi-TE and quasi-TM modes are the following:

$$L_{TE} = \frac{\pi}{\Delta\beta_{TE}} \approx \frac{\lambda}{2.\Delta n_{effTE}} \tag{5- 20}$$

$$L_{TM} = \frac{\pi}{\Delta\beta_{TM}} \approx \frac{\lambda}{2.\Delta n_{effTM}} \tag{5- 21}$$

Where, Δn_{effTE} and Δn_{effTM} are the differences of the effective indices of the supermodes for TE and TM polarization respectively.

With planar alignment conditions of the LC polymer, the TM mode has a lower effective index than the TE mode. Consequently, the confinement is higher for the TE mode than for the TM mode, and the coupling length of the TM mode will be shorter than for TE.

To separate properly the two polarization modes, the length L_C of the directional coupler needs to be an integer i of the TE coupling length and an integer j of the TM coupling length, with j>i and i, j having different parity. $L_c = i * L_{TE} = j * L_{TM}$ with j> i and (i even and j odd) or (i odd and j even).

5.3 Liquid Crystal as a Waveguide

So far we have seen the fundamentals of waveguides, formation of modes in the waveguide and the coupled mode theory. We have also taken a brief overview of polarisation issues and different techniques to overcome them. First we will answer the question of why liquid crystal has been used for the core and what is the role of liquid crystals in separating the polarisation of the propagating light wave. Liquid crystals are of potential interest for diversity of applications in optical communication because of large variety of interactions on electro-optic, magneto-optic and acousto-optic effects. Moreover, the electro-optic coefficient of the nematic liquid crystal is much larger than any available best electro-optic material [95]. One of the first waveguides based on liquid crystals were reported in [96]. One of the most important aspects of the liquid crystals for waveguide fabrication is that the liquid crystal material is birefrigent. We will be using this optical anisotropy to separate the polarisations of the input wave.

The idea is to fabricate zones of isotropic and anisotropic phase of liquid crystal on the same substrate. In other words, these two phases of liquid crystal will be trapped on single silicon substrate in the end helping us to separate the TE and TM modes from each other. Sensitivity to input polarisation has always been the issue for devices in optical communications; especially in guided optics TE and TM modes do not have same propagation properties. Polarisation sensitivity has turned out to be one of the drawbacks of the optical communications as the input polarisation cannot be controlled. Hence the use of liquid crystal will address the issue of separation of polarisation so that the devices based on our principle will behave in similar manner for all input polarisations.

In a general case, polarisation insensitive waveguide devices include three sections: the first contain the polarization splitter, the second one include the own function of the device: filtering, spatial routing, etc. While the last one recombines both polarisations in the output waveguide. However, the isotropic waveguides can not address the splitting of the polarisations. For many polarization sensitive optical devices, separation of orthogonal polarization states with polarization splitters is then the straightforward solution. This can be achieved only when the isotropic and anisotropic area of the material exists on the same substrate.

5.3.1 Principle of Anisotropic Coupling

When the physical separation of the waveguides is reduced, the two waveguide fields overlap and this allows the exchange of energy. The coupling length is given by the distance to obtain the complete the mode transfer from one guide to the other one. In the case of two anisotropic waveguides, two different coupling distances are present for TE and TM polarization. Knowing the coupling coefficient for each orthogonal mode, it is possible to adjust the coupling length to separate TE and TM orthogonal modes.

Most of optical devices use isotropic waveguides to achieve the targeted optical function. Therefore, obtaining simultaneously the polarization splitting and the optical function requires anisotropic and isotropic sections of the waveguide on the same substrate.

It is essential to take into account the degree of anisotropy while fabrication, lower is the anisotropy larger will be the coupling length. Hence it is necessary to use the materials which possess large anisotropy in order to restrict the coupling lengths to minimal.

5.4 Conclusions

So far in this chapter we have discussed that the polarisation sensitivity hampers the optical performance of any waveguide based optical device. We have also taken an overview of the possible solutions to overcome this issue but these solutions are expensive or can be very cumbersome to put into practise. The heart of addressing the polarisation sensitivity using liquid crystals lies in the birefringence nature of them. Liquid crystals allow us to achieve the separation of polarisation and decided optical function to be realised on the same substrate. This is one of the critical aspects to use the liquid crystal to address polarisation sensitivity. The design parameters and the fabrication of such a waveguide is discussed in the next chapter.

Chapter 6: Fabrication and Characterisation of Waveguide Coupler in Liquid Crystals

6.1 Introduction to reactive mesogens or liquid crystal polymers

Reactive mesogens are the photopolymerisable liquid crystals that can be manufactured by simple deposition of these materials into a birefrigent film [97]. Typical applications of these materials are viewing angle compensation films for liquid crystal display, optical retardation films, quarter waveplate and half waveplate fabrication to name a few. In order to obtain well oriented birefrigent film the substrate on which the film is going to be deposited should undergo the required alignment techniques. These techniques can be either photo-alignment or alignment by traditional rubbing of the surface. Various different types of reactive mesogen films can be produced namely homogeneously aligned, homeotropically aligned, hybrid aligned and cholesterics. These films are normally deposited on the polymer surface and the type of reactive mesogen depends upon the surface treatment of the polymer surface and the boundary conditions especially reactive mesogen-polymer boundary and also air-reactive mesogen boundary. In our case we will be using the homogeneous alignment of these liquid crystals. In these birefrigent films the nematic phase and the alignment of the liquid crystal can be "frozen" i.e. the film is in nematic phase after undergoing the polymerisation. This birefrigent film will remain in the nematic state over large of temperatures unlike the usual liquid crystals [98]. Generally speaking the concept of fabrication can be explained as the mixture of appropriate monomer, liquid crystal, the photo-initiator and appropriate surfactant all of them are dissolved in a solvent. This solution is known as liquid crystal polymer or reactive mesogen is eventually deposited on the surface which has already undergone the alignment treatment for desired alignment direction. These deposited films are sometimes readily aligned depending upon the anchoring energy provided or they need to undergo a heat treatment which is normally dictated by the manufacturer in the datasheet of the reactive mesogen. This particular heat treatment makes sure the removal any possible alignment defects and also evaporation of the solvent. Once the film is coated and aligned (after the heat treatment) it is polymerised forming a dense network of polymer chain and the liquid crystal molecules are frozen in these chains. Photo-polymerisation of the monomer ensures that the anisotropic characteristics of the liquid crystal are conserved. Another important characteristic of these materials is to make complex alignment structures on the same substrate by using the masks i.e. the patterning of the reactive mesogen can be achieved with different liquid crystal orientation on the same substrate. This particular feature can be easily exploited using the photo-alignment technique. Using rubbing technique it is not possible to have two different molecular orientations on the same substrate. Another remarkable feature of these reactive mesogens is the possibility of the temperature dependent polymerisation. The phase of the liquid crystal can be trapped by polymerising the birefrigent film at different temperature to trap the desired phase of the same [98]. Since the patterning of the film is possible, the thermal patterning of these films is equally

possible. Therefore, one can polymerise different zones of the substrate at different temperatures by trapping different phases of liquid crystal in these zones notably nematic and isotropic phase of the liquid crystal. Thermal patterning can be achieved by traditional buffing method as well. Therefore, such a material presents with wide variety of designs by using polymerisation under the mask. Birefringence of a nematic liquid crystal is a function of temperature i.e. as the temperature increases the birefringence decreases. Hence if we can polymerise the optical film of a reactive mesogen at different temperature, the birefringence value of such material can be tuned. If the temperature goes beyond nematic-isotropic temperature, then the isotropic phase of the liquid crystal can be polymerised with a birefringence equal to zero. This allows us to have two different phases of the nematic liquid crystal (isotropic and anisotropic) on the same substrate.

6.1.1 Isotropic and Anisotropic phase on the same substrate

The process of achieving the isotropic and anisotropic phase on the same substrate was carried using two different alignment techniques namely photo-alignment and alignment by rubbing. The liquid crystal polymer used for these two techniques were different. First, we will mention the process using photo-alignment. We used the similar photo-alignment materials which we have mentioned and detailed in the chapter 2. As mentioned earlier the first step of the photo-alignment is exposure of linearly photopolymerisable polymer by using the polarised UV. Since our objective is to have the isotropic and anisotropic on same substrate we need not use the mask for making the first exposure with polarised UV light. Once the first exposure of LPP after it underwent deposition and the baking of the same; the deposition of the LCP was carried out in order to have the thickness of 1.5 microns. Thereafter, the deposited LCP underwent the heat treatment i.e. it was baked at 52°C during 3 min to align the unaligned areas. Now the substrate was kept under the mask and the uncovered areas of the mask were exposed by UV under the nitrogen atmosphere in order to trap the anisotropic phase of the LCP because this particular material does not return to aligned anisotropic phase once it is treated at temperature above nematic-isotropic temperature. Thereafter the covered areas are exposed at temperature of 65°C, well above the nematic-isotropic temperature of the LCP again under the nitrogen atmosphere with the same UV energy as for the anisotropic phase. Below diagram shows how the process was carried out.

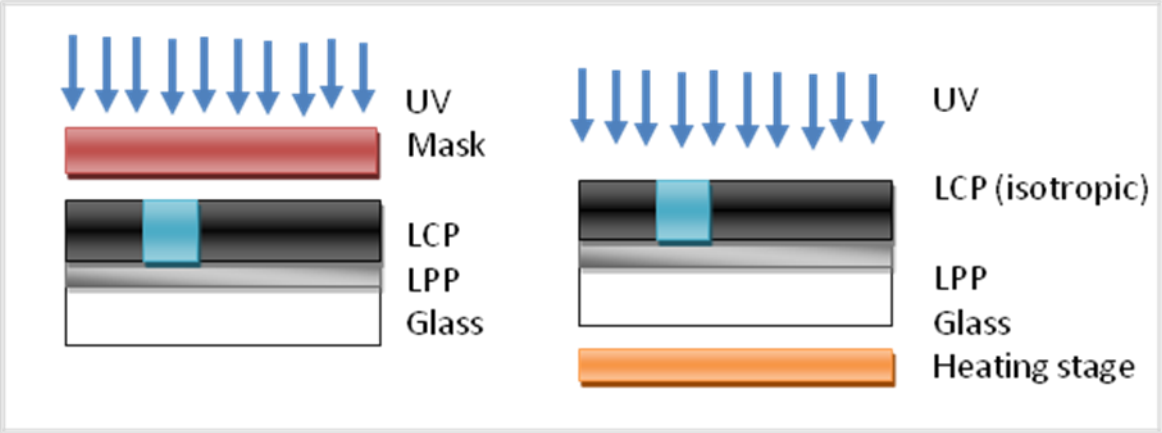

FIGURE 6- 1: POLYMERISATION OF ISOTROPIC AND ANISOTROPIC PHASES ON THE SAME SUBSTRATE

The same experiment was performed using the rubbing method as we had to change the alignment technique due to the fact that the availability of the LCP and LPP was scarce and it was not evident to buy the product. For the traditional rubbing method we used the conventional polyimide as an alignment layer while the reactive mesogen was RMS-03-001C provided by the Merck. In order to carry out the entire process we used polyimide Nissan 410 for homogeneous alignment diluted 10 times in a varnish provided by same manufacturer so as to have a very thin film (approximately 50 nm) deposited on the glass surface. After the deposition of polyimide it underwent the traditional heat treatment of baking at 180°C for 2 hours. Once the polyimide surface is dried it was rubbed in a desired direction. Then the reactive mesogen was spin coated to have the appropriate thickness of it. Coated film underwent a heat treatment of 5 min at 60°C to remove the defects in the film and to improve the alignment quality. Then, it is polymerised under the mask using UV light with the energy of $1J/cm^2$ to trap the anisotropic part of the reactive mesogen. Once the anisotropic part was polymerised the mask was removed and the temperature of the substrate was raised up to 100°C and polymerisation was carried out at this temperature. Both the polymerisation processes were carried out under constant flow of nitrogen to avoid the oxygen affecting the film.

6.2 Fabrication of the waveguides

We have already seen the theory of waveguides and their importance in the telecommunication industry. We have also overviewed the liquid crystal waveguides and their need in the waveguide fabrication. It should be noted that the above mentioned experiments were carried out on the glass substrates; however, the fabrication of the actual waveguide will be fabricated on the silicon substrates. The advantage of carrying out the process on silicon wafers is for the final cleaving of the waveguides. In order to have a clean cut cleaving of the wafer a mark where the wafer should be cleaved after the entire process was made.

6.2.1 Design considerations of the waveguide

It is very essential to know the design of the waveguide which will allow us to separate the polarisations in different branches. It is also necessary to see selection of material for the cladding of the waveguide. The minimum thickness required for the cladding as well as the core. Especially the core thickness which should limit propagation of single mode and hence single mode propagation conditions should be satisfied. The necessity to have single mode propagation through the waveguide is because the multimode waveguides can cause problems with crosstalk and the waveguide becomes lossy. The anisotropic zone on the waveguide will perform the operation of polarisation separation while the isotropic zone will perform the optical function assigned.

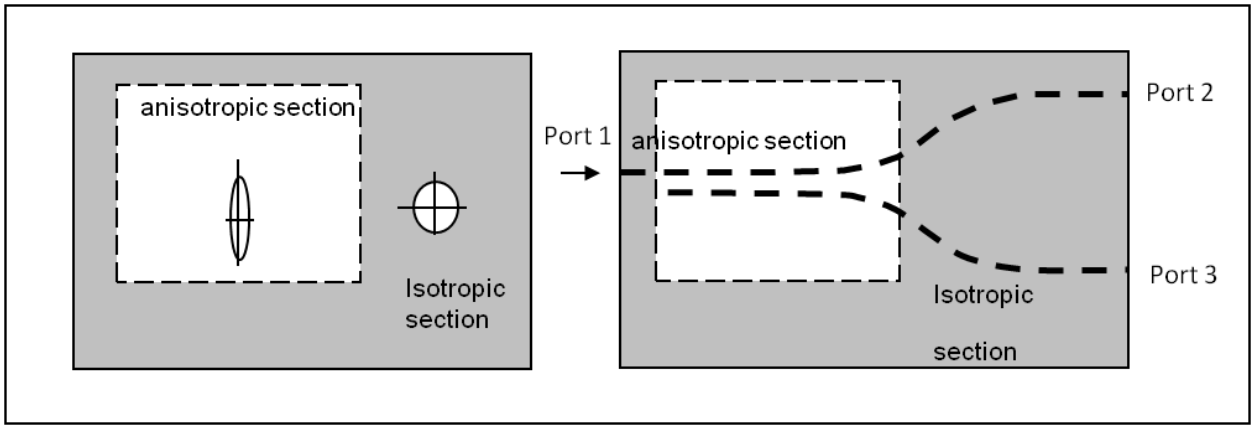

FIGURE 6- 2: SUBSTRATE WITH ANISOTROPIC AND ISOTROPIC AREA. PRINCIPLE OF ANISOTROPIC COUPLING AND DESIGN OF A WAVEGUIDE

The waveguide in consideration is a square waveguide. Above diagram shows that the light enters the anisotropic section where the length of this region has been adjusted so as to make the coupling of 2 modes in two different branches.

The directional couplers have been already achieved using anisotropic material [82], a geometry of waveguide induced anisotropy, etc. However, for all tested solutions, the devices are made up by the same material or they use the induced anisotropy with asymmetrical waveguides. In the last case, the induced birefringence is very low; this leads a very large coupling length. To overcome this difficulty, we propose to use a Liquid Crystal photo-Polymer or reactive mesogen (RM). The thermotropic liquid crystal pre-polymer has the property to have both isotropic (liquid) and anisotropic (liquid crystal) phases that depend on the temperature. The mesophase of photopolymer is the nematic phase which has uniaxial symmetrical property. An alternative technology has been already use by polymer poling but the induce material birefringence is very low about 10^{-3} [99].

This material can be easily deposited onto a substrate by a standard spin coating process to make a thin film compatible with the geometrical and optical targeted characteristics of waveguide core. Moreover, the birefringence of liquid crystal in nematic phase depends on the temperature. This property provides a degree of freedom on the value of the birefringence of the waveguide. Depending of the temperature of the LC pre-polymer polymerization; we obtain either an anisotropic or an isotropic film.

These two optical characteristics can be obtained on the same substrate by using a specific mask to imprint anisotropic section in isotropic film of LC polymer. On the cladding layer, the pre-polymer is spin-coated. The polymerization process will be achieved in two steps at two different temperatures: At room temperature, the anisotropic sections are obtained by photo-polymerization through a specific mask. Removing the mask and heating the substrate in isotropic temperature, all the substrate is exposed to UV light so that previously unexposed areas will be trapped in the isotropic phase. The substrate with these two sections is then etched to fabricate the waveguides.

Due to large birefrigent properties i.e. with extra-ordinary refractive index of 1.63 and ordinary refractive index of 1.51 the coupling lengths were considerably reduced to only few microns. Coupling lengths for TE mode and for TM mode were calculated as a function of the gap between the two branches in the anisotropic zone. The ratio of coupling lengths for TE and TM mode were calculated in order to make the complete transfer of power for TM mode in one of the branches while the complete transfer of power for TE mode in the other branch of the waveguide. These lengths were also optimised for extinction ratio. Higher extinction rations can be obtained by increasing the coupling length. According to the coupled mode theory we have a coupling length $L_c = i * L_{TE} = j * L_{TM}$ for our waveguide where j>i (since $L_{TE} > L_{TM}$) and (i is even and j is odd/ is odd and j is even) i.e. the coupling lengths for TE and TM mode are integral multiple of each other.

6.2.2 Geometrical characteristics of the coupler

The design of the waveguide was not done by the author but was realised by one of the members of the project (Prof. Michel Gadonna, ENSSAT, Lannion, France) and author is summarising the results with his permission. We have designed a directional coupler using a liquid crystal polymer as the core material of the waveguide. The liquid crystal polymer used was the mesogen RMS-03-001C from Merck Corporation with n_o of 1.51 and n_e of 1.63 at the wavelength of 1.55 µm. The cladding layer was a low refractive index polymer from SSCP Corporation with an index value of 1.40 at 1.55µm. First we analyze the PLC waveguide with BPM software for the quasi-TE and the quasi-TM modes. We have considered a square waveguide core with a side from 1 to 2 µm. The limit for single mode propagation for the quasi-TE mode was found to be 1.8µm. The coupling length increases with the confinement value and with the core side. In order to have a short coupling length, the core side is chosen to be 1.5 µm. In this case the effective indexes are 1.441 for TM and 1.540 for TE, giving a birefringence (n_{effTE} - n_{effTM}) of 0.1. In a first time, the analysis of the directional coupler by the supermodes of the two waveguides system considers that the coupler is a straight coupler. This device layout is also analysed with full 3-D vector BPM and FDTD software. As shown in figure 2 there is only slight difference between the different methods.

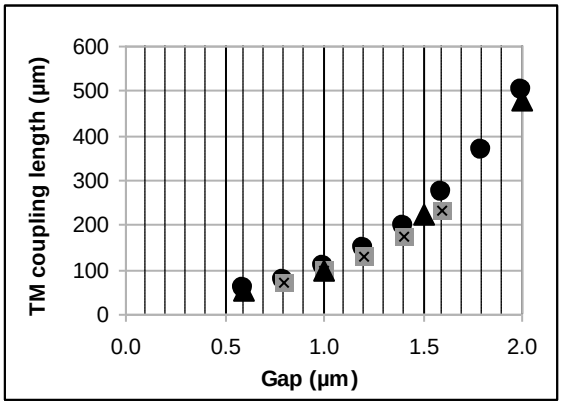

GRAPH 6- 1: TE COUPLING LENGTH IN FUNCTION OF THE GAP WITH SUPERMODES ANALYSIS (CIRCLES), 3-D BPM (TRIANGLES) AND FDTD (SQUARES)

The coupling length of the TE mode becomes twice the TM coupling length (i=1, j=2)at a gap of 0.7 µm and with a TE coupling length of 150 µm. The TE mode is coupled only once and exits at the port 3, while the TM mode is coupled twice and is detected at the port 2. The case of i=1 and j=4 is obtained at a gap of 1.3 µm and a coupler length of 650 µm.

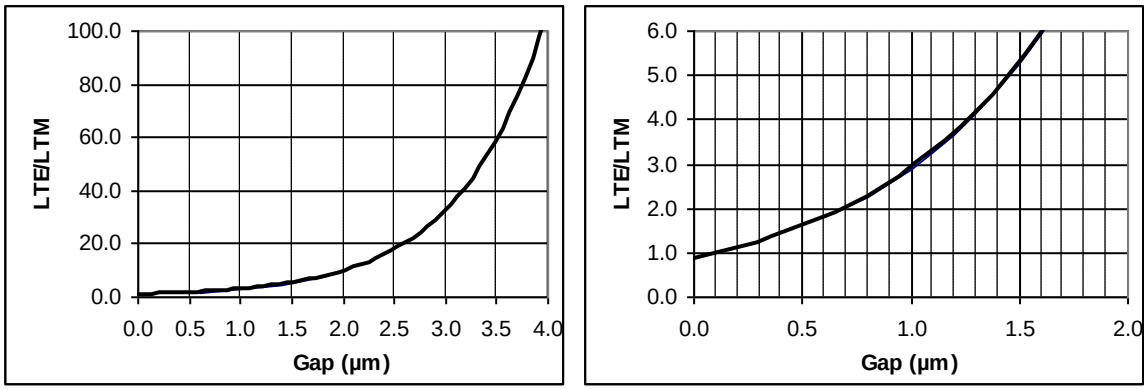

GRAPH 6- 2: RATIO OF TE COUPLING LENGTH ON TM COUPLING LENGTH

In the following we used the values obtained with the straight directional coupler to do the analysis of the polarization splitter shown figure 1 with S-bends at the port 2 and 3. For taking account of the s-bends we will use full vector 3-D BPM for these analysis. The S-bend has a length of 500 µm and a 1.5 mm radius. The coupling contribution of the S-bends will modified the effective length of the straight coupling part.

In a first step the analysis was made for (i=1, j=2) and (i=1, j=4) in order to have the shorter polarization splitter. The results are shown in Table 1. The tolerance against fabrication errors are also given as well as the wavelength bandwidth in function of the extinction ratio (ER) level. The extinction ratio is given as the power of the desired rejected polarization on the input power. We see that for these two configurations the tolerances are very low and below the lithography resolution available in our laboratory. To increase the fabrication tolerance it is necessary that the coupler length for (i=1, j=2) is longer and for that the waveguide birefringence must be lower. A PLC with a lower anisotropy must be used.

Taking account of these conclusions we studies the behaviour of a polarization splitter with quasi-no coupling for TE mode and the TM mode coupled to the second waveguide (i=0, j=1). In order to have a good transmission for the TE mode, the TE coupling length must be as high possible compared to the TM coupling length. In our work we limit the coupler length at 1 mm. At a gap of 2.5 µm the TM coupling length is 940 µm, and the TE coupling length is about 20000 µm, giving a ratio of 20. This value gives an extinction ratio for TE mode of more than 20 dB. Except for the gap, the tolerances are in fabrication capacity, for a 30 dB ER the gap needs to be well controlled but for a 20 dB ER the tolerance is greater.

(i, j)	Gap g (μm)	Length L_c (μm)	Tolerance / ER =20 dB			Tolerance / ER=30 dB		
			L_c (μm)	G(μm)	λ e(mm)	L_c	G	Λ
(1, 2)	0.6	40	±12	±0.01	±0.01	±1	±0.001	±0.01
(1, 4)	1.3	580	±10	±0.01	±0.01	±3	±0.001	±0.01
TM (0,1) TE	2.5	940	±60	±0.05	±100	±15 NA	±0.01 NA	±50 NA

TABLE 6- 1: PARAMETERS AND TOLERANCE AGAINST FABRICATION ERRORS AND WAVELENGTH FOR THREE POLARIZATION SPLITTER CONFIGURATIONS

Taking into account these observations based on simulation, we studied the behaviour of a polarization splitter with quasi-no coupling for TE mode and for TM mode coupled to the second waveguide (i=0, j=1). In order to have a good transmission for the TE mode, the TE coupling length must be as high as possible compared to the TM coupling length. In our work we limit the coupler length at 1 mm. At a gap of 2.5 μm the TM coupling length is 940 μm, and the TE coupling length is about 20000 μm, giving a ratio of approximately 20. This value gives an ER for TE mode of more than 20 dB.

On a concluding remark, the accuracy in the results will depend upon the configuration we have chosen. However, we should remind that this solution is strongly correlated to the photolithography process.

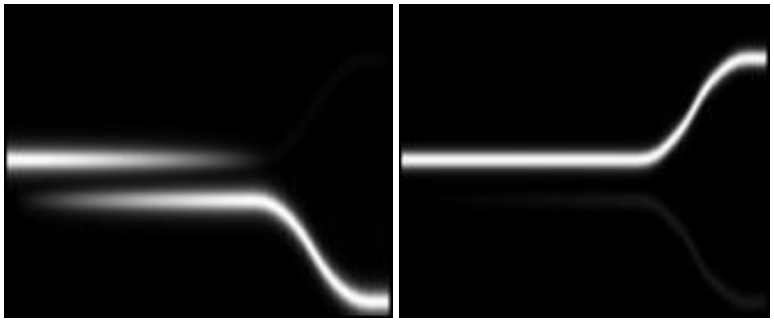

FIGURE 6- 3: BEAM PROPAGATION SIMULATION FOR A POLARIZATION SPLITTER WITH A GAP OF 2.5 μM AND LC OF 940 μM FOR TM AND TE MODES AT 1.55 μM WAVELENGTH RESPECTIVELY

Above figure shows the coupling of the TM mode and quasi no coupling of TE mode. In the picture on the right slight transmission for the TE mode in other coupler can be seen.

6.2.3 Process of waveguide fabrication

Process with photo-alignment

Initially the process was carried out using the photo-alignment technique. We had done some preliminary experiments on the substrate with LPP and LCP. For the low refractive index glue PC 373 (1.37 at 850nm) from SSCP Corporation was initially used as a cladding layer. Initial waveguides were fabricated on the glass substrate. The glue PC 373 was dissolved in the solvent cyclopentanon with a concentration of 70% -30% by weight and was filtered using 0.45 microns PTFE membrane filters. Thereafter, it was deposited on the glass substrate for 40 seconds with the speed of 3000RPM. Uniform film of PC373 was obtained. This film was polymerized under nitrogen atmosphere using the 254nm UV as the photoinitiator for this glue triggers at that wavelength. Since the surface of PC373 is highly fluorinated the wetability of this surface is very feeble which makes the deposition of any film very difficult. Hence the substrate underwent the plasma oxygen treatment to improve the temporary wetability of the surface.

Immediately after plasma oxygen treatment, a layer of LPP was deposited at the speed of 3000RPM for 60 seconds. Then, the substrate was baked at 180°C for 5 min to evaporate excess solvent from the film. This substrate with PC373 and LPP was then exposed to linearly polarised UV light where the direction of polarisation decided the direction of alignment with the UV energy of 500mJ/cm^2.

Then a layer of LCP was deposited at a speed of 1500 RPM for 120 seconds. Thereafter, the substrate underwent the process mentioned in section 6.16.1.1. This substrate was further was etched to form the waveguides. The etching process for these waveguides in mentioned in section 6.2.4

Process with rubbing

Since we had the problem relating to photo-alignment products we went for the rubbing process. PC373 was replaced by low refractive index glue PC404F (1.38 at 850nm) from SSCP Corporation was used as a cladding layer. The reason for the change is because this material has photoinitiator at 365nm it was technologically easier to handle for nitrogen polymerisation. This material has no mesogenic property and after spin-coating process an isotropic layer is obtained.

The material for core was reactive mesogen RMS-03-001-C (Consult datasheet from the manufacturer for more details: see appendix) from Merck Corporation. Polyimide SUNEVER 410 from Nissan Corporation served as an alignment layer for the reactive mesogen. Deposition of PC404F i.e. cladding was carried out in 2 steps in order to achieve

thickness around 10 microns as the theoretical limit for the cladding thickness as 7 μm. The reason to carry the deposition in two steps as it is difficult to achieve the thickness of 10 μm and also have the required flatness using spin coating that is why this two step spin coating approach was adapted. PC404F was first dissolved in 30 % by weight of cyclopentanon. The dissolved solution was then filtered using PTFE membrane 0.45 micron filters. Filtered solution was then deposited on well cleaned Silicon wafer at the speed of 3000 RPM at 40 seconds; immediately after the bid-edge was removed using the same solvent at lower speed by putting few drops of cyclopentanon on the edge of the wafer while spinning. The wafer was kept at 130°C (Temperature at which cyclopentanon evaporates) for 1 minute in order to ensure there is no solvent left in the film. The film was polymerized under nitrogen atmosphere at 365 nm with the energy of 2 J/cm^2. Wafer was treated in plasma oxygen for 2 minutes in order to improve the adhesion for second deposition. Since PC404F is highly fluorinated plasma oxygen treatment is necessary.

The second deposition was carried out exactly similar manner as the first one. Just before the deposition of polyimide, wafer with PC404F was kept in plasma oxygen for 2 minutes to improve the adhesion of polyimide on the cladding layer. A fine layer of polyimide was deposited on PC404F at the speed of 3000 RPM at 20 seconds. According to conventional heat treatment for polyimide the wafer was kept at 180°C for the period of 2 hours. In order to achieve a good alignment of reactive mesogen we put the silicon wafer with polyimide in plasma oxygen for 2 minutes and subsequently rubbing it in desired direction. In order to achieve the desired thickness of reactive mesogen spin coating was performed in 2 cycles (measured thickness was approximately 10 μm) The first cycle the wafer was spun at 1000 RPM for 5 seconds and the second cycle the wafer was spun for 120 seconds at the speed of 600 RPM. The bid-edge removal for reactive mesogen was carried at lower speed by putting few drops of solvent PGMEA (solvent used for RMS03-001-C) at the edge of the wafer while spinning. After the spin coating it was observed that there were quite a lot of defects on the reactive mesogen surface which were removed by keeping the wafer 65°C for 5 minutes. It was observed over the period of time these defects they disappear and one can obtain a uniform alignment of reactive mesogen layer. It should be noted that hardly any de-wetting was observed during the period of 5 minutes. Polymerisation of anisotropic and isotropic was carried under the mask (the mask was not in contact with the liquid crystal polymer during the exposure). First polymerization of anisotropic phase was achieved at room temperature by exposing the areas not covered with UV protecting film at the energy of 1 J/cm^2. However, the areas under UV protecting film are not polymerized and therefore the wafer was kept at 100°C while polymerizing at same energy by removing the mask.

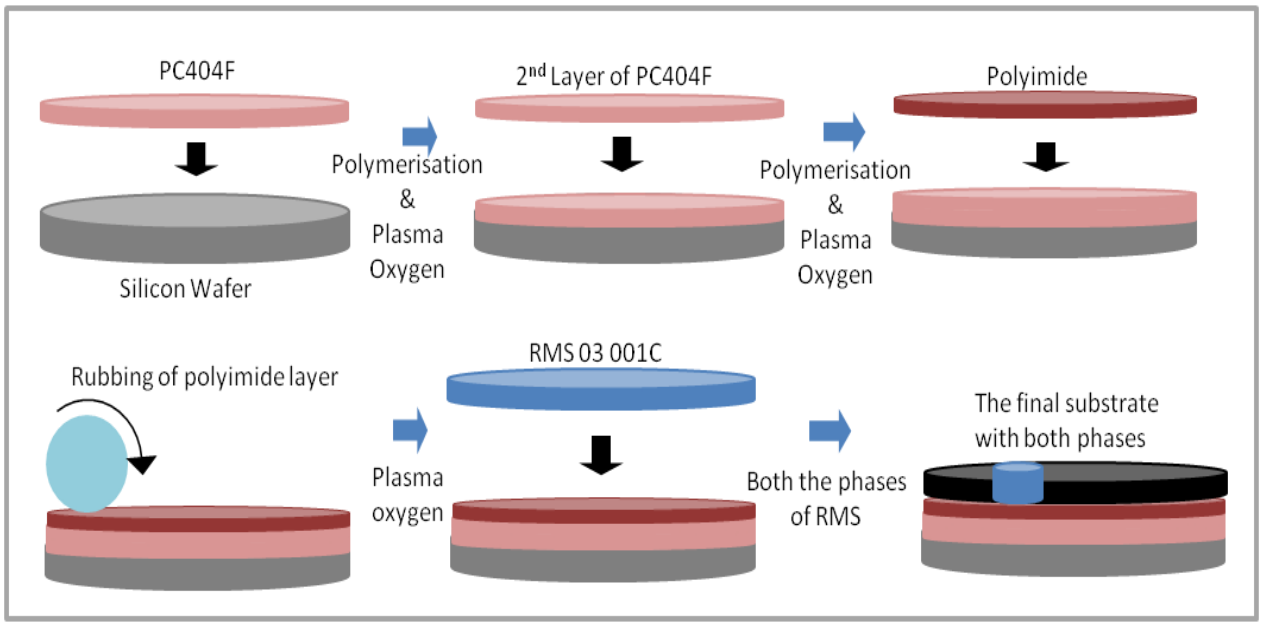

FIGURE 6- 4: ENTIRE FABRICATION PROCESS ON SILICON WAFER

Above diagram explains the step by step fabrication of the cladding and core assembly on the silicon wafers. Now we will explain in brief the process of etching the waveguides.

6.2.4 Etching of the waveguides

Etching experiments were performed in CCLO, Lannion. The experiments were not performed by the author but were done by the authors mentioned in the [100]. However, we will take a brief overview of how they were done. Also, they were done on the glass substrates and also on the silicon substrates provided by the authors of this manuscript. The thermal patterning process leaves a wafer with a cladding and a core layer featuring anisotropic and isotropic regions. The next step is to etch waveguides in this core layer. This is done by oxygen plasma reactive ion etching (RIE) with a silica mask [100].

First we will mention the etching process for the samples with photo-alignment. Initially, a layer of SiO_2 approximately 30nm was deposited on the substrate followed by adhesion improving agent HMDS was spin coated. Then a layer of photoresist (SPR 700) was deposited on the substrate. This substrate was then placed on the mask aligner and then the photoresist was exposed under the designed mask for 3.5secs. After development, the sample was brought in etching chamber. Then, the film was etched in 4 steps with 120secs, 420secs, 720secs and 1420secs. Etching was performed across two zones.

A silica layer (~25 nm) is first deposited on the sample by sputter coating. Then, a layer of SPR700 photoresist (~0.14 µm) is deposited by spin coating and the image of the

waveguides is transferred from a mask to the photoresist by contact photolithography. After development, the sample is brought in the RIE chamber and the uncovered silica is etched in SF_6 plasma. Next, the polymer core layer is etched in oxygen plasma, where the remaining silica pattern acts as a mask. The progression is followed by laser interference and the etching is stopped when the cladding layer is uncovered.

6.3 Results and Discussion

Here we will discuss the results of the thermal patterning; also we will make certain observations regarding the preliminary fabrication process of the waveguide. The brief overview of the etching experiments where we will demonstrate the etched waveguides. Finally, we will consider the injection of light in the waveguides and losses of the light. Also, we will show whether the principle of polarisation separation actually works.

6.3.1 Thermal Patterning of the reactive mesogens

To begin with we will analyse the substrate with isotropic and anisotropic phase using two different alignment techniques as well as two different liquid crystal polymers. A photo below shows the isotropic and anisotropic phase using photo-alignment technique. The brighter area shows the anisotropic part while the dark area shows the isotropic part. The photograph has been taken under polarising microscope. The border between the isotropic and anisotropic phase is diffusing because the mask was not touching the LCP film.

FIGURE 6- 5: ANISOTROPIC AND ISOTROPIC PHASE ON THE SAME SUBSTRATE

The photo below shows the same process using rubbing technique with RMS-03-001C as reactive mesogen.

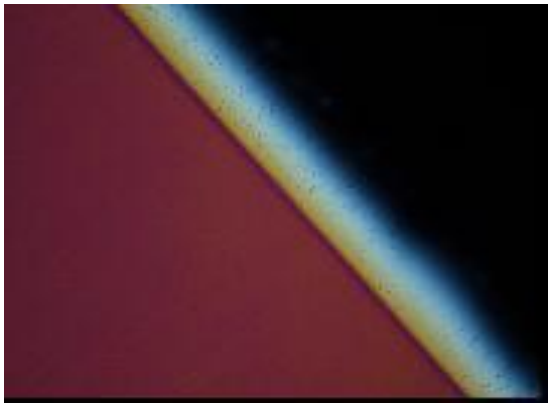

FIGURE 6- 6: ANISOTROPIC AND ISOTROPIC PHASE ON THE SAME SUBSTRATE WITH RUBBING TECHNIQUE

The thickness of the LCP is approximately 1.5 μm. The picture above shows the anisotropy and isotropy on the same substrate taken under the polarising microscope. Red side of the picture is an anisotropic phase while the dark side shows the isotropic phase. The border between these two phases is not very sharp because it was found that the mask was not touching the surface of the RMS03001C. However, both these pictures justify the objective of the experiment.

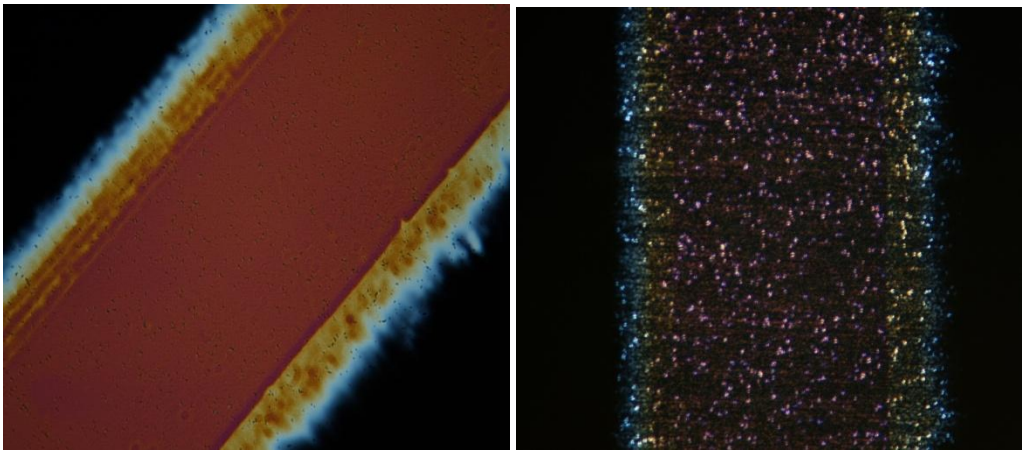

FIGURE 6- 7: BRIGHT AND DARK AREAS OF AN ANISOTROPIC ZONE

Above photographs are the substrate which has a red stripe as an anisotropic zone while the areas besides are the isotropic zone. When the sample was turned by 45° under polarising microscope; as anisotropic phase has birefringence it will have bright and dark states at 45° from each other. The photo on the right we can see that the dark of the anisotropic zone is not completely dark and also it has a pixellic nature, which comes from the defects which were not removed during the heat treatment or the alignment is not well made.

6.3.2 Experimental observations of waveguide fabrication

To begin with it is necessary to know whether the core and the cladding have appropriate thicknesses. We took the profile of each of the layer deposited using a profilometer. Thickness of the cladding layer was observed to be 10 microns with modulation of 30 nm on the surface. The deposition of the polyimide was possible without any apparent defects or de-wetting of the surface. Adhesion of reactive mesogen on the polyimide was very good at temperature required for heat treatment (65° C) as hardly any de-wetting was observed. However, there was some de-wetting at the edges while polymerizing in isotropic state i.e. at 100° C. Thickness of 1.5 microns for the reactive mesogen layer was achieved with modulation of again 30-40 nm on the surface, which is well within the flatness requirements according to simulation results. Presence of plasma oxygen treatment before each and every deposition ensures the adhesion and also the quality of the deposition. Heat treatment for the reactive mesogen after the spin coating is necessary in order to remove the defects. Complete removal of defects can only be achieved by increasing the anchoring energy, hence by increasing number times the polyimide surface has been rubbed. Thorough cleaning of silicon substrates ensures proper deposition of the cladding layer henceforth the following layers. Boundaries of isotropic and anisotropic areas were diffused because of the home made mask, made up of UV protecting film. The results can be improved by using a proper mask under the mask aligner. Following figures represent topology of the cladding layer.

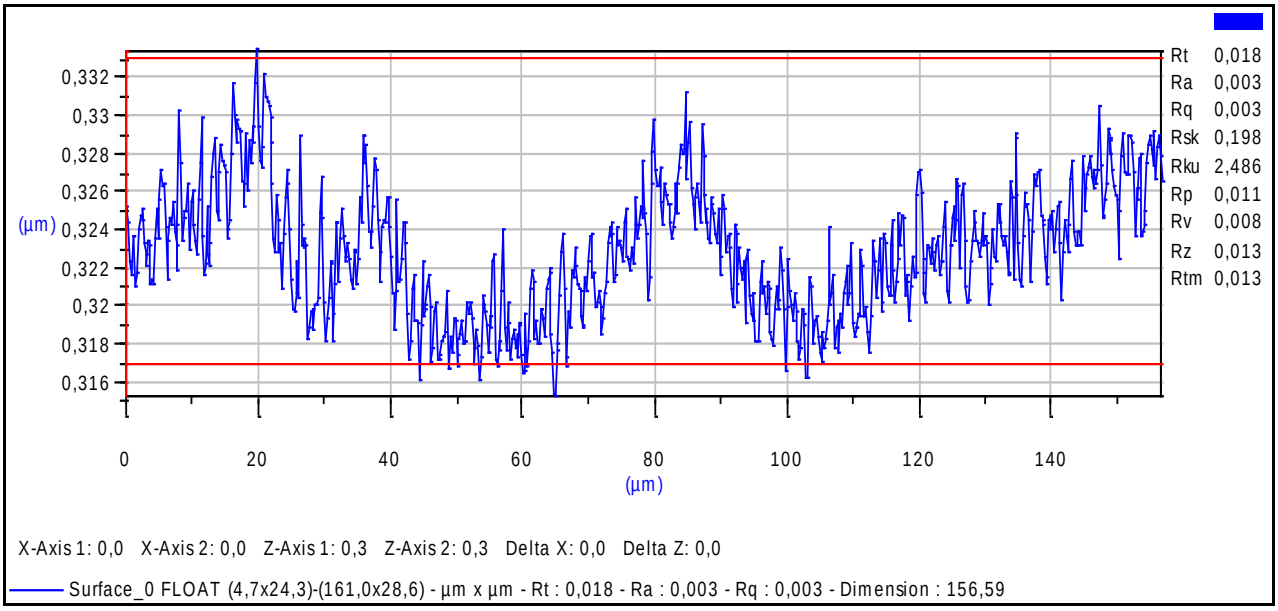

FIGURE 6- 8: TOPOGRAPHY OF THE CLADDING LAYER

6.3.3 Profile of the etched waveguide

First we will discuss the samples with LPP and LCP combination. It is mentioned that the etching of the waveguide was done in 4 steps and after 1420secs the etched depth for isotropic zone was between 1.4 microns to 1.6 microns and for anisotropic zone there was a lot of fluctuation of the etched depth. The maximum was observed at 0.5 microns.

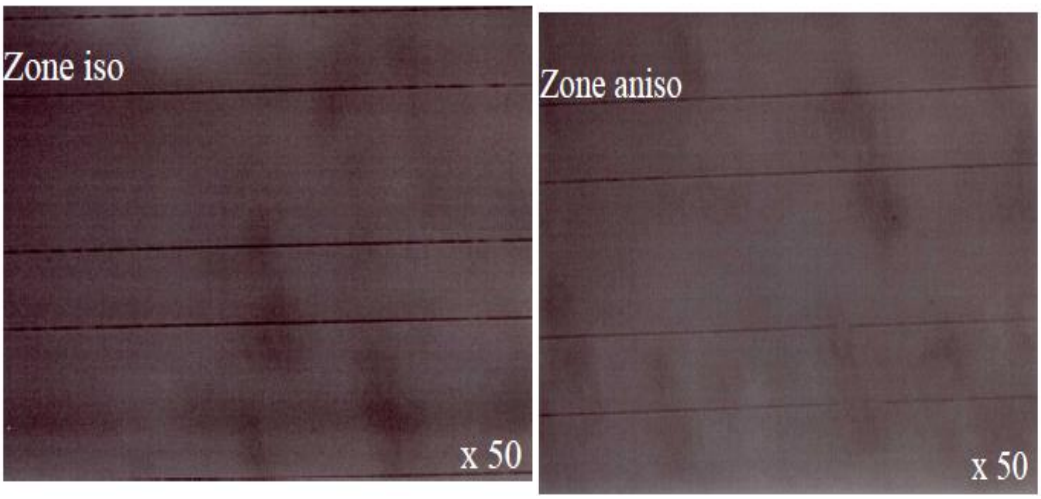

FIGURE 6- 9: ETCHED WAVEGUIDES ON ISOTROPIC AND ANISOTROPIC ZONES

One can clearly see that the anisotropic zones are badly etched. It can be improved by increasing the etching time. It is likely that the edges had bigger thickness due to spin to coating was done on square substrates. Therefore, when the mask was pressed on the film it was not touching the actual film because of the higher thickness at the borders. Therefore, it is necessary to remove the bid edge just after spin coating in order to make sure that the uniformity of the film across the film.

Now, we will take into consideration the waveguide profile on the silicon wafers. Photographs below demonstrate the quality of the etching and also the structure of the waveguides. The photograph is made of two branches of waveguide which in the end will separate the polarisation modes i.e. each branch will carry a TE and a TM mode.

Figure 6- 10: Waveguide with two branches which separate the polarisations

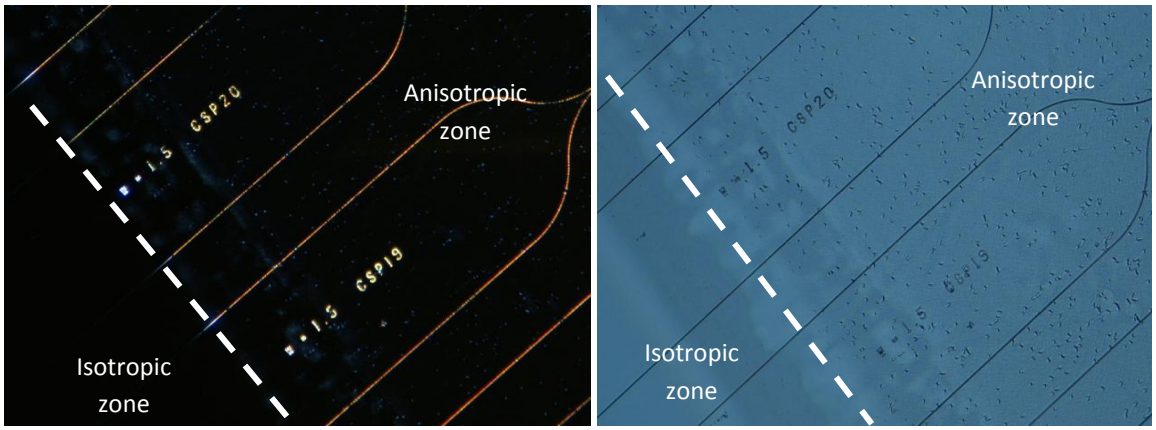

FIGURE 6- 11: DIFFERENT WAVEGUIDE STRUCTURES WITH IMAGES WITH AND WITHOUT CROSS POLARISERS

Polymer waveguide etched in anisotropic area are red coloured due to the birefringence (observed in crossed polarised microscope). On left, in the isotropic area, waveguide appear dark on this picture. We observe a progressive disappearance of anisotropy: Red colour turn to the white and finally extinction of Newton colour that correspond to isotropic optical property. It can be seen that the waveguide will act as a polarisation separator as soon as the mode sees high birefringence when it enters the anisotropic zone and it will continue. One can also see that the waveguides are the remaining part of the anisotropic and isotropic zones the rest of these zones is etched. Two photos show the effect of using crossed polarisers while taking photograph.

We have successfully demonstrated the initial fabrication of the waveguides in liquid crystal i.e. the liquid crystal polymers can be etched to give desired pattern in our case we had the waveguides etched in them. Waveguides were fabricated in liquid crystal polymer which was aligned using photo-alignment; it was observed that the etching depth were variable for the isotropic and anisotropic zones. Perhaps, this was due to different

refractive indices of these zones. Also there might have been thickness variations when they underwent the polymerisation at different thicknesses. In case of RMS-03-001C we have demonstrated slightly better in terms of uniformity of the waveguides.

6.3.4 Preliminary results on light injection and coupling of light

Some couplers have been fabricated with a mask available in the laboratory, but not optimized for PLC materials. The waveguides were etched in an entirely anisotropic PLC layer and studied without upper cladding. Transmission measurements were carried out with a tunable laser, a polarizer and a polarization maintaining fibre at the input. A micro-lens was provided on the tip of the input fibre, so that the waist of the injected beam has a diameter of 2.3 μm. The fibre could be rotated so as to align the input polarization with TE or TM waveguide polarization. The output fibre was a standard single-mode fibre.

The device was observed from above with an infrared camera. Due to the many defects present in this first attempt a lot of light was leaking through the waveguides suggesting the waveguides are far from perfect; however, it was possible to follow the path of the light because of the scattering from the defects. Figure below was obtained by rotation the input polarization so that the light is coupled to both output waveguides. The coupling zone and the waveguide separation can be clearly seen.

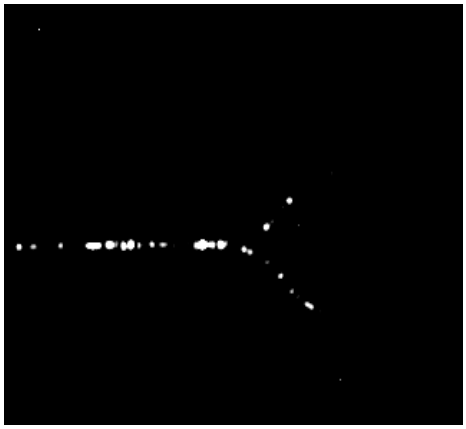

FIGURE 6- 12: TOP VIEW OF THE POLARISATION SEPARATION TAKEN WITH INFRARED CAMERA

The maximum level of transmission was about -23 dB for TE and TM. This value is much lower than the expected value for transmission but the causes for this low transmission were: the insertion losses through the cleaved facets; the scattering from the defects along the waveguide; and the scattering due to the roughness of the waveguide walls, enhanced by the fact that the upper cladding was air. To improve the transmission i.e. reduce the transmission losses, a drop of index-matching gel was deposited on the coupler to act as an

upper cladding (with refractive index 1.45). This reduced the losses to a maximal transmission of about -15 dB, as seen in FIGURE 6- 13. This figure also shows the differences between the TE and TM coupling behaviour. Although the system is not completely optimised a clear difference is observed for the transmission of the two modes. At 1570 nm, the extinction ratio is about 9 dB for both TM and TE polarizations, which demonstrates the principle of this polarization splitter.

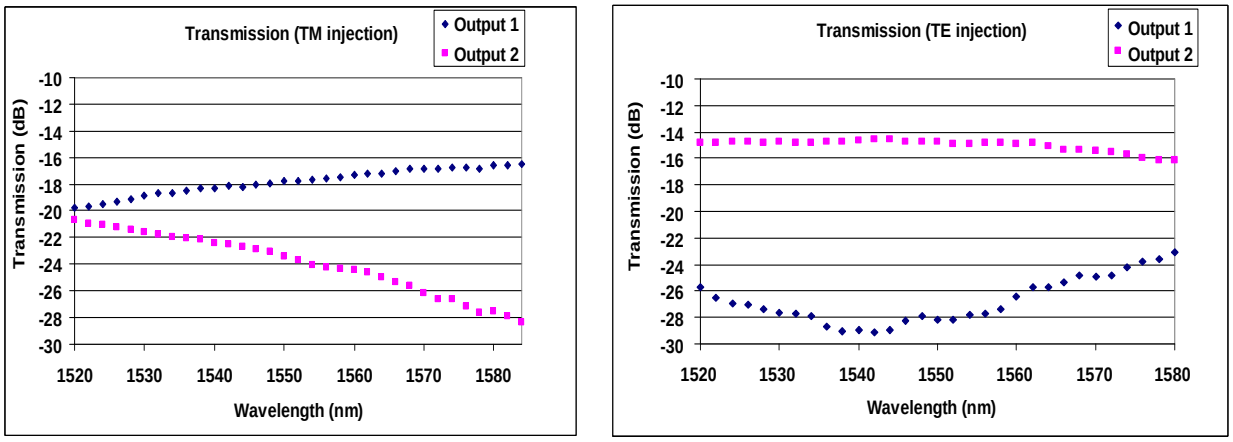

FIGURE 6- 13: COUPLER TRANSMISSION FOR (A) TM AND (B) TE INPUT BEAM POLARIZATIONS INDEX-MATCHING GEL IS USED AS AN UPPER CLADDING

We demonstrated the technical feasibility to fabricate two adjacent domains (isotropic and anisotropic) and finally to etch continuous waveguides on both domains. Optical measurement (propagation losses, extinction ratio, wavelength bandwidth, etc.) will be achieved in a next step.

6.4 Conclusions

Thermal patterning of liquid crystals allows us to fiddle with birefringence value of the reactive mesogens or the liquid crystal polymers. This possibly opens a door for many liquid crystal based applications one of which we have envisaged in this work. Another important advantage with thermal patterning is that it allows patterning even using the traditional rubbing method. This can be useful from the point of mass production of optical devices. In our case, we have instigated the work related to polarisation from the point of view of optical communications. Thermal patterning is an integral of this work and would help in eventual separation of TE and TM modes. This process was established for different liquid crystal polymers and also it was proved using different alignment methods like photo-alignment and the rubbing of the polymer layer. We have successfully demonstrated "freezing" the isotropic state of the liquid crystal and also having different phases of the

liquid crystal on the same substrate at the same time which are temperature independent after they are “frozen”.

Simplicity in the fabrication process is one of the major advantages of this work. This work demonstrates the new approach for the polarisation beam splitter for optical waveguide based devices. Birefrigent properties of liquid crystal play important role in the polarisation separation. This method is very useful for the treatment of polarization diversity in numerous optical waveguide functions that have different propagation behaviours for TE and TM modes. The splitting takes place in anisotropic zone while the optical function is being done isotropic zone, specialised design for TE and TM modes. The obtained beam splitter exhibits a high waveguide birefringence due to the large intrinsic anisotropy of liquid crystal material that allows very short coupling lengths.

Chapter 7: Conclusions and Perspectives

7.1 General Conclusions

Different optical functions have been investigated and for each targeted application. The engineering work is to define the structure of the device, the choice of the liquid crystal and the technological process for the device fabrication. The choice of the liquid crystal was made according to the desired performances e.g. pure liquid crystal, polymer stabilized, Polymer dispersed, reactive mesogen. The work can be divided into three different applications *viz.* Switchable mirrors and filters, shutters for 3D glasses and waveguide based polarisation splitters.

Switchable mirrors and filters

Polymer stabilised cholesteric liquid crystals showed better switching time than pure cholesterics and also the ability to sustain higher electric fields. Hence the Fabry-Perot cavity was successfully realised using polymer stabilised cholesteric liquid crystal by using photo-alignment and traditional rubbing. The monolithic fabrication of this cold cavity makes it interesting from the point of view fabrication. Having a quarter waveplate inside the cavity is essential for the cavity to function as Fabry-Perot cavity and without it the cavity will not function as Fabry-Perot. Presence of isotropic area in Fabry-Perot using both the alignment methods ensured the possibility of having more than one peak in the stop band of the cholesteric liquid crystal. One can tailor the thickness of this isotropic area to control the Free Spectral Range of the cavity. Tunability of the Fabry-Perot cavity was observed only due to temperature and not with electric field. However, cavity can be switched using both these parameters. Therefore, electric addressing cannot be used for tunability in such arrangement. Control of the input polarisation is essential which can be ensured by polarisation diversity systems.

One of the applications of nematic liquid crystals we demonstrated was isotropic cavity i.e. the output of the cavity remains the same irrespective of input polarisations. In other words this cavity is independent of input polarisations what makes it an extremely useful component for optical telecommunications. However, this insensitivity to input polarisation was observed only in 50 nm window. Since the quarter waveplate fabrication depends upon the wavelength at which it was fabricated; this waveplate will not behave as a quarter waveplates for all other wavelengths the ones in the vicinity of the wavelength for which it was fabricated. This causes the formation of elliptical modes rather than circular modes has led to the shift in the Fabry-Perot peaks for the wavelengths far from quarter waveplate wavelength. Successful and wide tunability was achieved using applied electric field. However, even a tunability of 50 nm is of great interest for telecommunications.

Shutters for 3D glasses

The idea to use high speed liquid crystal seems to be obvious to fabricate high quality 3D glasses. The ferroelectric liquid crystal has this property; however, the alignment without defects remains the main difficulty. Alignment of ferroelectric was realised in different manner i.e. the introduction of twist while fabricating a cell using rubbing method as well as using the photo-alignment method. The coupling between twist distribution and the chevron structure of the smectic layers has been tested to evaluate the possibility to reduce the tilt of these layers and then to reduce the density of defects.

This coupling between director distribution and tilt of smectic layer has been already expressed in different articles. However, a complete model with twisted distributed solutions for smectic layers has not been proven experimentally.

Another important point is that the value of twist given during alignment has some correlation with the effective tilt angle of the ferroelectric liquid crystal. At this juncture we do not have enough results to justify our preliminary observations. From the point of view of electro-optical properties the applied twist seems to have given some possible indication for the upper limit but the results are not lucid enough to establish a definite correlation. Asymmetric boundary conditions do prove to be successful in aligning the liquid crystal. This particular method can be cost effective as only one substrate undergoes any kind of treatment. No apparent trade-off was observed on the bistability of the cell as the response time and the contrast ratio were not affected because only one substrate was buffed. In case of polymer stabilised ferroelectric liquid crystals the concentration of polymer plays an important role in alignment quality.

Cells with higher concentration of polymer need higher electric fields because the polymer network binds the liquid crystal tightly (elastic torque).

The fabrication of the shutters for active 3D glasses with polymer stabilized liquid crystal was successfully shown, even a residual scattering effect is observed. The response times and contrast ratio well within the requirement of the 3D cinema viewing were achieved. The chromatic response of the glasses and also the viewing angle of them clearly satisfy the requirements of the 3D cinema.

Waveguide based polarisations splitter

Thermal patterning of liquid crystals allows us to have different birefringence value of the reactive mesogens or the liquid crystal polymers at zones of the substrates. In our case, we have instigated the work related to separation of polarisation from the point of view of optical communications. This process can be achieved using different alignment techniques. Isotropic and anisotropic phases of the liquid crystal can be trapped on the same substrate. Moreover, these new trapped phases will be independent of applied temperature as reactive mesogens or liquid crystal polymers are already polymerised.

Liquid crystal polymers can be successfully etched to give the desired pattern in our case we had the step index waveguides. Both the alignment techniques were used to demonstrate the possibility of waveguide fabrication and both were successfully demonstrated. Depths of waveguides etched were found to be slightly different for anisotropic and isotropic region. However this difference between two areas is not significant to induce Alignment using rubbing has been continued because of the problems we had discussed regarding photo-alignment. This novel process on silicon was successfully established.

Simplicity in the fabrication process is a key feature of this waveguide fabrication. It is a novel approach for the polarisation beam splitter for optical waveguide based devices. This method is very useful optical waveguide functions that show different propagation behaviours for TE and TM modes. Anisotropic zone splits the polarisation and isotropic zone performs the optical function. Large anisotropy of liquid crystal restricts the coupling lengths to smaller values to fabricate highly compact devices.

We have successfully demonstrated coupling of light in the waveguide. It is clearly observed that there has been a lot of leakage of light through the waveguide. This confirms that the waveguides are not homogeneous. The separation of polarisation has been demonstrated, but not yet optimised.

7.2 Future Scope

There is always a scope for improvement and our work is no exception. This section will be dedicated to possible future applications of few technologies or possible improvement in the present technologies.

The concept of tunable and switchable mirror is also novel concept and there are number of possible improvements in the fabrication. There is a possibility of converting the cold

cavity into a laser by doping the liquid crystal with appropriate gain medium like coloured dyes. This kind of laser will be an optically pumped laser in the visible range.

If the isotropic layer present inside the cavity is removed then there will be only one mode resonating inside the cavity i.e. the cavity becomes single mode and if one of the mirrors can be switched off; then there is a possibility of fabricating switchable Fabry-Perot with single mode output.

The isotropic nematic cavity can behave as input polarisation insensitive cavity for 50 nm then there is possibility of investigating some applications in the C band of telecommunications as sensitivity to input polarisation has been the constraint in the devices for optical communications.

The alignment of ferroelectric liquid crystal using twist presents some ambiguous results and we believe that there is a need for a theoretical analysis to overcome these ambiguities; also the experiments which will observe the chevron like structure for instance, X-ray diffraction to observe the smectic layers at a molecular level. We strongly believe that there is a scope for further analysis of this particular result. The authors think that there are few parameters which can influence the alignment *viz.* azimuthal and polar anchoring energy, pre-tilt angle etc. In order to establish a possible correlation one has to perform experiments, in which one can control all these parameters.

Scattering has remained the problem for the shutters for 3D cinema. It is essential to improve or to overcome this defect. Nonetheless, this kind of shutter can find numerous other applications when it is used in optical setup resilient to scattering effect. For example, use this kind of shutter as switchable half-waveplate in front of video-projector to switch between the left and the right circular polarisation for 3D system with passive glasses.

One of the challenges with the thermal patterning is that the size of the zone achieved or the resolution that can be achieved. In this work we have realised zones of millimetres over the entire substrate. However, the challenge lies in making microscopic zones with different birefringence. If it is possible to do micro level fabrication of such zones then it opens a door really wide variety of applications as the birefringence can be adjusted on the same substrate.

Polarisation beam splitter has a lot of potential in the world of optical communications. Sensitivity to polarisation has always been a constraint. The principle we presented here opens a door for potentially all the applications based on optical waveguides. Also, robust

and simple fabrication method allows us for mass production. Single substrate fabrication of entire optical system makes it cost effective, smaller in size and easy to package. It is quite clear that our present system needs improvement in all these aspects but firstly the homogeneity of the waveguide should be achieved, then control over the scattering losses is necessary. One needs to improve the extinction ratio and eventually one need to prove the separation of the polarisation. If the objectives set for this work are achieved then the system has the potential to be one of the milestones of optical communications research.

References

[1] I. C. Khoo, *Liquid Crystals*, Second ed.: Wiley Interscience, 2007.

[2] S. Chandrasekhar, *Liquid crystals*: Cambridge University Press, 1992.

[3] D. Demus, *Handbook of Liquid Crystals: Fundamentals*: Wiley-VCH, 1998.

[4] P. G. de Gennes, *The Physics of Liquid crystal*: Oxford Science Publications, 1993.

[5] D. Dunmur and T. Sluckin, *Soap, science, and flat-screen TVs: a history of liquid crystals*: Oxford University Press.

[6] N. A. Clark and S. T. Lagerwall, "Submicrosecond bistable electrooptic switching in liquid crystals," *Applied Physics Letters,* vol. 36, pp. 899-901, 1980.

[7] P. Watson, P. J. Bos, and J. Pirs, "Effects of surface topography on formation of defects in SmC* devices explained using an alternative chevron description," *Physical Review E,* vol. 56, p. R3769, 1997.

[8] P. Watson, P. J. Bos, and J. Pirs, "Effects of Surface Topography on Formation of Zig-Zag Defects in SSFLC Devices," *Society of Information Display International Symposium Digest of Technical Papers,* pp. 743-746, 1997.

[9] S. M. Kelly and M. ONeil, "Liquid crystals for electro-optic applications," in *Handbook of Advanced Electronic and Photonic Materials and Devices*. vol. 7, 2000.

[10] L. M. Blinov and V. G. Chigrinov, *Electrooptic Effects in Liquid Crystal Materials*: Springer, 1996.

[11] M. Mucha, "Polymer as an important component of blends and composites with liquid crystals," *Progress in Polymer Science,* vol. 28, pp. 837-873, 2003.

[12] K. Takatoh, M. Hasegawa, M. Koden, N. Itoh, R. Hasegawa, and M. Sakamoto, *Alignment Technologies and Applications of Liquid Crystal Devices*: Taylor and Francis, 2005.

[13] I. Dierking, M. A. Osipov, and S. T. Lagerwall, "The effect of a polymer network on smectic phase structure as probed by polarization measurements on a ferroelectric liquid crystal," *Eur. Phys. J. E,* vol. 2, pp. 303-309, 2000.

[14] T. J. Scheffer and J. Nehring, "A new, highly multiplexable liquid crystal display," *Applied Physics Letters,* vol. 45, pp. 1021-1023, 1984.

[15] T. Alkeskjold, L. Scolari, D. Noordegraaf, J. Lægsgaard, J. Weirich, L. Wei, G. Tartarini, P. Bassi, S. Gauza, S.-T. Wu, and A. Bjarklev, "Integrating liquid crystal based optical devices in photonic crystal fibers," *Optical and Quantum Electronics,* vol. 39, pp. 1009-1019, 2007.

[16] H. Lin, M. Khan, and T. Giao, "Dynamic Liquid Crystal Hot Spot Examination of Functional Failures on Production Testers," in *20th International Symposium for Testing and Failure Analysis*, 1994, p. 81.

[17] V. I. Kopp, B. Fan, H. K. M. Vithana, and A. Z. Genack, "Low-threshold lasing at the edge of a photonic stop band in cholesteric liquid crystals," *Opt. Lett.,* vol. 23, pp. 1707-1709, 1998.

[18] S. H. Rumbaugh, M. D. Jones, and L. W. Casperson, "Polarization control for coherent fiber-optic systems using nematic liquid crystals," *Journal of Lightwave technology,* vol. 8, pp. 459-465, 1990.

[19] A. Chen and D. Brady, "Real-time holography in azo-dye-doped liquid crystals," *Optics Letters,* vol. 17, pp. 441-443, 1992.

[20] Y.-H. Fan, H. Ren, and S. T. Wu, "Switchable Fresnel lens using polymer-stabilized liquid crystals," *Optics Express,* vol. 11, pp. 3080-3086, 2003.

[21] A. D. Kiselev, V. Chigrinov, and D. D. Huang, "Photo-induced ordering and anchoring properties of azo-dye films," *Phys. Rev. E,* vol. 72, 2005.

[22] M. Schadt, K. Schmitt, V. Kozinkov, and V. Chigrinov, "Surface Induced Alignment of Liquid Crystals by Linearly Polarised Photopolymers," *Japanese Journal of Applied Physics,* vol. 31, pp. 2155-2164, 1992.
[23] Maugin, vol. 34, 1911.
[24] D. W. Berreman, "Solid Surface Shape and the alignment of an adjacent nematic liquid crystal," *Physical Review Letters,* vol. 28, pp. 1683-1686, 1972.
[25] J. P. Castellano, "Surface anchoring of liquid crystal molecules on various substrates," *Molecular Crystal Liquid crystal,* vol. 294, pp. 33-41, 1983.
[26] J. M. Geary, J. W. Goodby, A. R. Kmetz, and J. S. Patel, "The mechanism of polymer alignment of liquid-crystal materials," *Journal of Applied Physics Letters,* vol. 62, pp. 4100 - 4108 1987.
[27] M. Toney, T. Russell, J. Logan, and H. Kikuchi, "Near-surface alignment of polymers in rubbed films," *Nature,* vol. 350, pp. 709-711, 1995.
[28] X. Zhuang, L. Marucci, and Y. R. Shen, "Surface-Monolayer-Induced Bulk Alignment of Liquid Crystals," *Physical Review Letters,* vol. 73, pp. 1513-1516, 1994.
[29] W. Chen, O. T. Moses, Y. R. Shen, and Yang, "Surface electroclinic effect on the layer structure of a ferroelectric liquid crystal," *Physical Review Letters,* vol. 68, pp. 1547-1550, 1992.
[30] M. Feller, W. Chen, and Y. Shen, "Investigation of surface-induced alignment of liquid-crystal molecules by optical second-harmonic generation," *Phys. Rev. A* vol. 43, 1991.
[31] J. Stohr and M. G. Samant, "Liquid crystal alignment by rubbed polymer surfaces: a microscopic bond orientation model," *Journal of Electron Spectroscopy and Related Phenomena,* vol. 98-99, pp. 189-207, 1999.
[32] S. Ishihara, "How Far Molecular Alignment has been elucidated?," *IEEE/OSA Journal of Display Technology,* vol. 1, pp. 30-39, 2005.
[33] A. Lien, R. A. John, M. Angelopoulos, K. W. Lee, H. Takano, and K. Tajima, "UV modification of surface pretilt of alignment layers for multidomain liquid crystal displays," *Applied Physics Letters,* vol. 67, 1995.
[34] J. C. Dubois, M. Gazard, and A. Zann, "Liquid crystal orientation induced by polymeric surfaces," *Journal of Applied Physics,* vol. 47, pp. 1270-1274, 1976.
[35] S. Lee, C. S. Ha, and J. K. Lee, "Syntheses and characteristics of polyimides for the applications to alignment film for liquid crystal display," *Journal of Applied Polymer Science,* vol. 82, pp. 2365–2371, 2001.
[36] S.-M. Kim, Y. M. Koo, and J. D. Kim, *Polymer surfaces and interfaces: characterization, modification and application*, 1997.
[37] J. Jenning, "Thin film surface orientation for liquid crystals," *Applied Physics Letters,* vol. 21, 1972.
[38] L. Goodman, J. T. Mcginn, C. Anderson, and F. Digeronimo, "Topography of obliquely evaporated silicon oxide films and its effect on liquid-crystal orientation," *IEEE TRANSACTIONS ON ELECTRON DEVICES,* vol. 7, pp. 795-804, 1977.
[39] D.-R. Chiou and L.-J. Chen, "Pretilt Angle of Liquid Crystals and Liquid-Crystal Alignment on Microgrooved Polyimide Surfaces Fabricated by Soft Embossing Method," *The ACS Journal of Surfaces and Colloids,* vol. 22, pp. 9403-9408, 2006.
[40] J. P. Doyle, P. Chaudhari, J. L. Lacey, E. A. Galligan, S. C. Lien, A. C. Callegari, N. D. Lang, M. Lu, Y. Nakagawa, H. Nakano, N. Okazaki, S. Odahara, Y. Katoh, Y. Saitoh, K. Sakai, H. Satoh, and Y. Shiota, "Ion beam alignment for liquid crystal display fabrication," *Nuclear Instruments and Methods in Physics Research Section B: Beam Interactions with Materials and Atoms,* vol. 206, pp. 467-471, 2003.
[41] K. Ichimura, Y. Suzuki, T. Seki, A. Hosoki, K. A. Ichimura, Y. Suzuki, T. Seki, A. Hosoki, and K. Aoki, "Reversible change in alignment mode of nematic liquid crystals regulated photochemically by

command surfaces modified with an azobenzene monolayer," *Langmuir,* vol. 4, pp. 1214-1216, 1988.
[42] W. M. Gibbons, P. J. Shannon, S. T. Sun, and B. J. Swetlin, "Surface-mediated alignment of nematic liquid crystals with polarized laser light," *Nature,* vol. 351, pp. 49-50, 1991.
[43] J. Hoogboom, T. Rasing, A. E. Rowan, and R. J. M. Nolte, "LCD alignment layers. Controlling nematic domain properties," *Journal of Materials Chemistry,* vol. 16, pp. 1305-1314, 2006.
[44] D. Olenik, M. W. Kim, A. Rastegar, and T. Rasing, "Probing photo-induced alignment in poly(vinyl cinnamate) films by surface second-harmonic generation," *Applied Physics B: Lasers and Optics,* vol. 68, pp. 599-603, 1999.
[45] O. Yaroshchuk, V. Kyrychenko, D. Tao, V. Chigrinov, H. S. Kwok, H. Hasebe, and H. Takatsu, "Stabilization of liquid crystal photoaligning layers by reactive mesogens," *Applied Physics Letters,* vol. 95, pp. 021902-021902-3, 2009.
[46] A. Denisov and J.-L. de Bougrenet de la Tocnaye, "Resonant gratings in planar Grandjean cholesteric composite liquid crystals," *Appl. Opt.,* vol. 46, pp. 6680-6687, 2007.
[47] P. Yeh and C. Gu, *Optics of Liquid Crystal Displays*: Wiley, 2009.
[48] A. Denisov, "Reconfigurable Photonic Crystals: External Field Structuring of Liquid Crystals - Polymer Composites," in *Department of Optics*. vol. Ph.D Brest: Telecom Bretagne, 2009, p. 133.
[49] J. M. Vaughan, *The Fabry-Perot interferometer: history, theory, practice, and applications*: A. Hilger, 1989.
[50] E. Hecht and A. ZajÄ…c, *Optics*: Addison-Wesley Pub. Co., 1974.
[51] B. E. A. Saleh and M. C. Teich, *Fundamentals of photonics*: Wiley-Interscience, 2007.
[52] J. E. Stockley, G. D. Sharp, and K. M. Johnson, "Fabry Perot etalon with polymer cholesteric liquid-crystal mirrors," *Optics Letters,* vol. 24, pp. 55-57, 1999.
[53] N. Fraval, P. Joffre, S. Formont, and J. Chazelas, "Electrically tunable liquid-crystal wave plate using quadripolar electrode configuration and transparent conductive polymer layers," *Appl. Opt.,* vol. 48, pp. 5301-5306, 2009.
[54] J. S. Patel, "Polarization insensitive tunable liquid-crystal etalon filter," *Applied Physics Letters,* vol. 59, pp. 1314-1316, 1991.
[55] Y. Morita and K. M. Johnson, "Polarization-insensitive tunable liquid crystal Fabry-Perot filter incorporating polymer liquid crystal waveplates," in *Liquid Crystals II*, San Diego, CA, USA, 1998.
[56] G. P. Crawford and S. Žumer, *Liquid crystals in complex geometries: formed by polymer and porous networks*: Taylor & Francis, 1996.
[57] G. Chilaya, "Cholesteric Liquid Crystals: Optics, Electro-Optics and Photo-Optics," in *Chirality in Liquid Crystals*, H.-S. Kitzerow and C. Bahr, Eds.: Springer, 2001, p. 501.
[58] G. Chilaya, "Effect of Various External Factors and Pretransitional Phenomena on Structural Transformations in Cholesteric Liquid Crystals," *Crystallography Reports,* vol. 45, pp. 871-886, 1999.
[59] L. Lipton, "The stereoscopic cinema: From film to Digital projection," *Society of Motion Picture and Television Engineers Journal,* vol. 110, pp. 586-593, 2001.
[60] I. Sexton and P. Surman, "Stereoscopic and autostereoscopic display systems," *Signal Processing Magazine, IEEE,* vol. 16, pp. 85-99, 1999.
[61] A. K. Srivastava, J. L. de Bougrenet de la Tocnaye, and L. Dupont, "Liquid Crystal Active Glasses for 3D Cinema," *Journal of Display Technology,* vol. 6, pp. 522-530, 2010.
[62] A. Woods and T. Rourke, "Ghosting in anaglyphic stereoscopic images " in *Stereoscopic Displays and Virtual Reality Systems XI*, San Jose, California, United States, 2004, p. 12.
[63] M. Weissman and A. Woods, "A simple method for measuring crosstalk in stereoscopic displays," in *Proceedings of SPIE Stereoscopic Displays and Applications XXII*, San Francisco, California, United States, 2011.

[64] S. T. Lagerwall, *Ferroelectric and Antiferroelectric Liquid Crystals*: WILEY-VCH 1999.
[65] C. Wang and P. J. Bos, "Bistable C1 ferroelectric liquid crystal device for e-paper application," *Displays,* vol. 25, pp. 187-194, 2004.
[66] L. Limat, "A Model of Chevrons in Smectic C* Liquid Crystals: Uniform and Twisted "Soliton" States," *J. Phys. II France,* vol. 5, pp. 803-822, 1995.
[67] E. Pozhidaev, V. Chigrinov, D. Huang, and H. Kwok, "Alignment of ferroelectric liquid crystals with photoanisotropic azodye aligning layers," in *Proceedings Eurodisplay* Nice, France, 2002, pp. 137-140.
[68] B. Caillaud, L. Dupont, and J. L. de Bougrenet de la Tocnaye, "Planar-Homeotropic Transition in PS-FLC Induced by an Electric Field During Photopolymerization in the Nematic Phase," *Molecular Crystals and Liquid Crystals,* vol. 469, pp. 59-68, 2012/01/19 2007.
[69] E. Pozhidaev, V. Chigrinov, D. Huang, A. Zhukov, J. Ho, and H. S. Kwok, "Photoalignment of Ferroelectric Liquid Crystals by Azodye Layers," *Japanese Journal of Applied Physics,* vol. 43, pp. 5440-5446, 2004.
[70] J. L. de Bougrenet de la Tocnaye, L. Dupont, D. Stoenescu, K. Sathaye, and V. Nunes Henrique Silva, "Liquid crystal for 3-D active glasses," in *LCP 2010: 3rd International workshop on liquid crystals for photonics* Elche, Spain, 2010.
[71] B. Caillaud, B. Bellini, and J. L. De Bougrenet de la Tocnaye, "High speed, large viewing angle shutters for triple-flash active glasses," Bellingham, WA, United States, 2009.
[72] Y.-H. Fan, Y.-H. Lin, H. Ren, S. Gauza, and S.-T. Wu, "Fast-response and scattering-free polymer network liquid crystals for infrared light modulators," *Applied Physics Letters,* vol. 84, pp. 1233-1235, 23 February, 2004.
[73] I. Kaminow, "Polarization in optical fibers," *Quantum Electronics, IEEE Journal of,* vol. 17, pp. 15-22, 1981.
[74] Telcordia, "Generic Requirements for Passive Optical Components," 2010.
[75] K. Wörhoff, C. G. H. Roeloffzen, R. M. d. Ridder, A. Driessen, and P. V. Lambeck, "Design and Application of Compact and Highly Tolerant Polarization-Independent Waveguides," *Journal of Lightwave Technology,* vol. 25, pp. 1276-1283, 2007.
[76] G. Hanisch, R. P. Podgorsek, and H. Franke, "Origin of optical anisotropy in planar polymer waveguides," *Sensors and Actuators B: Chemical,* vol. 51, pp. 348-354, 1998.
[77] A. Shibukawa and M. Kobayashi, "Optical TE-TM mode conversion in double epitaxial garnet waveguide," *Applied Optics,* vol. 20, pp. 2444-2450, 1981.
[78] M. Campoy-Quiles, P. G. Etchegoin, and D. D. C. Bradley, "On the optical anisotropy of conjugated polymer thin films," *Physical Review B,* vol. 72, pp. 045209-1-045209-16, 2005.
[79] H. Zou, K. W. Beeson, and L. W. Shacklette, "Tunable Planar Polymer Bragg Gratings Having Exceptionally Low Polarization Sensitivity," *J. Lightwave Technol.,* vol. 21, p. 1083, 2003.
[80] D. X. Xu, P. Cheben, D. Dalacu, A. Delâge, S. Janz, B. Lamontagne, M. J. Picard, and W. N. Ye, "Eliminating the birefringence in silicon-on-insulator ridge waveguidesby use of cladding stress," *Opt. Lett.,* vol. 29, pp. 2384-2386, 2004.
[81] Y. Shi, D. Dai, and S. He, "Proposal for an Ultracompact Polarization-Beam Splitter Based on a Photonic-Crystal-Assisted Multimode Interference Coupler," *IEEE Photonics Technology Letters,* vol. 19, pp. 825-827, 2007.
[82] Q. Wang, G. Farrell, and Y. Semenova, "Design of Integrated Polarization Beam Splitter With Liquid Crystal," *IEEE Journal of Selected Topics in Quantum Electronics,* vol. 12, pp. 1349-1353, 2006.
[83] W.-H. Hsu, K.-C. Lin, J.-Y. Li, Y.-S. Wu, and W.-S. Wang, "Polarization Splitter With Variable TE-TM Mode Converter Using Zn and Ni Codiffused LiNbO3 Waveguides," *IEEE Journal of Selected Topics in Quantum Electronics,* vol. 11, pp. 271-277, 2005.

[84] S. M. Garner, V. Chuyanov, S.-S. Lee, A. Chen, W. H. Steier, and L. R. Dalton, "Vertically Integrated Waveguide Polarization Splitters Using Polymers," *IEEE Photonics Technology Letters,* vol. 11, pp. 842-844, 1999.
[85] W. Pei-Kuen and W. Way-Seen, "A TE-TM mode splitter on lithium niobate using Ti, Ni, and MgO diffusions," *Photonics Technology Letters, IEEE,* vol. 6, pp. 245-248, 1994.
[86] S. M. Garner, V. Chuyanov, L. Sang-Shin, C. Antao, W. H. Steier, and L. R. Dalton, "Vertically integrated waveguide polarization splitters using polymers," *Photonics Technology Letters, IEEE,* vol. 11, pp. 842-844, 1999.
[87] E. Schonbrun, Q. Wu, W. Park, T. Yamashita, and C. J. Summers, "Polarization beam splitter based on a photonic crystal heterostructure," *Opt. Lett.,* vol. 31, pp. 3104-3106, 2006.
[88] T. Liu, A. R. Zakharian, M. Fallahi, J. V. Moloney, and M. Mansuripur, "Design of a compact photonic-crystal-based polarizing beam splitter," *Photonics Technology Letters, IEEE,* vol. 17, pp. 1435-1437, 2005.
[89] T. K. Liang and H. K. Tsang, "Integrated polarization beam splitter in high index contrast silicon-on-insulator waveguides," *Photonics Technology Letters, IEEE,* vol. 17, pp. 393-395, 2005.
[90] K. Okamoto, *Fundamentals of optical waveguides*: Elsevier, 2006.
[91] A. Yariv, "Coupled-mode theory for guided-wave optics," *Quantum Electronics, IEEE Journal of,* vol. 9, pp. 919-933, 1973.
[92] J. R. Pierce, "Coupling of Modes of Propagation," *Journal of Applied Physics,* vol. 25, pp. 179-183, 1954.
[93] A. Yariv and P. Yeh, *Photonics: optical electronics in modern communications*: Oxford University Press, 2007.
[94] X. H. Wang, *Finite element methods for nonlinear optical waveguides*: Gordon and Breach, 1996.
[95] J. Whinnery, H. Chenming, and Y. Kwon, "Liquid-crystal waveguides for integrated optics," *Quantum Electronics, IEEE Journal of,* vol. 13, pp. 262-267, 1977.
[96] T. G. Giallorenzi and J. M. Schnur, "Liquid crystal waveguide " United States: The United States of America as represented by the Secretary of the Navy (Washington, DC) 1976.
[97] Y. Kurioz, O. Buluy, Y. Reznikov, I. Gerus, and R. Harding, "Orientation of a Reactive Mesogen on Photosensitive Surface," *SID Symposium Digest of Technical Papers,* vol. 38, pp. 688-690, 2007.
[98] J. Lub, D. J. Broer, R. T. Wegh, E. Peeters, and B. M. I. v. d. Zande, "Formation of Optical Films by Photo-Polymerisation ofLiquid Crystalline Acrylates and Application of TheseFilms in Liquid Crystal Display Technology," *Molecular Crystal Liquid crystal,* vol. 429, pp. 77-99, 2005.
[99] M. C. Oh, S. Y. Shin, W. Y. Hwang, and J. J. Kim, "Poling-induced waveguide polarizers in electrooptic polymers," *IEEE Photonics Technology Letters,* vol. 8, pp. 375-377, 1996.
[100] D. Bosc, A. Maalouf, F. Henrio, and S. Haesaert, "Strengthened poly(methacrylate) materials for optical waveguides and integrated functions," *Optical Materials,* vol. 30, pp. 1514-1520, 2008.
[101] Tamir, *Integrated Optics*, Second ed.: Springer-Verlag, 1975.
[102] M. J. Adams, *An introduction to optical waveguides*: Wiley, 1981.
[103] R. J. Black and L. Gagnon, *Optical waveguide modes: polarization, coupling, and symmetry*: McGraw-Hill, 2009.
[104] A. W. Snyder and J. D. Love, *Optical waveguide theory*: Chapman and Hall, 1983.
[105] A. Boudrioua, *Photonic waveguides: theory and applications*: ISTE, 2009.

Appendix I

Cleaning of Silicon Wafers

Silicon wafers were washed in deionised water for half hour in an ultrasonic bath. The water in the ultrasonic bath was heated before commencing the cleaning process, this ensures better cleaning quality. 5% of decon was added for cleaning purpose. After first ultrasonic bath the water with decon was replaced by pure deionised water and the wafers were again kept in ultrasonic bath for the period of half hour. Wafers were afterwards dried at temperature of above 100° C for half hour minutes. This ensures no residual water is left on the surface. Presence of decon and entire ultrasonic bath treatment ensures thorough cleaning of the wafers. Similar process can be followed for the cleaning of glass substrates.

Fabrication of a liquid crystal cell

A liquid crystal cell comprises of two substrates. Normally these substrates are glasses and have already been coated with an alignment layer. This alignment layer has been coated normally by means of spin coating or by other means depending upon the alignment technique. Then, these glasses undergo the treatment required for the coating normally a heat treatment. Then these coated films undergo the alignment technique like buffing of the layer or photo-alignment of the layer. Then, a mixture of polymer glue (NOA 63, NOA65, UVS 91 etc) is made with glass fibre spacers of appropriate thickness (from 1.5 microns to 100 microns). In this mixture the spacer concentration is 0.5%-1% as compared to that of glue. Then, this mixture is deposited on the corners of one of the substrates using pressure dispenser. The other substrate is placed with slight off-set on top of the first substrate. This assembly is kept under UV to polymerise the glue and hence to stick substrates together. Interestingly, the off-set given is to have access to apply the voltage in the future as sometimes glasses with transparent electrodes (Indium Tin Oxide - ITO) are used as substrates. Another important aspect is that the direction of orientation for molecules is decided by the surface treatment to the alignment layer. Subsequently, the evolution of liquid crystal inside the cell depends upon how these two substrates are assembled i.e. whether the direction is anti-parallel, parallel or twisted.

Appendix II

Polarisation insensitive passive cholesteric mirrors

The fabrication of this kind of passive optical component has been previously done. In order to achieve this objective we made 2 mixtures. First mixture was made using S811 (a left handed chiral dopant from Merck) with nematic MLC-100-6846 of very low birefringence (0.09) at a concentration of 30%-70% respectively and was subsequently filled in a cell with two rubbed polyimide glasses. Second mixture was made using R811 (a right handed chiral dopant from Merck) with same nematic at a same concentration, which was also filled in a cell. These two cells were stuck together.

The left handed cholesteric liquid crystal reflects 50% of light while right handed cholesterics reflects the other 50% of light in the cholesteric stop band. Therefore, for any incoming light in the stop band, the light will experience a complete reflection in the cholesteric stop band. The graph is a transmission spectrum taken with unpolarised light. It can be observed that there is 90% of reflection in the cholesteric band. This can be due to the losses because multiple reflections on glass substrates.

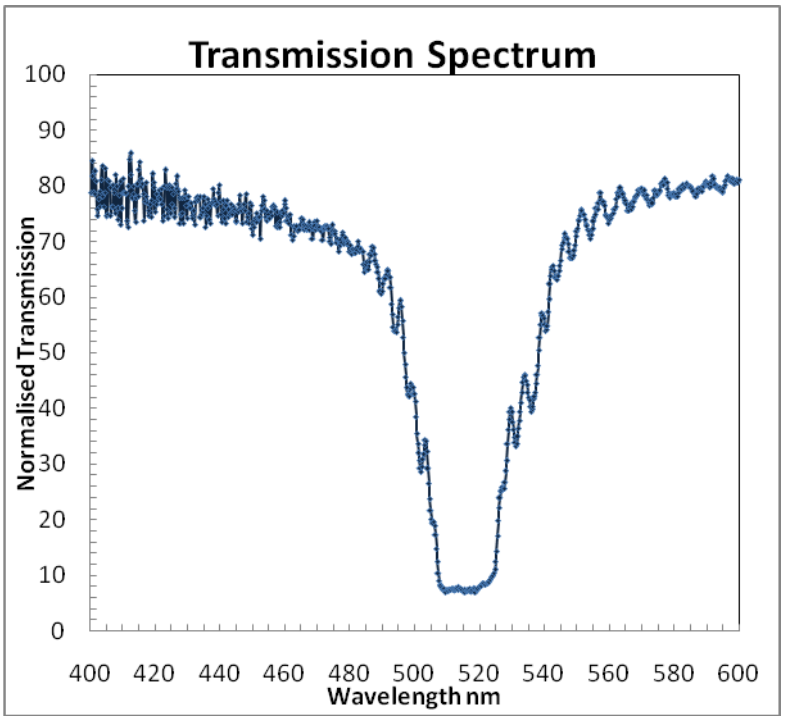

Appendix III

Molecular structure of RM257

We have seen so far that the reactive mesogen RM257 has been extensively used in this work. It would be a good idea to know about the molecular structure of the same. This particular monomer is a diacrylate mesogen and it is crystalline at room temperature. The molecular structure is as follows. The chemical name is 4- (3-acryloyloxypropyloxy) -benzoic acid 2-methyl-1, 4-phenylene ester. Two side chains make the molecule diacrylate. For more information consult Merck datasheet for RM257.

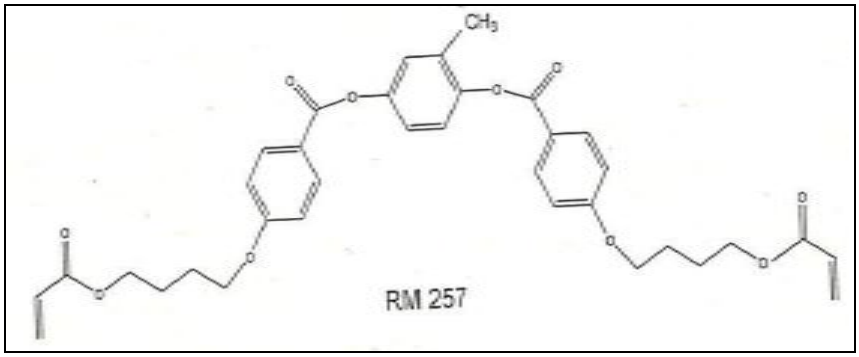

Molecular structure of Igracure 651

Photoinitiator Igracure 651 is highly efficient photoinitiator which normally used in prepolymers like acrylates and also in combination with monomers. Hence it is ideal to use in combination with RM257. The chemical name is 2,2-Dimethoxy-1, 2-diphenylethan-1-1. For more information consult the datasheet of Ciba Igracure 651.

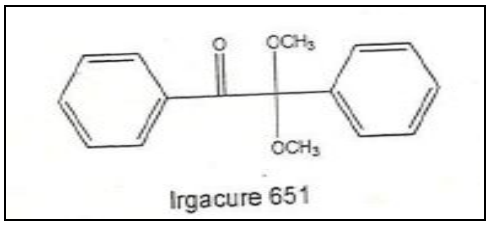

Appendix IV

Mode formation in an optical waveguides

Optical waveguides can be considered as the dielectric solid state materials wherein the optical waves are confined along the path of the waveguide due to the phenomenon of total internal reflection [90]. The index of refraction of the guiding medium is larger than the outer mediums of the waveguide. The condition to satisfy the phenomenon of total internal reflection is given as

$$n_1 \sin\theta(\pi/2 - \phi) \geq n_0 \qquad \textbf{(Equation 1)}$$

Where, n_1 is the refractive index of the core and n_0 is the refractive index of the cladding; θ is the incident angle, ø is the angle of refraction. However, the incident angle and refraction angle are related by Snell's law. Therefore, by substituting the right values in above equation we obtain

$$\theta \leq \sin^{-1}\sqrt{n_1^2 - n_0^2} \equiv \theta_{max} \qquad \textbf{(Equation 2)}$$

Where θ_{max} is the maximum value of the incident angle allowed also known as the numerical aperture of the waveguide. Numerical aperture can be expressed in terms of the refractive indices of the core and the cladding. Therefore, we have the relative refractive index of the waveguide given by,

$$\Delta = \frac{n_1^2 - n_0^2}{2n_1^2} \cong \frac{n_1 - n_0}{2n_1} \qquad \textbf{(Equation 3)}$$

Hence the numerical aperture can be given as

$$NA = \theta_{max} \cong n_1\sqrt{2\Delta} \qquad \textbf{(Equation 4)}$$

However, light waves with all the angles below this value can not propagate through the waveguide i.e. each mode associated with the waveguide travels at a discrete value which can be seen using electromagnetic wave analysis. In order to prove this condition we have to take into account the fundamentals of the waveguide theory. When a linearly polarised light beam undergoes a total internal reflection then there is small phase shift occurring in

the beam. This optical phenomenon is known as the Goos-Hänchen shift [101], which is given by,

$$\Phi = -2\tan^{-1}\frac{\sqrt{n_1^2 cos^2\phi - n_0^2}}{n_1 sin\phi} = -2\tan^{-1}\sqrt{\frac{2\Delta}{sin^2\phi} - 1} \qquad \textbf{(Equation 5)}$$

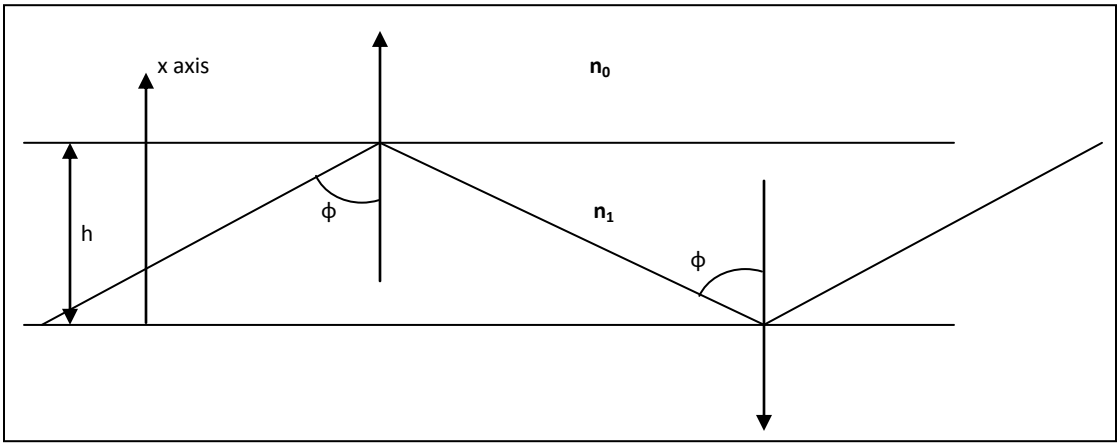

FIGURE 1: BASIC WAVEGUIDE STRUCTURE

Above phase shift takes place at both the interfaces of the waveguide. The refractive index of the cladding is considered to be equal on upper and lower side of the core for simplicity purpose i.e. the waveguide in consideration is a symmetric waveguide. As shown in above diagram when we moved from the lower interface (x=0) to upper interface (x=h) and back again to the interface where we started, there will be phase shifts occurring at each interface. The sum of all the phase shifts taking place in the waveguide will be integral multiple of 2π. For the waveguide with thickness h the phase shift for the transverse of the film is $kn_1 h\cos\phi$ for one passage and similar phase shift the passage down the waveguide in addition to the phase shifts occurring at each interface. Therefore, the total phase shift will be

$$2kn_1 h\cos\phi - 2\Phi = 2m\pi \qquad \textbf{(Equation 6)}$$

By making appropriate substitutions in above equation we have

$$tan\left(kn_1 h sin\phi - \frac{m\pi}{2}\right) = \sqrt{\frac{2\Delta}{sin^2\phi} - 1} \qquad \textbf{(Equation 7)}$$

We have the dispersion equation for the guided modes. It can be seen that the above equation is discrete and has a solution for only allowed values of ϕ. The optical field distribution that matches the phase matching condition is known as *mode.* The minimum

value of angle ϕ that satisfies above equation is known as the fundamental mode (m=0). Formation of modes is also known as the standing wave condition and for a waveguide to guide a wave through it one has to satisfy both the conditions i.e. the condition for total internal reflection and the condition for the standing wave [102]. Now we have seen the conditions for the formation of the modes and basic structure of the waveguide. We shall now proceed to coupled mode theory and conditions for propagation of single mode through the waveguide.

Formation of TE and TM modes in optical waveguides

In order to explain the formation of TE and TM modes in an optical waveguide it is necessary to understand the polarisation dependency of modes and the sources of anisotropy which give rise to polarisation sensitive behaviour of the optical waveguide [103]. In an optical waveguide any variation of refractive index of the core leads to anisotropic behaviour of the waveguide. Broadly speaking, there can be two types of refractive index variations; first being the index change on microscopic level while the second being the index change on macroscopic level. The origin for the former can be considered as the wave travelling through the waveguide travels with different phase velocities and thus it experiences different refractive indices depending upon the electric field distribution. The origin of the macroscopic anisotropies in one dimensional case i.e. in case of a slab waveguide there is a splitting of polarisation seen by modes; one is parallel to the electric field while the other is perpendicular to the electric field [103]. Geometrical anisotropy can occur if the waveguide is elliptical the effective indices will depend on the polarisations along major and minor axes. Such waveguides are considered as the globally anisotropic waveguides. In case of optical fibres also there is a degree of birefringence which is associated with the radial component of the polarisation and the axial component of the polarisation. In other words in case of waveguides with both the core and cladding being perfectly isotropic materials there is always a degree of anisotropy associated with it. The degree of the splitting of polarisations depends upon the core-cladding refractive index difference [104]. In case of the slab waveguides the splitting of the refractive indices based on the parallel and perpendicular to electric polarisations are nothing but the TE and TM modes in the waveguide.

Let us now consider the wave analysis of TE and TM modes inside the slab waveguide in terms of Maxwell's equations. Consider a slab waveguide with n_1 as the refractive index of the core, n_0 as the refractive index of the cladding or the upper layer and n_s as the refractive index of the substrate.

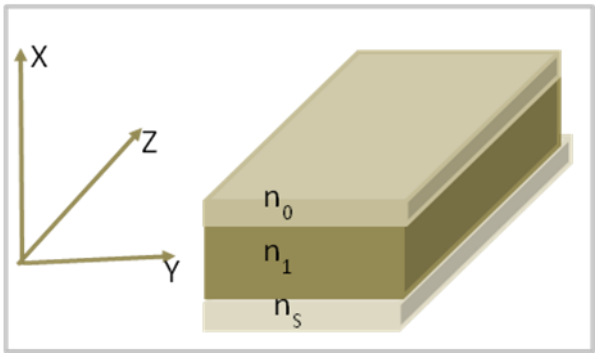

FIGURE 2: SLAB WAVEGUIDE

Consider the slab waveguide with infinite length in the z-direction. We have considered that the above waveguide is a dielectric waveguide. Therefore, the permittivity and the permeability of the waveguide is $\varepsilon = \varepsilon_0 n_1^2$ and $\mu=\mu_0$. According to Maxwell's equation we have,

$$\nabla \times E = -\mu_0 \frac{\partial H}{\partial t} \quad \textbf{(Equation 8)}$$

$$\nabla \times H = -\varepsilon_0 n_1^2 \frac{\partial E}{\partial t} \quad \textbf{(Equation 9)}$$

The wave propagation in such a media in terms of electric and magnetic fields is given by,

$$E = E(x, y)^{j(wt-\beta z)} \quad \textbf{(Equation 10)}$$

$$H = H(x, y)^{j(wt-\beta z)} \quad \textbf{(Equation 11)}$$

Where, β is the propagation constant in the medium and ω is group velocity in the z direction. It can be seen from the diagram that the electric field and the magnetic field do not have any component in the y direction; therefore we can consider that the change of these fields with respect to y-direction is 0. Thus by substituting equations 10 and 11 in equation 8 and 9 respectively we have two following equations wherein eliminating the change of electric and magnetic field with respect to y-direction we get following equations for TE and TM modes [105];

$$\frac{d^2 E_y}{dx^2} + \left(k^2 n_1^2 - \beta^2\right) E_y = 0 \quad \textbf{(Equation 12)}$$

Where,

$$H_x = -\frac{\beta}{\omega \mu_0} E_y \quad \textbf{(Equation 13)}$$

$$H_z = -\frac{j}{\omega\mu_0}\frac{dE_y}{dx} \quad \textbf{(Equation 14)}$$

$$\frac{d^2H_y}{dx^2} + \left(k^2n_1^2 - \beta^2\right)H_y = 0 \quad \textbf{(Equation 15)}$$

Where,

$$E_x = -\frac{\beta}{\omega\mu_0}H_y \quad \textbf{(Equation 16)}$$

$$E_z = -\frac{j}{\omega\mu_0}\frac{dH_y}{dx} \quad \textbf{(Equation 17)}$$

Where k is the propagation constant in free space; we now will take into consideration the effective refractive index based on the propagation constants. The mode travelling along the core will remain confined to the core and it will decay exponentially if the mode enters either cladding or the substrate as the refractive indices of them are lower than of the core. Therefore, the electric field will be exponentially decreasing or it will be evanescent if the mode enters either cladding or the substrate. This exponential decay in the energy is called as the radiation mode. We shall now see the dispersion equation for TE mode using which we will derive the cut-off condition for and also the condition for single mode propagation inside the waveguide. Based on the boundary conditions of the waveguide and by introducing transverse wavenumbers for the cladding, the core and the substrate respectively we can evaluate change in y-component of electric field with respect to the x-direction i.e. the thickness of the waveguide. Hence we have,

$$\frac{dE_y}{dx} = \begin{cases} -\sigma A\cos(\kappa a - \phi)e^{-\sigma(x-a)} \dots\dots\dots\dots\dots\dots\dots\dots\dots\dots x > a \\ -\kappa A; sin(\kappa x - \phi) \dots\dots\dots\dots\dots\dots\dots\dots\dots\dots -a \le x \le a \\ \xi A\cos(\kappa a + \phi)e^{\xi(x+a)} \dots\dots\dots\dots\dots\dots\dots\dots\dots\dots x < -a \end{cases} \quad \textbf{(Equation 18)}$$

Where, σ, κ and ξ are the transverse wavenumbers in the cladding, the core and the substrate respectively. These transverse wavenumbers are the function of refractive index and the propagation constant [90]. Φ is the phase and ±a is the thickness of the waveguide as the x-axis passes exactly in the midpoint of the thickness. As one can notice the propagation of wave dissipates exponentially in the substrate and the cladding. dE_y/dx will be continuous at the boundaries of the core. Hence we have the equation,

$$\kappa A\sin(\kappa a + \phi) = \xi A\cos(\kappa a + \phi) \quad \textbf{(Equation 19)}$$

$$\sigma A\cos(\kappa a - \phi) = \kappa A\sin(\kappa a - \phi) \quad \textbf{(Equation 20)}$$

Getting rid of the constant A we have following equation,

$$tan(u+\phi) = \frac{w}{u} \quad \textbf{(Equation 21)}$$

$$tan(u-\phi) = \frac{w'}{u} \quad \textbf{(Equation 22)}$$

Where u=κa, w'=σa, w=ξa. Hence we get the eigen value equation for u and Φ as [90];

$$u = \frac{m\pi}{2} + \frac{1}{2}tan^{-1}\left(\frac{w}{u}\right) + \frac{1}{2}tan^{-1}\left(\frac{w'}{u}\right) \quad \textbf{(Equation 23)}$$

$$\phi = \frac{m\pi}{2} + \frac{1}{2}tan^{-1}\left(\frac{w}{u}\right) - \frac{1}{2}tan^{-1}\left(\frac{w'}{u}\right) \quad \textbf{(Equation 24)}$$

These equations are nothing but the dispersion equations for TE modes; similar equations can be derived for TM mode. Here we introduce another parameter called normalised frequency v which can be found out from the phase matching

$$v = kn_1 a\sqrt{2\Delta} \quad \textbf{(Equation 25)}$$

In order to maintain the mode inside the core of the waveguide it is necessary to see the cut-off condition for the mode to be a guided and not radiating. Hence there will be an exponential component associated with the propagation of the wave in case of radiation mode. This exponential component will depend upon the boundary conditions and also the refractive indices of the cladding and the substrate. Considering the waveguide as an asymmetric waveguide with refractive index of cladding smaller than that of the substrate; we have the normalised propagation constant β/k will give us the cut-off condition as;

$$n_s \leq \frac{\beta}{k} \leq n_1 \quad \textbf{(Equation 26)}$$

In above equation we β/k is a dimensionless parameter and is known as the effective refractive index n_e of the waveguide. Therefore, if $n_e < n_s$ then the mode will dissipate into the radiation mode. If $n_e = n_s$ is the cut-off condition for the guided mode. Here we introduce another dimensionless parameter defined by;

$$b = \frac{n_e^2 - n_s^2}{n_1^2 - n_s^2} \quad \textbf{(Equation 27)}$$

Therefore, the condition for guided mode is given by $\mathbf{0 \leq b \leq 1}$ suggesting that b=0 is the cut-off condition and any value below this value will result into the radiation mode. Now we will write the dispersion equation 23 for TE in terms of normalised frequency and normalised propagation constant;

$$2v\sqrt{1-b} = m\pi + tan^{-1}\sqrt{\frac{b}{1-b}} + tan^{-1}\sqrt{\frac{b+\gamma}{1-b}} \qquad \textbf{(Equation 28)}$$

Where γ is the parameter which defines the asymmetry of the waveguide and can be expressed as;

$$\gamma = \frac{n_s^2 - n_0^2}{n_1^2 - n_s^2} \qquad \textbf{(Equation 29)}$$

This equation is used in designing of the waveguide. The condition for single mode waveguide can be obtained by substituting the value of m=1 in equation 28. The graph of b versus v normally gives adequate information about the cut-off condition, single mode waveguide parameters and choice of material for the cladding, the core and the substrate.

Résumé

L'objectif de cette thèse est de fabriquer différents dispositifs optiques basés sur la structuration des cristaux liquides. Nous avons tout d'abord présenté différentes méthodes pour aligner les molécules de cristaux liquides et détaillé celles que nous avons utilisées au cours de ce travail. L'alignement et certaines propriétés physiques des cristaux liquides ont permis de fabriquer des dispositifs optiques. Ces dispositifs se divisent généralement en trois catégories : les filtres optiques, les modulateurs spatiaux et les guides d'ondes optiques. Ils sont présents dans divers secteurs et particulièrement dans le domaine des télécommunications. La structure des cristaux liquides cholestériques a une biréfringence périodique qui donne lieu à une réflexion sélective de la polarisation circulaire de la lumière. Nous avons tiré profit de cette propriété en fabricant un miroir de Bragg commutable. Ce miroir nous a permis de fabriquer un filtre de Fabry-Perot commutable et accordable. Un réseau de polymère a été utilisé pour stabiliser le cristal liquide cholestérique, afin d'apporter résistance mécanique et durabilité aux champs électriques. Les cristaux liquides ferroélectriques présentent des propriétés électro-optiques efficaces, en particulier un temps de réponse élevé. Cette propriété a été exploitée pour fabriquer des obturateurs optiques pour lunettes 3D actives basées sur des cristaux liquides ferroélectriques. Malgré un temps de réponse élevé, les cristaux liquides ferroélectriques présentent certains défauts structurels. Nous avons proposé une nouvelle technique pour pallier ces défauts. Enfin, nous avons fabriqué des guides d'ondes gravés dans le polymère à cristaux liquides. Nous avons fabriqué ce polymère à cristaux liquides de manière à obtenir deux phases de cristal liquide différentes : isotrope et anisotrope, sur le même substrat. Le substrat a ensuite été gravé afin de créer un séparateur de polarisation séparant le mode TE et TM dans les deux branches du guide.

Mots-clés: cristaux liquides, d'alignement de cristaux liquides, Fabry-Perot, PSCLC (polymer stabilsed cholesteric liquid crystals), les cavités accordables, des modulateurs spatiaux, des obturateurs optiques pour lunettes 3D actives, des guides d'ondes à cristaux liquides.

Abstract

The objective of this thesis is to engineer different optical devices based on structuring of the liquid crystals. Initially, we presented various methods to align the liquid crystal molecules and we have detailed the ones which we used during the course of this work. In combination with alignment of liquid crystals we exploited certain physical properties of the liquid crystals to engineer few optical devices. Broadly speaking one can divide these types of devices in three categories *viz.* Optical filters, spatial modulators and optical waveguides. All three of these devices have an application in telecommunication sector as well as in the other sectors. The structure of cholesteric liquid crystals has a periodic birefringence and gives rise to selective reflection of the circularly polarised light. We exploited these properties to fabricate a switchable Bragg mirror. This Bragg mirror made up of cholesteric liquid crystals was later on used to fabricate switchable and tunable Fabry-Perot interferometer. A polymer network was used to stabilise the cholesteric liquid crystal in order to give the mechanical strength and sustainability to the electric fields. The ferroelectric liquid crystals have very pertinent electro-optical properties especially the response times. This property was exploited to fabricate optical shutters for 3D active glasses based on ferroelectric liquid crystals. Although, the response times for these liquid crystals are higher than nematics, they have some structural defects. We have proposed a new alignment to technique to overcome such defects. Lastly, we have fabricated the waveguides etched in the liquid crystal polymer. We have patterned the liquid crystal polymer in such a way that we have two different phases of liquid crystal namely isotropic and anisotropic present on the same substrate. Waveguides were etched on such a substrate with two different phases to give rise to the polarisation separator to separate TE mode and TM mode in two different branches of the waveguide.

Keywords: Liquid crystals, Alignment of liquid crystals, Fabry-Perot, Polymer stabilised cholesteric liquid crystals, tunable cavities, spatial modulators, optical shutters for 3D active glasses, liquid crystal waveguides.

Résumé

1. Introduction

Cette thèse discute de la structuration des cristaux liquides pour les technologies optiques. Divers types de cristaux liquides ont été utilisés pour fabriquer les technologies employées dans les différents domaines optiques. Les différents types de cristaux liquides seront dans un premier temps passé en revue avant d'examiner en détails les raisons pour lesquelles ces cristaux liquides ont été choisis pour certaines technologies optiques.

1.1. Pourquoi les cristaux liquides pour les technologies optiques?

Les cristaux liquides sont des matériaux qui ont les propriétés d'un cristal et d'un liquide isotrope. Par conséquent, leur état de la matière se trouve entre celui d'un cristal et d'un liquide. Ces matériaux sont optiquement biréfringents, c'est-à-dire ils possèdent deux indices de réfraction différents. Leur biréfringence est également plus élevée que n'importe quel cristal existant. La technologie des cristaux liquides est compatible avec celle des autres technologies existant dans le domaine optique. L'adaptation de la biréfringence en venant modifier le champ électrique, le champ magnétique et la température permettre d'utiliser cette technologie dans des domaines variés. Différents types de cristaux liquides offrent diverses propriétés optiques ; nous avons essayé d'exploiter ces propriétés pour faire des applications différentes. Cette technologie est compatible avec des substrats macroscopiques et microscopiques.

1.2. Les structures des cristaux liquides

Il existe différents types de matériaux à cristaux liquides dont les principaux sont les cristaux liquides nématiques, cholestériques et smectiques. Chacun de ces cristaux liquides possède des propriétés optiques spécifiques que nous avons exploitées pour la fabrication de composants. Ainsi, les cristaux liquides nématiques ont été choisis pour la construction de guides d'ondes et de cavités isotropes. De tels composants peuvent être utilisés pour le contrôle de la polarisation dans les réseaux optiques. Les cristaux liquides cholestériques ont servi pour la fabrication de miroirs ou de filtres accordables et commutables. Ces filtres sont d'une grande utilité dans le domaine des réseaux optiques. Les cristaux liquides smectiques, en raison de leur faible temps de réponse, ont été utilisés pour la conception de modulateurs spatiaux de lumière. L'application ciblée dans notre cas était les obturateurs optiques pour les lunettes actives 3D. Ces dernières représentent l'épine dorsale du cinéma 3D. Avant d'entrer dans le vif du sujet concernant la réalisation de chaque dispositif, on se focalisera tout d'abord sur les détails structurels des principaux types de cristaux liquides cités ci-dessus.

Les molécules présentes dans les cristaux liquides nématiques ne possèdent pas d'ordre de positionnel mais disposent néanmoins d'un certain ordre orientationnel dont le sens est défini par son vecteur directeur.

Dans le cas d'un cristal liquide cholestérique, le directeur dispose d'une structure hélicoïdale. Le pas correspond à la longueur de la période hélicoïdale. Ce pas couvre un large spectre pouvant aller de quelques nanomètres à plusieurs microns. Les cholestériques sont également connus sous l'appellation de nématiques chiraux où le dopant chiral peut faire varier le pas de sorte à obtenir la longueur d'onde désirée. Ce type de cristaux liquides possède des propriétés structurelles remarquables conduisant à certaines fonctions optiques. Nous avons essayé d'exploiter ces propriétés dans notre travail. La structure du cholestérique ne possède pas de directeur dans le plan perpendiculaire à l'axe de l'hélice et s'enroule de manière à effectuer une rotation complète de 360°.

Les cristaux liquides smectiques peuvent être divisés en plusieurs catégories. Cependant, lors des travaux de thèse, nous avons utilisé seulement trois phases de cristaux liquides smectiques : smectique A, smectique C et smectique C*. Ces cristaux liquides présentent des ordres orientationnel et positionnel. Dans le cas du smectique A, le directeur est perpendiculaire aux couches smectiques tandis que pour le smectique C, il est légèrement incliné par rapport aux couches smectiques.

1.3. Couplage diélectrique

Le couplage diélectrique s'occupe de la commutation des molécules dans le cas des cristaux liquides nématiques. Lorsque le champ électrique est appliqué à ces derniers, selon le signe de l'anisotropie diélectrique, le directeur suivra la direction du ou celle opposée au champ électrique. La première situation se produit pour un cristal liquide nématique avec une anisotropie positive tandis que la seconde a lieu lorsqu'elle est négative.

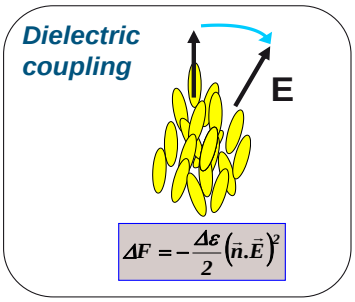

Fig. 1 : Couplage diélectrique.

1.4. Couplage ferroélectriques

La phase smectique C* est une phase smectique chirale où le directeur effectue une rotation hélicoïdale le long de chaque couche smectique. Cette torsion hélicoïdale est macroscopique et n'est pas similaire à celle présente dans les cristaux liquides cholestériques. Dans cette phase, chaque couche smectique possède un moment dipolaire permanent qui donne lieu à une polarisation spontanée. Le vecteur de polarisation est tangent au plan smectique et tourne librement dans le plan du cône smectique. Cependant, le moment dipolaire net de cette phase est nul et le phénomène de ferroélectricité se produit lorsque la symétrie de la structure est rompue. La rupture de la symétrie peut être obtenue selon deux méthodes : la première consiste à effectuer une compression des couches smectiques tandis que l'autre revient à appliquer un champ électrique. Une fois la symétrie de la structure brisée, le mouvement moléculaire est restreint et les molécules ne peuvent occuper que deux états. Les molécules restent dans l'état dans lequel elles étaient lors de l'enlèvement du champ électrique. Cela donne lieu à un effet mémoire. Puisque les deux états sont stables, les vitesses de commutation sont élevées car les molécules ne peuvent basculer qu'entre ces deux états. Cette phase smectique démontre donc bien une commutation bistable.

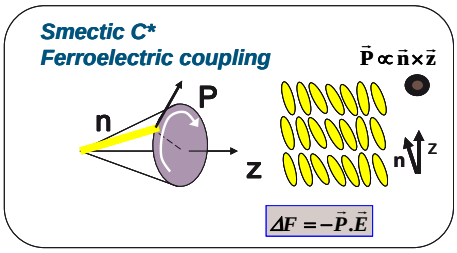

Fig. 2 : Couplage ferroélectrique.

1.5. Alignement de cristaux liquides

L'un des aspects les plus critiques de l'étude des cristaux liquides est l'orientation des molécules dans une direction souhaitée. La base pour la réalisation de nombreuses applications est une couche d'alignement déposée sur un substrat qui induit une interaction entre le substrat et les molécules des cristaux liquides et éventuellement décide de l'orientation de ces molécules. Cette couche d'alignement est en général un film polymère qui est déposé sur un substrat selon un procédé de revêtement par centrifugation, immersion, pulvérisation, etc. Cette couche permet d'aligner les molécules des cristaux liquides soit parallèlement (planaire), soit perpendiculairement (homéotrope) au substrat. La qualité du cristal liquide, après avoir subi le traitement d'alignement, est primordiale pour le comportement électro-optique. La qualité d'alignement conditionne donc la performance électro-optique du dispositif à base de cristaux liquides. Les travaux de thèse consistaient à utiliser deux techniques d'alignement de base : l'alignement par brossage et le photo-alignement. La première est la méthode traditionnelle utilisée pour aligner les cristaux liquides. Dans ce procédé, le substrat est revêtu d'un

polymère qui est brossé dans une direction spécifique. La direction du brossage décide de l'orientation moléculaire. Cette méthode souffre de quelques carences : elle n'est pas très propre et peut laisser des charges électrostatiques sur le substrat. Pour pallier à ces inconvénients, une autre alternative consiste à réaliser l'alignement en utilisant la lumière. La lumière UV polarisée permet de décider de la direction de l'orientation. Un film de polymère linéairement photopolymérisable (LPP) est revêtu sur le substrat. Lorsque ce film est exposé à la lumière UV polarisée, les molécules s'alignent le long de la direction de la polarisation. L'avantage de cette méthode est que le motif du cristal liquide sur un substrat unique est possible alors que ce n'est pas le cas avec la méthode traditionnelle d'alignement par brossage.

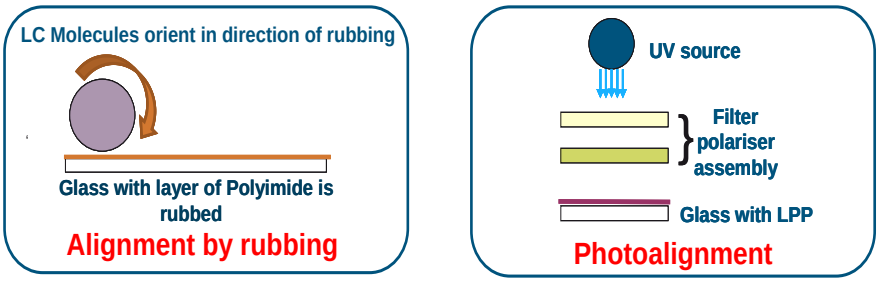

Fig. 3 : Alignement des cristaux liquides par brossage et photo-alignement.

2. Les dispositifs à cristaux liquides

Il existe plusieurs technologies optiques à base de cristaux liquides. Nous en avons ciblées trois utilisables dans différents domaines de l'optique. Les dispositifs concernés sont les filtres sélectifs en longueurs d'onde, les modulateurs spatiaux et les guides d'ondes.

2.1. Les miroirs ou les filtres commutables

Un miroir est un dispositif qui reflète toutes les longueurs d'onde de la lumière alors que le filtre optique réfléchit et transmet peu de longueurs d'onde. Comme mentionné précédemment, les cristaux liquides cholestériques sont préconisés pour la fabrication de composants sélectifs en longueurs d'onde en raison de leurs propriétés structurales remarquables. L'auto-organisation des molécules des cristaux liquides cholestériques donne lieu à des bandes interdites photoniques. Ces dernières exhibent les propriétés de réflexion des miroirs de Bragg. En choisissant le matériau à cristaux liquides et le dopant chiral appropriés, on peut adapter la longueur d'onde de réflexion ainsi que la largeur de bande de réflexion.

2.1.1. *Réflexion sélective dans les cristaux liquides cholestériques et les effets électro-optiques*

La structure périodique dans les cristaux liquides cholestériques permet la réflexion sélective. Cependant, cette réflexion est sélective seulement pour la lumière polarisée circulairement. Cette propriété de réflexion sélective a été utilisée pour la conception du filtre accordable. Dans le cas d'un cristal liquide cholestérique gauche, la lumière à polarisation circulaire gauche sera complètement réfléchie alors que celle à polarisation circulaire droite sera transmise sans aucune absorption. La particularité intéressante est que la polarisation de la lumière réfléchie est conservée et garde une polarisation circulaire gauche. Si la lumière incidente est non polarisée, le taux maximal de réflexion est de 50%.

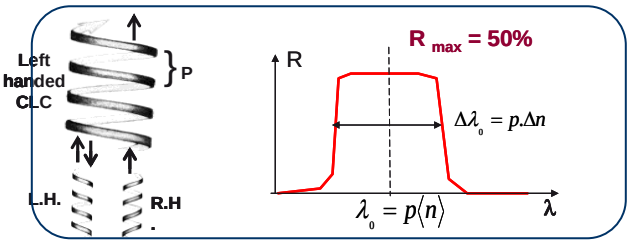

Fig. 4 : Réflexion de la lumière dans les cristaux liquides cholestériques.

La longueur d'onde de réflexion et la largeur de bande dépendent du pas "cholestérique" et de l'indice de réfraction moyen de l'empilement hélicoïdal de lamelles qui constituent les cristaux liquides cholestériques.

Les effets électro-optiques dans les cristaux liquides cholestériques sont tout aussi importants que ceux présents dans les autres matériaux à cristaux liquides. L'application d'un champ électrique à un cristal liquide cholestérique aligné dans une configuration plane donne lieu à des structures à coniques focales. L'augmentation supplémentaire du champ électrique conduit à un positionnement des molécules de manière à ce qu'elles soient perpendiculaires au substrat, c'est-à-dire en alignement homéotrope. Cet effet est réversible puisque la suppression du champ électrique entraîne une transition d'un alignement homéotrope vers des structures à coniques focales et celles à coniques focales vers un alignement plane.

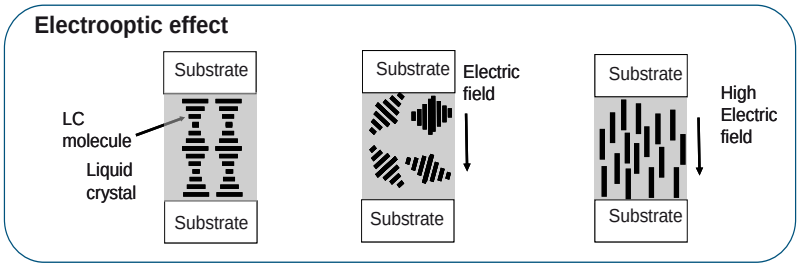

Fig. 5 : Effet électro-optique dans les cristaux liquides cholestériques.

2.1.2. *Le miroir de Bragg cholestérique accordable*

La fabrication du miroir de Bragg cholestérique a été réalisée à l'aide d'un polymère cholestérique stable et une lame quart d'onde. La nécessité d'avoir un polymère avec le cristal liquide cholestérique sera détaillée dans la section suivante. La fabrication de ce type de miroir de Bragg est la première étape dans la réalisation de cavité Fabry-Perot.

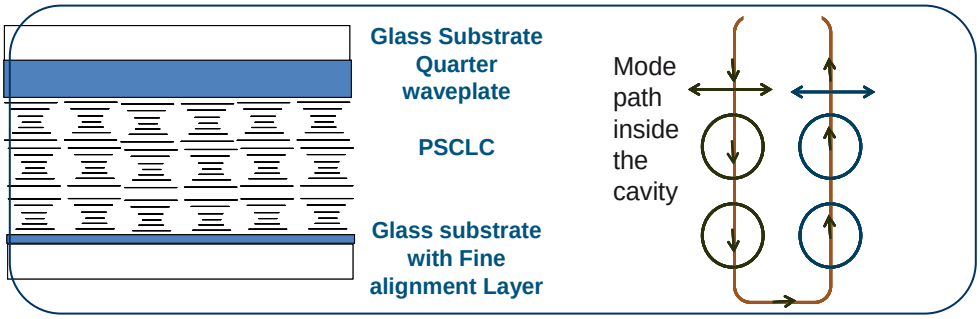

Fig. 6 : Le miroir de Bragg cholestérique accordable.

On peut voir sur la figure ci-dessus le trajet optique du mode à l'intérieur de la cavité. Lorsque la lumière avec une polarisation rectiligne est transmise à travers la lame quart d'onde, elle se transforme en lumière polarisée circulairement. Comme elle possède la même chiralité que celle du cholestérique, elle est réfléchie en retour avant de ressortir en tant que lumière polarisée linéairement. La structure décrite constitue une demi-cavité. La présence de la lame quarte d'onde à l'intérieur de la cavité représente l'originalité de la technique.

2.1.3. *Nécessité d'avoir un polymère dans les cristaux liquides cholestériques*

Un polymère nématique a été utilisé suivant différents niveaux de concentration avec un cristal liquide cholestérique. Nous verrons dans un premier temps l'impact de ce polymère sur la bande passante et la réflectivité du miroir de Bragg. La figure suivante illustre les détails sur la bande passante et la réflectivité pour différentes concentrations du polymère et pour des cristaux liquides cholestériques purs en l'absence du polymère.

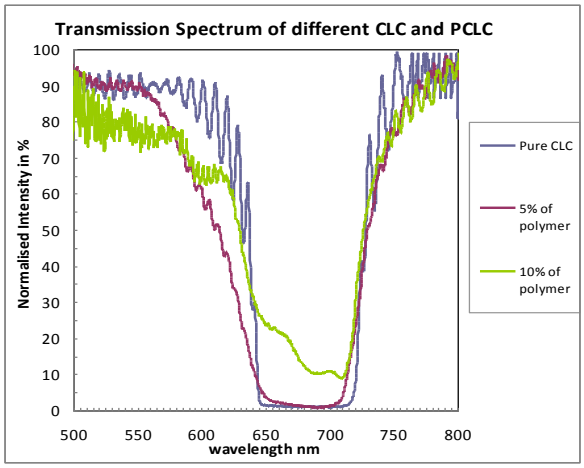

Fig. 7 : Effet d'un polymère sur la largeur de bande et la réflectivité.

D'après la figure 7, on peut voir que la largeur de bande du miroir de Bragg demeure plus ou moins constante après l'addition du polymère. Toutefois, la réflectivité diminue avec augmentation de ce dernier. Afin de prouver l'importance du polymère dans le cristal liquide cholestérique, nous évaluons l'impact des polymères concernant la stabilité sur les propriétés électro-optiques. Il a été observé que le miroir de Bragg avec cholestérique pur requiert un champ électrique faible pour s'éteindre. Cependant, le temps de relaxation de l'état homéotrope à l'état planaire est vraiment lent (de l'ordre de quelques secondes à quelques minutes). L'ajout de polymère permet de réduire drastiquement ce temps de relaxation à 50 ms pour 5% de polymère, voire même 30 ms pour 10% de polymère. Néanmoins, l'intensité du champ électrique requise avec 10% de polymère est vraiment élevée (20 V/µm). Par conséquent, le cristal liquide cholestérique avec 5% de polymère a été considéré comme un bon compromis : un apport de 10% de polymère diminue la réflectivité et nécessite un champ électrique élevé alors qu'avec les cholestériques purs, le temps de relaxation est relativement long.

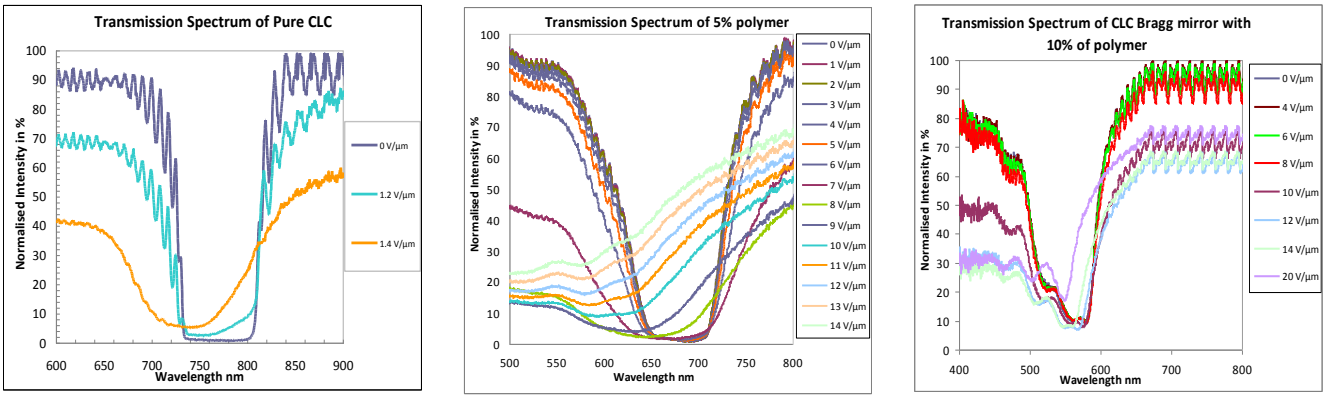

Fig. 8 : Spectres de transmission du miroir de Bragg avec cholestériques pour différentes concentrations de polymère selon différentes intensités du champ électrique (a) CLC Pur (b) CLC avec 5% de polymère (c) CLC avec 10% de polymère.

2.1.4. *Cavité Fabry-Perot accordable et asymétrique utilisant le miroir de Bragg avec cholestérique*

La cavité Fabry-Perot (FP) utilisant le cristal liquide cholestérique est asymétrique puisque l'un des miroirs est constitué d'un miroir cholestérique tandis que l'autre est métallique. Les étapes relatant la fabrication du miroir sont décrites sur la figure 9.

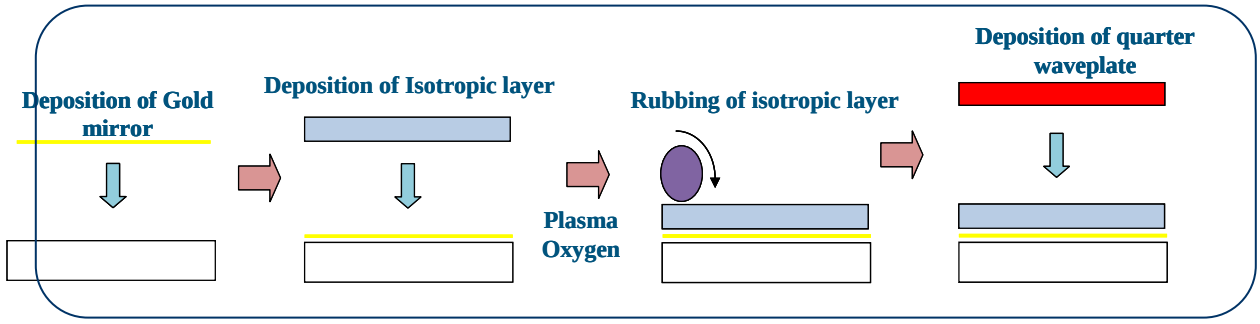

Fig. 9 : Fabrication du Fabry-Perot avec le miroir de Bragg avec cholestérique.

Ces étapes décrivent la réalisation du premier substrat alors que le second substrat est juste une couche alignée de polyimide frotté. Le schéma descriptif final de la cavité Fabry-Perot et le trajet optique du mode dans la cavité sont donnés sur la figure 10. La présence de la lame quarte d'onde à l'intérieur de la cavité représente une nouvelle technique pour la fabrication de cavité Fabry-Perot. La propagation du mode dans la cavité montre clairement que la lame quart d'onde en est une partie intégrante. Son absence fait que le dispositif n'exhibe plus le comportement d'une cavité Fabry-Perot.

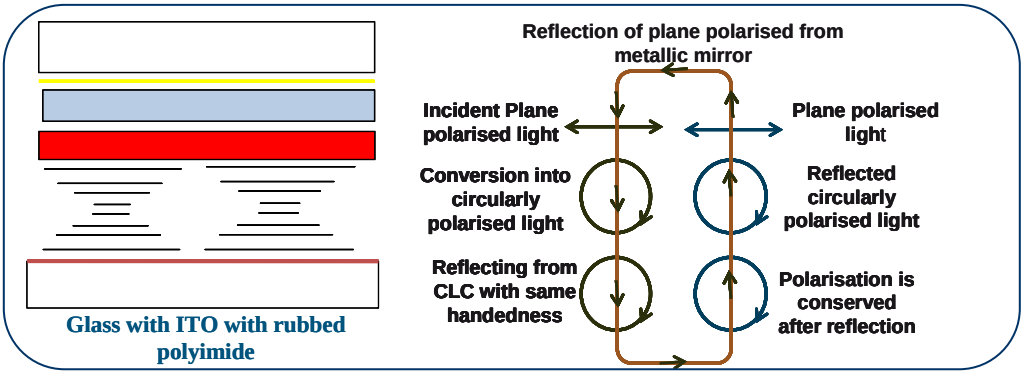

Fig. 10 : Fabry-Perot avec miroir de Bragg avec cholestérique.

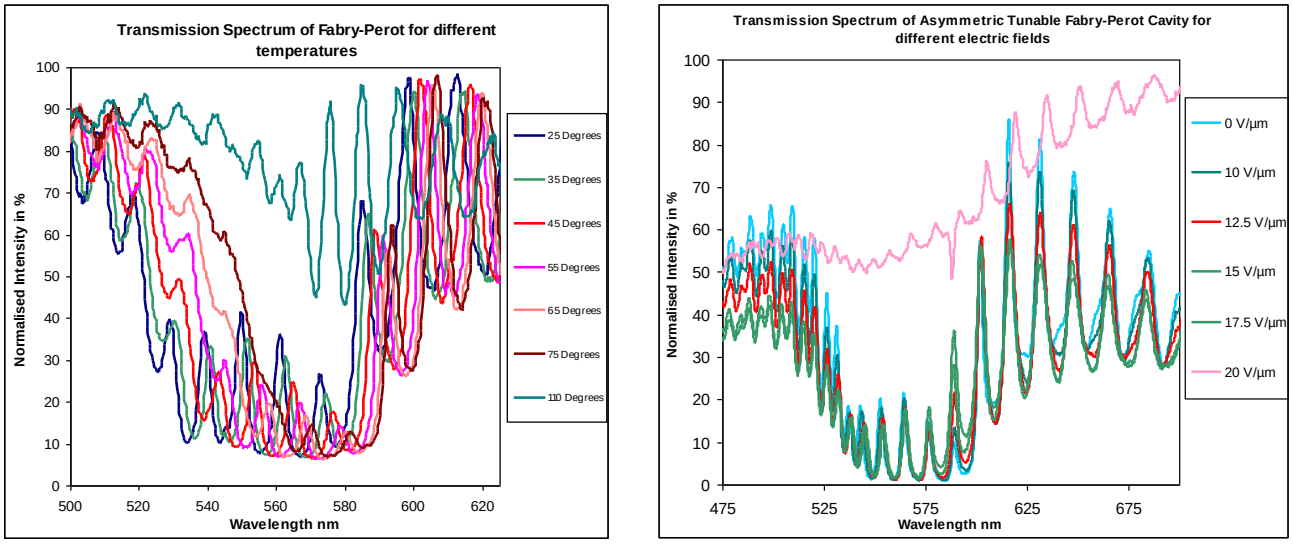

Fig. 11 : Spectre de transmission for tunable Fabry-Perot using temperature and electric field.

On peut voir sur la partie gauche de la figure 11 que la commutabilité et l'accordabilité peuvent être modulées en jouant sur la température. Lorsque ce paramètre augmente le pas des cholestériques, ces derniers commencent à se dérouler tout en entraînant un décalage en longueur d'onde vers le rouge. Le décalage total observé est de 8 nm. La température à laquelle se produit l'extinction complète de la cavité de Fabry-Perot est atteinte lorsque la transition nématique-isotrope est réalisée. En ce qui concerne la partie droite de la figure 11, aucune accordabilité n'a été obtenue avec l'application d'un champ électrique. Néanmoins, l'extinction de la cavité Fabry-Perot est possible lorsque l'intensité du champ électrique atteint une certaine valeur seuil. La distance de 7 µm entre les cholestériques et l'une des électrodes est une raison possible pour laquelle aucune accordabilité ne fut observée.

2.2. Modulateurs Spatiaux

Les modulateurs spatiaux ont été conçus avec des cristaux liquides ferroélectriques. Ce choix de ce type de cristaux liquides est du au fait de leurs caractéristiques électro-optiques concernant la commutation.

2.2.1. Cinéma 3D

Le principe du cinéma 3D en utilisant des lunettes actives est d'envoyer à des fréquences élevées et de manière alternée des images sur l'œil gauche et l'œil droit. Afin de créer le sentiment de profondeur, l'obturateur optique pour chaque œil doit se refermer très rapidement. La grande vitesse des images permet une synchronisation avec la vitesse d'obturation. Les obturateurs doivent également

posséder un taux de contraste élevé afin de limiter la fuite de d'images d'un œil à l'autre. Ce phénomène est appelé "ghosting" ou phénomène d'images fantômes.

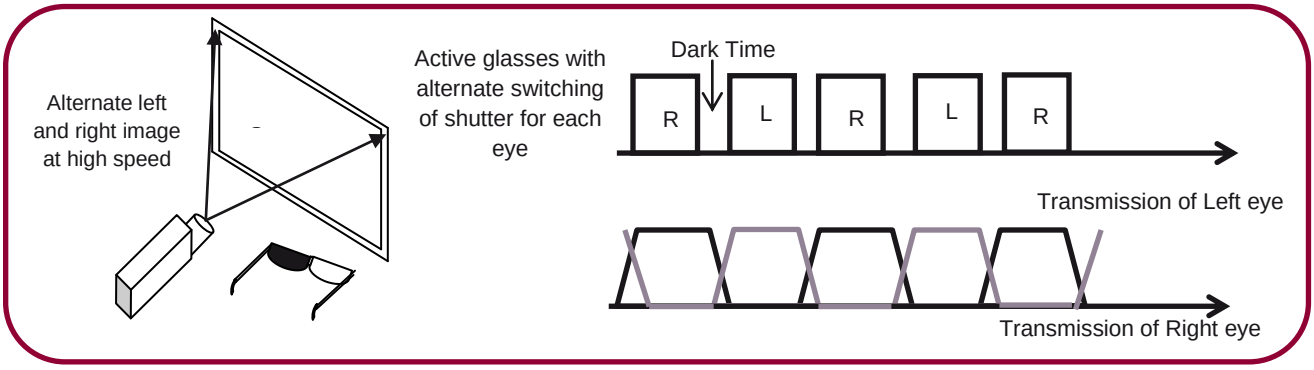

Fig. 12 : Le principe du cinéma 3D avec les lunettes actives.

Plusieurs raisons peuvent expliquer le phénomène de "ghosting" dans les lunettes actives : un temps de commutation trop faible (figure 12), un faible taux de contraste ou une isolation insuffisante due à la fermeture incomplète des obturateurs.

2.2.2. Cristaux liquides Ferroélectriques pour la fabrication d'obturateurs optiques

Les paramètres à prendre en compte lors de la conception d'obturateurs à cristaux liquides sont le temps de commutation, le taux de contraste et la lumière résiduelle. Il est important de restreindre le temps de commutation afin de réduire le "ghosting" et les bandes de couleur. Ce temps de commutation est fortement lié aux temps noirs entre deux images. Ces temps noirs varient entre 1 et 2 ms selon le système 3D utilisé. Ils sont évalués en prenant en compte les paramètres concernant la commutation pour les lunettes actives existantes. Toutefois, une réduction trop importante du temps noir peut conduire à une augmentation non négligeable de la luminosité pour une trame d'une durée d'environ 6 ms. Un temps de commutation proche d'une milliseconde (temps de relaxation de commutation) est réalisable avec les cristaux liquides nématiques alors que les cristaux liquides ferroélectriques offrent un temps de réponse de l'ordre de 100 microsecondes et permettent une commutation symétrique. Les cristaux liquides ferroélectriques ont donc une influence non négligeable sur la luminosité et les images fantômes. Une attention particulière doit être prise en ce qui concerne la valeur du taux de contraste afin d'éviter le "ghosting" résiduel. Une caractéristique fondamentale de tout commutateur optique est qu'il doit laisser passer le maximum de lumière à l'état "ON" et tout bloquer à l'état "OFF". Le taux de contraste est le rapport de l'intensité lumineuse transmise à l'état "ON" à celle transmise à l'état "OFF". Les obturateurs optiques avec un rapport de contraste élevé sont donc privilégiés puisqu'ils offrent un visionnage de meilleure qualité des films en 3D.

2.3. Guides d'onde à cristaux liquides

L'un des aspects fondamentaux des cristaux liquides pour la fabrication de guides d'onde est la biréfringence du matériau cristal liquide. On utilise cette anisotropie optique pour séparer les polarisations de l'onde incidente en entrée du dispositif. L'idée est de fabriquer des zones de phase isotrope et anisotrope du cristal liquide sur le même substrat. En d'autres termes, ces deux phases de cristaux liquides sont créées sur un seul substrat de silicium afin de permettre la séparation entre les modes TE et TM. La sensibilité à la polarisation d'entrée a toujours posé problème en ce qui concerne les dispositifs pour les communications optiques, notamment en optique guidée où les modes TE et TM ne possèdent pas les mêmes propriétés de propagation. Elle est indésirable dans les communications optiques puisque la polarisation d'entrée ne peut pas être contrôlée. L'utilisation des cristaux liquides permet la séparation de polarisation de telle sorte que les dispositifs basés sur notre principe vont se comporter de façon similaire pour toutes les polarisations d'entrée.

2.3.1. Problèmes de polarisation dans les guides d'onde optiques

La sensibilité à la polarisation des guides d'ondes optiques demeure, depuis plusieurs années, l'un des problèmes les plus complexes à traiter dans les communications optiques. La polarisation d'entrée du signal optique ne peut pas être contrôlée lors de sa propagation et est totalement instable en raison de contraintes mécaniques subies pas la fibre optique. Cette sensibilité provient principalement de l'anisotropie induite dans les circuits de guides d'onde. Il existe plusieurs sources d'anisotropie qui peuvent être d'origines géométriques telles que les courbures et les sections asymétriques des guides d'onde et technologiques comme la croissance épitaxiale ou les techniques de conception de guides d'onde et l'effet photoélastique en raison de du désaccord de réseau entre la couche de guidage et le substrat. Nous nous sommes basés sur la nature anisotrope des guides d'ondes afin de résoudre le problème lié à la sensibilité à la polarisation. Nous proposons une solution originale qui consiste à réaliser des guides d'onde à base de polymères à cristaux liquides. Ces guides contiennent à la fois une section anisotrope et isotrope. Les matériaux polymères possèdent des qualités indéniables : ils permettent la production en masse à faible coût et peuvent être facilement intégrés sur une large gamme de matériaux constituant le substrat tels que le verre, le dioxyde de silicium et le silicium. La section anisotrope est dédiée à la séparation de polarisation tandis que la section isotrope est consacrée à la réalisation de fonctions optiques. Un exemple de fonction à tester est un filtre de longueur d'onde.

2.3.2. Le principe des "supermodes"

Lorsque deux guides d'onde sont symétriquement espacés comme ceux illustrés dans la figure 13, la structure totale est longitudinalement invariante. Cependant, l'excitation du mode fondamental

dans l'un des guides conduit à l'excitation de deux modes normaux de la structure totale. Ces deux modes sont également appelés supermodes. Chaque supermode a sa propre vitesse de phase : leur propagation dans le double guide d'onde conduit à l'oscillation de la lumière présente, c'est-à-dire, il se produit un transfert continu de la puissance lumineuse d'un guide à l'autre. Quand un faisceau lumineux est incident par exemple sur le guide 'a' (figure 13), il excite les supermodes qui sont également appelés supermodes pair et impair ou modes symétrique et antisymétrique. Pour une distance de propagation égale à la longueur de couplage un déphasage de π se produit entre ces supermodes. La quasi-totalité de la puissance lumineuse sera transféré au guide 'b'. Comme on vient de le voir, le principe d'un coupleur directionnel est basé sur le phénomène d'interférence entre les deux (ou plusieurs pour un couplage à guide d'onde multiple) supermodes. L_c est la longueur de couplage et correspond à la distance sur laquelle la puissance lumineuse est transmise d'un guide à l'autre. Il faut toutefois souligner que le transfert total de puissance d'un guide à l'autre n'est strictement pas possible puisque les supermodes pair et impair ne peuvent pas s'annuler complètement dans un guide en raison de la distribution de leur champ électromagnétique respectif dans un seul guide.

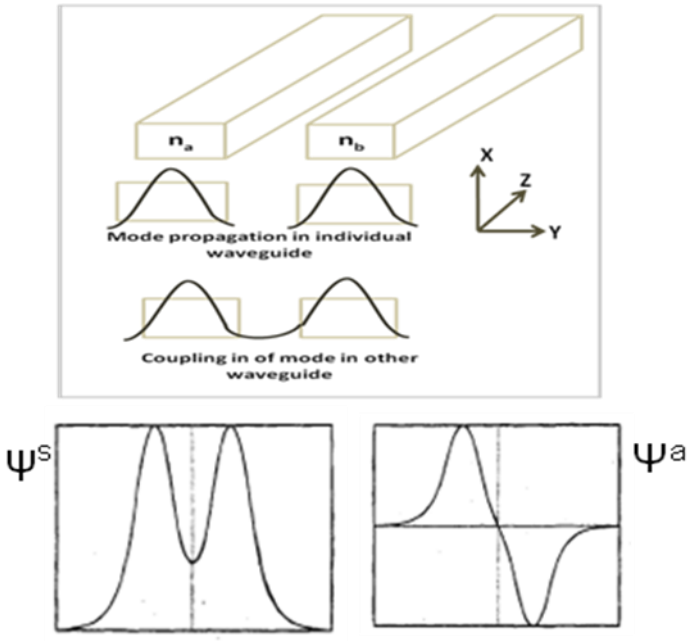

Fig. 13 : Couplage de la lumière dans les guides d'onde et les supermodes.

La longueur de couplage est la longueur nécessaire pour avoir un transfert d'énergie complet. Les longueurs de couplage pour les modes quasi-TE et quasi-TM sont données par les relations suivantes :

$$L_{TE} \approx \frac{\pi}{\Delta\beta_{TE}} \approx \frac{\pi}{2\Delta n_{effTE}} \quad \text{.....1- 12}$$

$$L_{TM} \approx \frac{\pi}{\Delta\beta_{TM}} \approx \frac{\pi}{2\Delta n_{effTM}} \quad \text{.....1- 13}$$

Afin de séparer correctement les deux modes de polarisation, la longueur de couplage du coupleur directionnel doit être un nombre entier i de la longueur de couplage du mode TE et un entier j de celle du mode TM, avec j>i et i ayant une parité différente par rapport à j.

$$L_C = i * L_{TE} = j * L_{TM} \quad \text{.....1- 14}$$

où j>i et (i pair et j impair) ou (i impair et j pair).

2.3.3. Les guides d'onde et les coupleurs anisotropes

De manière générale, les guides d'onde insensibles à la polarisation comprennent trois sections : la première contient le séparateur de polarisation, la seconde inclut la fonction propre réalisée par le dispositif (filtrage, routage spatial, etc.) tandis que la dernière concerne la recombinaison des deux polarisations dans le guide d'onde de sortie. Toutefois, les guides d'ondes isotropes ne peuvent pas effectuer la séparation des polarisations. Pour la plupart de composants optiques insensibles à la polarisation, la séparation des états orthogonaux de polarisation avec les séparateurs de polarisation est la solution la plus simple. Cette séparation ne peut être réalisée que lorsque les zones isotrope et anisotrope issues de la même matière existent sur le même substrat. Lorsque la séparation physique des guides d'ondes est réduite, les champs électromagnétiques dans les deux guides d'ondes se recouvrent, permettant ainsi le transfert d'énergie. La longueur de couplage correspond à la distance nécessaire pour le transfert de mode complet d'un guide à l'autre. Dans le cas de deux guides d'onde anisotropes, les longueurs de couplage pour les polarisations TE et TM diffèrent entre elles. Connaissant le coefficient de couplage pour chaque mode orthogonal, il est possible d'ajuster la longueur de couplage afin de séparer les modes TE et TM. La plupart des dispositifs optiques utilisent des guides d'onde isotropes pour réaliser la fonction optique ciblée. Pour obtenir simultanément la séparation de polarisation et la fonction optique que doit réaliser le dispositif, les sections anisotrope et isotrope du guide d'onde doivent être sur le même substrat. Il est primordial de prendre en compte le degré d'anisotropie lors de la fabrication. Une anisotropie plus faible nécessite une longueur de couplage plus grande. On comprend alors l'utilisation de

matériaux à forte anisotropie tels que les cristaux liquides dans le but de limiter les longueurs de couplage.

2.3.4. *Fabrication de différentes zones sur le même substrat*

La fabrication des deux zones sur le même substrat est réalisée grâce à une technique traditionnelle de brossage utilisant du polyimide comme couche d'alignement et un mésogène réactif comme couche de cristal liquide. Une couche très fine (environ 50 nm) de polyimide est déposée sur la surface du verre et est brossée dans la direction souhaitée (figure 14). Le mésogène réactif subit ensuite un revêtement par centrifugation pour avoir l'épaisseur appropriée. Il est ensuite polymérisé sous le masque en utilisant la lumière UV afin de retenir la partie anisotrope du mésogène réactif. Une fois la partie anisotrope polymérisée, le masque est retiré et la température du substrat est élevée jusqu'à 100°C. La polymérisation est réalisée à cette température. Ces deux procédés de polymérisation sont réalisés sous flux constant d'azote pour éviter que la couche de polyimide soit affectée par l'oxygène.

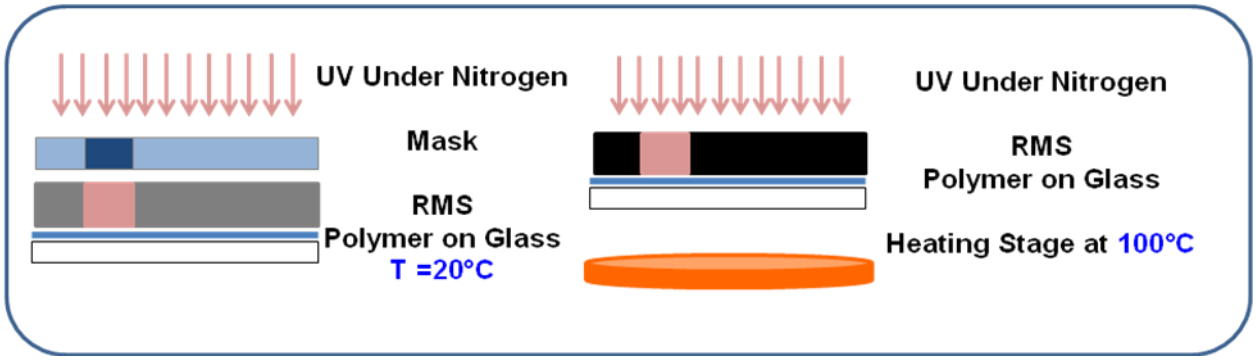

Fig. 14 : Impression thermique pour la création de motifs sur un polymère à cristaux liquides.

2.3.5. *Fabrication du séparateur de polarisation*

Une colle possédant un faible indice de réfraction est utilisée pour réaliser la gaine. Le matériau utilisé pour le cœur est un mésogène réactif. Un polyimide sert en tant que couche d'alignement pour le mésogène reactif. La polymérisation de la phase anisotrope est effectuée à température ambiante en exposant les zones non couvertes par le film de protection UV. Cependant, les zones couvertes par ce dernier ne sont pas polymérisées. Le wafer de silicium est maintenu à 100°C et tout en maintenant, en enlevant le masque, la polymérisation à la même énergie. Des gravures ont été effectuées au Centre Commun Lannionnais d'Optique (CCLO) à Lannion. Le processus de structuration thermique laisse un wafer avec une gaine et un cœur possédant des zones anisotropes et isotropes. La dernière étape consiste à graver les guides d'onde dans la couche constituant le cœur. Ce procédé est réalisé au moyen d'une gravure ionique réactive (Reactive Ion Etching : RIE) en plasma d'oxygène avec un masque de silice.

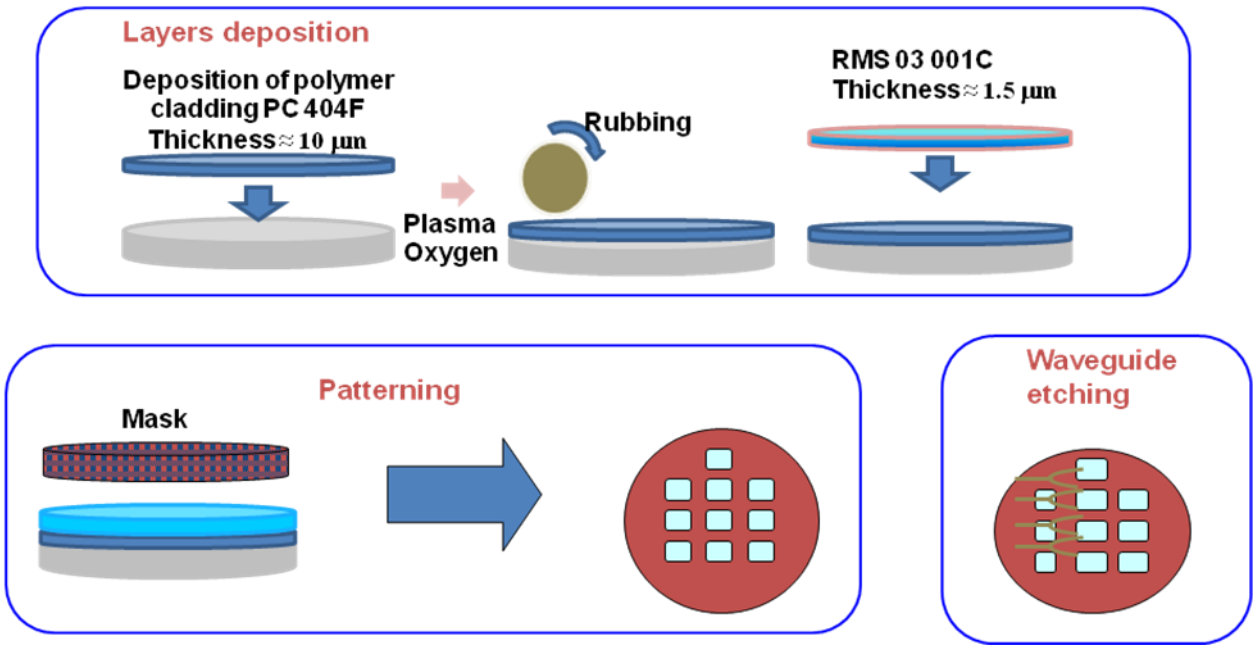

Fig. 15 : Fabrication de guides d'onde à base de cristaux liquides.

2.3.6. Résultats sur les séparateurs de polarisation

Nous avons démontré avec succès la fabrication de guides d'ondes à cristaux liquides : les polymères cristaux liquides peuvent être gravés de manière à obtenir le motif désiré. Dans notre cas les guides d'onde ont été gravés dans ces polymères. Le polymère cristal liquide utilisé est aligné à l'aide de la technique de photoalignement. Il a été observé que la profondeur de gravure variait selon les zones isotrope et anisotrope. Ce constat est peut-être dû aux valeurs différentes de l'indice de réfraction de ces zones. Il se peut qu'il y ait également des variations concernant l'épaisseur de ces zones car leur polymérisation a pu se faire à des épaisseurs différentes.

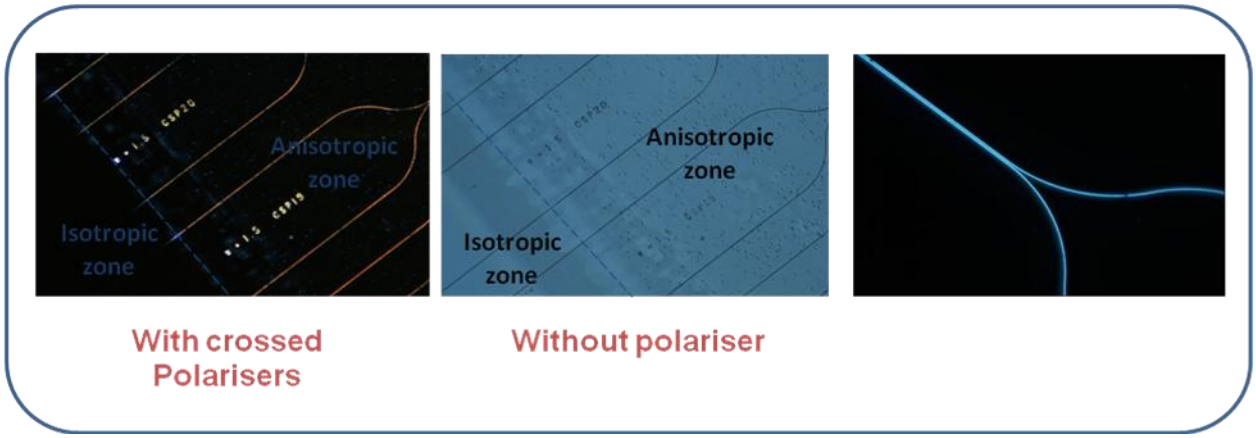

Fig. 16 : Guides d'onde à cristaux liquides dans les zones anisotrope et isotrope.

3. Conclusions

Les polymères cholestériques améliorent les temps de relaxation et la robustesse par rapport aux champs électriques intenses. Nous avons réussi à fabriquer des miroirs sélectifs en longueur d'onde ou cavités Fabry-Perot à base de cholestérique. La stabilisation de cholestérique avec du polymère anisotrope permet la commutation électrique réversible. Le traitement thermique a été utilisé pour permettre l'accordabilité et la commutabilité dans les cavités Fabry-Perot. Cependant, aucune accordabilité n'a été observée lors de l'application d'un champ électrique. Néanmoins, l'application d'un champ électrique faible, avec le concours d'un polymère conducteur, suffit pour causer l'extinction de la cavité Fabry-Perot.

La fabrication d'obturateurs pour les lunettes actives 3D actives avec des cristaux liquides stabilisés par polymère a été démontrée même si un effet de diffusion résiduelle est observé. Des temps de réponse et un taux de contraste bien en accord avec les exigences du cinéma 3D ont été obtenus. La réponse chromatique des lunettes et leur angle de vision répondent clairement aux normes établies pour le visionnage 3D.

La structuration thermique des cristaux liquides nous permet de jouer sur la valeur de la biréfringence des mésogènes réactifs ou les polymères cristaux liquides. La simplicité du procédé de fabrication constitue l'un des atouts majeurs. Ces travaux de thèse ont pu démontrer une nouvelle approche concernant la séparation de polarisation dans les dispositifs à guide d'onde optiques. Les propriétés biréfringentes des cristaux liquides jouent un rôle prépondérant dans la séparation de polarisation. Cette méthode est très utile pour le traitement de la diversité de polarisation qui est réalisé par divers dispositifs à guide d'onde où les modes TE et TM disposent de propriétés de propagation différentes. Le séparateur de faisceau conçu présente un guide d'onde avec une forte biréfringence qui est due à la forte anisotropie intrinsèque des matériaux à cristaux liquides. Cette importante anisotropie permet d'avoir des longueurs de couplage très courtes.